

# High Pressure Die Casting of Zamak alloys

*Steven Richard Pires de Oliveira*

**Dissertação de Mestrado**

Orientador na FEUP: Prof. Doutor Rui Jorge de Lemos Neto

Orientador no INEGI: Doutora Inês Vieira de Oliveira



**Mestrado Integrado em Engenharia Mecânica**

July 2018



*“The future will either be green or not all”*

*Bob Brown*



## Resumo

O processo da fundição injetada tem sofrido grandes avanços nos últimos anos, devido à sua crescente utilização no sector automóvel. Apesar das ligas de alumínio serem as mais utilizadas, a utilização das ligas de zinco também tem vindo a aumentar, principalmente devido às suas excelentes características de qualidade superficial e elevada cadência de produção. Estas características fazem com que as ligas de zinco sejam muito utilizadas em aplicações de pequenas dimensões, onde a qualidade superficial e baixo custo seja um requisito indispensável. Neste estudo, serão alvo de estudo a fundição injetada das ligas de zinco, mais precisamente as Zamak.

Devido ao regime turbulento do metal fundido, são produzidas grandes quantidades de porosidades durante o processo de injeção. Isto faz com que o ar fique aprisionado nas peças, o que deteriora as propriedades mecânicas. A existência de ar nas peças, faz com que não possam ser termicamente tratadas, devido à ocorrência de *blistering*. Uma das formas de minimizar este efeito, é na otimização dos sistemas de gitagem. O grande problema é que nem sempre este processo é suficientemente valorizado, pois muitas vezes recorre-se à experiência no seu dimensionamento. Por estas razões, é apresentado um manual de boas práticas de dimensionamento de sistemas de gitagem. Posteriormente, é aplicado num caso real, onde a falta de um sistema de gitagem otimizado traduz-se em taxas de rejeição de produção superior a 40 %. Esta solução é posteriormente validada por meio de um simulador, *ProCAST*, onde será analisado a ocorrência de defeitos. Foi verificado, que um sistema de gitagem otimizado resultou num enchimento onde o aprisionamento de ar ocorre em menor escala.

Mesmo com um sistema de gitagem otimizado, nem sempre é possível reduzir por completo o aprisionamento de ar durante o enchimento. A aplicação de vácuo na cavidade surge da necessidade de reduzir este problema. Esta tecnologia é largamente aplicada em ligas de alumínio e de magnésio. Contudo, nas ligas de zinco não é prática comum. Isto deve-se ao facto do mercado das ligas de zinco não ser muito exigente em termos de propriedades mecânicas e serem reservados para peças com um valor acrescentado menor. Contudo, pode ser necessário a utilização de vácuo para casos em que um sistema otimizado não seja suficiente. Um método de dimensionamento é proposto, onde é aplicado num caso real. Este dimensionamento tem por base a utilização do *Exco Engineering App*, que auxilia no dimensionamento de um sistema de vácuo. Este programa também possibilita a validação do dimensionamento com base na eficiência de vácuo.

## Palavras Chave

*Fundição injetada; ligas Zamak; sistema de gitagem; NADCA; ProCAST; Vácuo; Exco Engineering.*



## Abstract

The high pressure die casting process has undergone major advances in recent years, due to its increasing use in the automotive sector. Although aluminum alloys are the most widely used, the use of zinc alloys has been increasing, mainly due to their excellent characteristics of surface quality and production cycles. These characteristics make zinc alloys widely used in small applications, where surface quality and low cost are an indispensable requirement. In this study, more attention will be given to the high pressure die casting of zinc alloys, more precisely the Zamak alloys.

During the injection process, a turbulent molten metal flow is generated, as a result of the high injection velocities. For this reason, large amounts of air porosity are produced during the injection process. This causes the air to become trapped in the parts, which deteriorates the mechanical properties. Heat treatments cannot be applied to components with air porosity, since they will expand and cause blistering. An optimized gating system is a solution to minimize the occurrence of these defects. A major concern, is that this process is not valued enough, because many times only the designers experience is used for the design process of a gating system. For these reasons, a good practice manual for designing a gating systems is presented and then applied in a real case, where the lack of an optimized gating system results in production rejection rate of more than 40 %. This solution is later validated using a die casting simulator, ProCAST, where the occurrence of defects will be analyzed. It has been found that an optimized gating system resulted in a more uniform filling pattern, which resulted in less air entrapments.

Even with an optimized gating system, it is not always possible to completely reduce air entrapments during the filling process. The application of vacuum in the cavity arises from the need to reduce/minimize this problem. This technology is widely applied in aluminum and magnesium alloys. However, in zinc alloys it is not common practice. This is due to the fact that the zinc alloy market is not very demanding in terms of mechanical properties and is reserved for parts with a lower added value. However, it may be necessary to use vacuum in cases where an optimized system is not sufficient. A designing vacuum system method is proposed, where it is applied in a real case. This design is based on the use of the Exco Engineering App, which is a tool that calculates a number of parameters of the vacuum system. This program also enables the validation of the design based on the desired vacuum efficiency.

## KeyWords

High pressure die casting; Zamak alloys; Gating system; ProCAST; SolidWorks; Vacuum; Exco Engineering





## Acknowledgments

Firstly, a big thank you to my family for supporting me throughout the course of my degree and more importantly, during my master thesis internship.

To INEGI and my thesis advisor, Rui Neto, who provided me all the necessary working conditions for the thesis development.

My biggest appreciation would go for my supervisor, Inês Oliveira, who was always available and ensured that I was following the right path. Her suggestions on a variety of subjects, were a vital help to achieve the desired objectives.

I would like to thank all my colleagues that in some way contributed for my work. Last but not least, I would like to thank Marta Cerqueira for helping during my course and also for reviewing my thesis.

Also, I would like to thank my colleague, José Silva, for helping me in subjects related to the die casting simulation analysis.

*Este trabalho foi desenvolvido no âmbito do **projeto nº 24231 - HIVALOCK**, cofinanciado pelo Programa Operacional Competitividade e Internacionalização, através do Fundo Europeu de Desenvolvimento Regional (FEDER).*

Cofinanciado por:



UNIÃO EUROPEIA  
Fundo Europeu  
de Desenvolvimento Regional

Este trabalho foi desenvolvido no âmbito da operação **NORTE-01-0145-FEDER-000022 – SciTech – Science and Technology for Competitive and Sustainable Industries**, cofinanciado pelo Programa Operacional Regional do Norte (NORTE2020), através do Fundo Europeu de Desenvolvimento Regional (FEDER).



UNIÃO EUROPEIA  
Fundo Europeu  
de Desenvolvimento Regional



## References

1	Introduction.....	1
1.1	Motivation.....	1
1.2	INEGI- Instituto de Engenharia Mecânica e Gestão Industrial .....	2
1.3	Main goals.....	2
1.4	Scope and layout of the thesis.....	3
2	Die casting.....	5
2.1	Die casting processes .....	5
2.2	High pressure die casting .....	7
2.2.1	Historical review .....	7
2.2.2	High pressure die casting .....	9
2.2.3	Most common defects .....	11
2.3	Hot chamber machine .....	13
2.3.1	Zamak alloys .....	16
2.4	Die.....	20
2.4.1	Water-soluble salt cores .....	24
2.4.2	Lubricant .....	26
2.5	Hollow structures .....	28
2.6	Hot chamber semi-solid casting process .....	34
2.7	Heat treatments .....	36
3	Design and analysis of high pressure die casting components for zamak alloys.....	41
3.1	Gating system.....	41
3.2	Elements of a gating system.....	41
3.3	Gating system design .....	42
3.3.1	Casting quality requirements.....	43
3.3.2	Required flow pattern and ingate and outgate location.....	44
3.3.3	Cavity fill time and flow rates.....	45
3.3.4	Ingate parameters .....	46
3.3.5	PQ <sup>2</sup> analysis .....	47
3.3.6	Gate-runner design .....	48
3.3.7	Overflows and vents design .....	50
3.4	Case study .....	51
3.4.1	Iteration 1 .....	52
3.4.2	Iteration 2 .....	59
3.4.3	Iteration 3 .....	65
3.4.4	Conclusions .....	67
4	Vacuum high pressure die casting.....	69
4.1	Vacuum die castin.....	69
4.1.1	Effect of different slow shot speeds on the vacuum pressure and tensile properties.....	71
4.1.2	Influence of the second injection phase on the mechanical properties.....	73
4.2	Case study of an incorrect vacuum gate system design .....	74
4.3	Vacuum die casting system.....	76
4.3.1	Static vacuum shut-off valve.....	77
4.3.2	Dynamic vacuum shut-off valve .....	78
4.3.3	Choosing the evacuation device.....	79

4.4	CASTvac .....	81
4.5	Gibbs die casting machine .....	84
4.6	Vacuum system design .....	85
	4.6.1 Venting efficiency .....	85
	4.6.2 Vacuum tank size .....	86
	4.6.3 Vacuum pull time .....	87
	4.6.4 Discharge coefficient of the evacuation device .....	87
	4.6.5 Venting mass flow rate.....	88
4.7	Case study .....	90
	4.7.1 Vacuum tank sizing.....	90
	4.7.2 Vent Valve sizing .....	90
	4.7.3 Vacuum pull time .....	91
	4.7.4 Validation of the calculated vacuum system parameters .....	92
4.8	Design of vacuum runners .....	93
4.9	Conclusions.....	94
5	Conclusions and future studies.....	97
	5.1 Future studies.....	98
	References.....	99
	Appendix A.....	107

## List of figures

Figure 1- Comparison of properties of different foundry processes [1].....	5
Figure 2- Manufacturing conveniences of different foundry processes as function of production rate and casting weight [2].....	6
Figure 3- Representation of casting processes respecting velocity and pressure [3]. ....	6
Figure 4- Sturges die casting machine patent [5]. ....	7
Figure 5- Early die casting machine that required two people to operate [5]. ....	8
Figure 6- Pneumatic die casting machine [5]. ....	8
Figure 7- Left: Shock tower with an assembly of various sheet steel parts; Right: Same part with just a single part produced by aluminium die casting [10].....	9
Figure 8- High pressure die casting process [2]. ....	10
Figure 9- Left: Schematics of a conventional HPDC cold chamber machine [14]; Right: Typical layout of a component produced by a cold chamber machine [15].....	11
Figure 10- Classification of defects and their origins [16].....	12
Figure 11- Left: Schematics of a conventional HPDC hot chamber machine [14]; Right: Components produced by a hot chamber machine [22]. ....	14
Figure 12- Passage connecting the nozzle to the die cavity of a hot chamber machine [23]. ..	14
Figure 13- Projected area of casting which includes, die cavity, overflows, gating system, vacuum valves and runners [22].....	15
Figure 14- High pressure die casting process phases; representing piston speed and pressure as function of piston position [1]. ....	15
Figure 15- Zamak components ( Courtesy of Dynacast) [30]. ....	17
Figure 16- Left: Cast components being subjected to a grinding process; Right: abrasive chips [32]. ....	18
Figure 17- Left: Zamak 5; Right: Zamak 5 + 0.10 wt.% hf. Both allots at 200x magnification [35]. ....	18
Figure 18- Components of a unit die assembly [23]. ....	21
Figure 19- Flow chart of the simulation process based on ProCAST™ [43]. ....	22
Figure 20- Die casting mold manufactured with TOOLOX 44 to inject Zamak [40].....	23
Figure 21- Salt core and die casting with cavity [47].....	24
Figure 22- Left- “Triplet” salt core inserted in the die cavity; Right- Injected part of a zinc alloy [45]. ....	25
Figure 23- Water soluble salt core with bauxite powders and glass fibres for a zinc alloy casting [50]. ....	26
Figure 24- Thermal images of the die after spraying (left) with an average surface temperature of 180 °C, and before spraying (right) [52]. ....	27
Figure 25- Protrusions related to lamination. Left: magnified 25 x; Right: magnified 10 x [52]. ....	27
Figure 26- Deformation present on a manufactured part [52].....	28

Figure 27- Surface roughness duo to soldering [52].	28
Figure 28- Examples of components using the gas injection technology using a cold chamber [10].	29
Figure 29- Possible applications for gas injection technology in the high pressure die casting technology. Left: intake manifolds; Right: Hollow structures in clutch pedals [57].	29
Figure 30- Control-related of the die casting machine and thee gas unit [10].	30
Figure 31- Home position and filling phase [10].	31
Figure 32- Gas injection and opening of the cavity overflow [10].	31
Figure 33- Shot curve with different process parameters [10].	32
Figure 34- Simulation of die fill indicating cold metal near the gas injector for Gating [57].	32
Figure 35- Pressure die casting tool for gas injection and a 200 ton cold chamber casting machine. 1- Overflow Cavity; 2- Locking Pin; 3-Injector; 4- runner; 5-Runner 2 [57].	33
Figure 36- Zinc high pressure die casting with a cavity completely produced by gas injection [58].	33
Figure 37- Left: Non plana filling; Right: planar filing [60].	34
Figure 38- Hot chamber rheo-diecasting machine. The circle indicates de magnetic field around the nozzle [62].	35
Figure 39- Microstructure of a magnesium alloy, AZ91D. Left: conventional high pressure die casting, Right: hot chamber rheo-die casting [62].	36
Figure 40- Effect of test temperature (-35, 23,85 °C) and wall thickness on the tensile strength of Zamak 5 during different natural ageing durations [38].	38
Figure 41- Hardness evolution of a Zamak 5 alloy during 1 year natural ageing [38].	38
Figure 42- Artificial ageing of Zamak 5 alloy for 25 hours for 3 different temperatures [38].	39
Figure 43- Elements of a gating system [75].	42
Figure 44- Flow chart for die layout design [39].	43
Figure 45- Atomized flow [24].	47
Figure 46- Curve sided fan runner-gate [24].	48
Figure 47- Straight sided fan runner-gate [24].	48
Figure 48- Left: Top view of a curved sided fan divided into 9 sections; Right: Cross sectional view of a fan gate-runner and main runner [24].	49
Figure 49- Tapered tangential gate-runner that illustrates different flow angles [24].	50
Figure 50- Typical overflow sizes [24].	50
Figure 51- Overflow.	51
Figure 52- Location of vents on the die [24].	51
Figure 53- Left: Blistering; Right: Pin holes.	52
Figure 54- CAD model for a gating system which was responsible of a rejection rate of over 35 %.	52
Figure 55- Cross section of the die cavity for iteration 1.	53
Figure 56- Analysis of the cross-sectional area of the gating system.	54

Figure 57- Overview of the work flow for a simulation tool. ....	55
Figure 58- Velocity evolution at t=16.8ms and 35.2% filled. ....	56
Figure 59- Velocity evolution at each ingate.....	57
Figure 60- Velocity profile and representation of the metal front collision and creation of air pockets. ....	57
Figure 61- Air entrapment prediction during the filling process.....	58
Figure 62- Rx analysis after painting process. ....	58
Figure 63- Optimized gating system for iteration 2. ....	61
Figure 64- Simulation results of the entire component and gating system. ....	62
Figure 65- Molten metal velocity in function of die cavity filling time at 3 points. ....	63
Figure 66- Molten velocity profile representing 3 different points. ....	63
Figure 67- Air entrapment prediction using ProCAST <sup>TM</sup> . ....	64
Figure 68- CAD model of iteration 3. ....	65
Figure 69- Molten metal velocity profile function to cavity filling time. ....	66
Figure 70- Metal flow in the components die cavity, representing the occurrence of air pockets during the injection process.....	66
Figure 71- Prevision of air entrapments using simulation.....	67
Figure 72- Two examples of Zinc alloy components produced by vacuum high pressure die casting (Courtesy of Fondarex) [79].....	69
Figure 73- Comparison of conventional HPDC, vacuum-assisted HPDC and super-vacuum die casting [1]. ....	70
Figure 74- Case study presenting the internal die cavity pressure and air mass for a HPDC vacuum process including and excluding a leakage area [93].....	71
Figure 75- Die cavity pressure with respect to different slow shot speed [97]. ....	72
Figure 76- Average area of gas porosity with respect to different slow shot speeds [97].....	72
Figure 77- Influence of different slow shot speed on mechanical properties: UTS, YS, elongation [97].....	73
Figure 78- Mechanical properties variation with respect to different gate velocity [84]. ....	74
Figure 79- Incorrect vacuum gating system design, with blocked zones A and B [92].....	75
Figure 80- A- Incorrect vacuum gating design; B-Optimized design [92].....	75
Figure 81- Vacuum die casting system [98]. ....	76
Figure 82- Left- Schematic of a corrugated chill block [4]; Right- ProVac chill vent [99]. ....	77
Figure 83- Left: Chill block with a triangular cross-sectional shape; Right: Chill block with a trapezoidal cross-sectional shape [101]. ....	77
Figure 84- Mechanical shut-off vacuum valve with the Typhon vacuum runners [99]. ....	78
Figure 85- Vacuum runner for a mechanical vacuum valve [100]. ....	78
Figure 86- Left: Electro-pneumatic valve [102]; Right: Hydraulic vacuum shut-off valve [4]. ....	79
Figure 87- Performance comparing of a vacuum valve and chill vent [99]. ....	80

Figure 88- Pressure measurement of a vacuum shut-off valve. Left: Aspiration is opened; Right: Aspiration is closed [99].	80
Figure 89- Differences between a mechanical valve and a chill vent [99].	81
Figure 90- Left: Representation of one half, consisting of wedge-shaped inserts; Right: Engagement of two halves [100].	82
Figure 91- Left: Pressure changes in the vacuum line for a mechanical and a CASTvac valve; Right: Pressure changes in a 3L vacuum vessel for a chill vent and a CASTvac [100].	82
Figure 92- CASTvac installed in a die [100].	83
Figure 93- Different venting efficiencies for a CASTvac and a chill block with natural and vacuum venting [93].	83
Figure 94- Different venting efficiencies with for different venting methods and evacuation devices [93].	84
Figure 95- Gibbs vertical vacuum die casting process [14].	85
Figure 96- Discharge coefficient of vacuum valve and chill block [98].	88
Figure 97- Venting mass flow rates [98].	89
Figure 98- Vacuum tank sizing using the Exco Engineering application.	90
Figure 99- Vent valve sizing using Exco engineering application.	91
Figure 100- Vacuum pull time estimation using a mechanical vacuum valve.	92
Figure 101- Vacuum pull time estimation using a chill block.	92
Figure 102- Evolution of the die cavity pressure with respect to the plunger position [105].	93
Figure 103- Examples of a vacuum runner system layout with a mechanical vacuum valve [106].	93
Figure 104- Cross-sectional area variation of the vacuum runner system [106].	94
Figure A 1- Figure presenting different dimensions of the fan gate-runner calculated in Table A 6.	108
Figure A 2- Various dimensions of an overflow.	109
Figure A 3- Dimensions of a tangential gate-runner.	110



## List of tables

Table 1- Defects in HPDC [9; 17-21].....	12
Table 2- Mechanical properties [27; 30]. ....	19
Table 3- Creep Results [27].....	20
Table 4- Typical composition for TOOLOX 44 and hot working steel (H13), all elements are given in wt.% [40]. ....	22
Table 5- Surface finish in function to fill time and flow pattern design [24].....	44
Table 6- Recommended amount of Solidified material, S [24].....	45
Table 7- Model bodies of the CAD model supplied by STA. ....	55
Table 8- Input parameters supplied by STA.....	55
Table 9- Input and mesh information. ....	55
Table 10- Cavity filling time. ....	59
Table 11- Flow rates. ....	60
Table 12- Curved sided fan gate-runner and main runner dimension. ....	60
Table 13- Main runner dimensions.....	60
Table 14- Outgate dimensions.....	61
Table 15- Overflow dimensions. ....	61
Table 16- Vent dimensions.....	61
Table A 1- Cavity filling time.....	107
Table A 2- Flow rates. ....	107
Table A 3- Ingate data. ....	107
Table A 4- Nozzle data in second phase.....	107
Table A 5- Plunger date in the second phase. ....	108
Table A 6- Curved sided fan gate-runner and runner segment data.....	108
Table A 7- Outgates, overflows and vents. ....	109
Table A 8- Tangential gate-runner .....	110



# 1 Introduction

---

## 1.1 Motivation

In a world where a constant demand of lighter materials with higher mechanical properties are required, the high pressure die casting process plays an important role to achieve these requirements.

The high pressure die casting is a metal casting process, where liquid metal is injected into a reusable metal mould at high velocities along with high pressures.

In this process there are two types of die casting machines, the cold chamber machine and hot chamber machine. The hot chamber machine is reserved for lower melting point alloys such as zinc, tin, lead and some magnesium alloys. In this thesis, more emphasis will be placed into the high pressure die casting process of Zamak alloys. Zamak alloys, are a specific family with zinc as its main element, following aluminium, copper and magnesium. High density and high creep rate at low temperatures are the two main problems of using these alloys. This limits their usage on the “light weight” market. For these reasons, new ways to overcome these disadvantages are needed, so that Zamak alloys can have a wider market share.

This process offers a wide variety of advantages that are increasingly being appreciated for the automotive industry such as higher production cycles; production of thin walled near net shape components with good surface quality finishing; fully automated process; low requirement of post machining finishing's; the possibility to replace an entire assembly of components by a single cast component. Despite these advantages, a turbulent metal flow is generated during the filling process, which translates into components with a high porosity content.

The gating system design is a major task because it not only affects the manufacturing of the die but also the quality and cost of the produced components. This process heavily depends on the designer's experience but also on technical knowledge. Usually, this process requires a number of iterations which results in a longer lead time and increased die cost. For these reasons, a manual of good practices for the design of gating system is required. This manual surges from the need to create a standard design procedure, which allows the design of optimized gating systems.

The generation of high quantities of air during the filling process is a critical problem that often leads to air porosity related defects. This is a characteristic problem of this process, due to the high molten metal velocity, which causes turbulences. There are several reported procedures to reduce porosity levels such as modifying the alloy constituents, that leads to a higher metal fluidity and therefore an injection speed reduction is possible; optimization of process parameters such as metal injection velocity, applied casting pressure and molten metal temperature; applying vacuum to the die cavity and the use of other type of injection process such as squeeze casting or any semi-solid process.

The vacuum technology is being used to overcome defects related to air entrapments. However, there are few papers that discuss this process in detail. For this reason, a more detailed study in this topic is needed. Also, topics related to the designing process of vacuum systems are lacking from the literature. Therefore, a vacuum system designing method will be presented.

## 1.2 INEGI- Instituto de Engenharia Mecânica e Gestão Industrial

This thesis is developed in INEGI - Instituto de Engenharia Mecânica e Gestão Industrial.

INEGI is an interface Institution between University and Industry, oriented to the activities of Research and Development, Innovation and Technology Transfer. Being a private non-profit association and recognized by the Portuguese Government as being of public utility, INEGI is currently considered an active agent playing a significant role in the development of the Portuguese industry, and in the transformation of its competitiveness model. INEGI's core competences are experimental mechanics, engineering design, materials, industrial processes, renewable energies, and industrial engineering and management. INEGI hosts 137 PhD integrated members, and more than 100 associated members, being the largest Portuguese group on R&D and I&TT, in the field of Mechanical Engineering.

Its organizational structure relies on three pillars of activity in different technology readiness levels, maintaining a strong competence matrix element:

- Research with a special focus on applied research
- Innovation and technology transfer
- Consulting and advanced engineering services

The Institute's research activity is integrated in the national network of research funded by Portuguese Foundation for Science and Technology and has consistently been evaluated as excellent. INEGI is considered one of the most effective Research and Technology Organizations in transforming R&D investment in economic and social value.

More than 50% of its total turnover comes from R&D and innovation projects funded by industry. As a non-profit organization counts with 97 shareholders representing the University, public institutions, industrial associations and private companies.

INEGI's research infrastructure includes a broad set of well-equipped laboratories and an extensive engineering tools base for supporting its research and development activity as well as to support the production of industrial or commercial prototypes.

More information about INEGI please visit the website:

[www.inegi.up.pt](http://www.inegi.up.pt)

## 1.3 Main goals

The present work firstly focuses on describing every aspect of the high pressure die casting, more specifically for the hot chamber machine. More importantly, investigating new processes and procedures for the high pressure die casting of Zamak alloys is the main goal for this investigation.

Since a more scientific approach for the gating systems design is lacking for the current OEM's, another purpose of this thesis is to develop a more scientific approach for a gating system design, using Microsoft Excel. This spreadsheet automatically calculates every component of a gating system. Using this tool, a solution for a case study, which presents problems in its gating system, will be presented and validated experimentally using a CAE simulator, ProCAST™.

Lastly, the vacuum technology will be explained in detail and its viability in high pressure die casting process of Zamak alloys will be investigated. Also, an application that gives possibility to design a venting vacuum system will be explored and applied to a case study.

## 1.4 Scope and layout of the thesis

In the current chapter, is presented the motivation to develop this thesis; the problems that were proposed; solutions to these problems; reasons why these solutions were chosen; challenges that these solutions present. Also, the objectives are presented in a summarized way that anyone with a minimal scientific knowledge can understand what is proposed for this thesis.

Chapter two focuses on describing the principals behind the high pressure die casting process, more specifically for the hot chamber machine. Along this chapter, recent innovations are also pretended and discussed.

Chapter 3 is divided into three sections: the first section describes the basic principles of a gating system; in the second section, it is presented a designing procedure based on the NADCA's gating manual, that gives a good starting point to ensure an optimized gating system; in the third second, a real case study is analysed. For this case study three different gating systems are proposed, 1 and 3 by the company and the 2 by the author, using SolidWorks. For every iteration, a simulation tool (ProCAST™) will be used in order to determine the effectiveness of the proposed gating system. The gating system for iterations 1 and 3 are based on the designer's experience which lacks scientific analysis and calculations, while iteration 2 an optimized gating system is proposed.

Chapter 4 presents the application of the vacuum technology in the high pressure die casting process. A complete and detailed description of every component and the main challenges and benefits that this technology offers this process is presented as an introduction to this process. After this description, a venting system design procedure is presented and applied to proposed case study of iteration 2. Also, the Exco Engineering App is used which helps in the venting system design.



## 2 Die casting

### 2.1 Die casting processes

Die casting is a metal casting process that uses a permanent or reusable metal mould, also referred as a die. This process has three variants which depends mainly on the amount of pressure that is used to force the metal into the die [1]:

- Permanent mould casting, or gravity casting. In this process the molten metal is poured into the die and it solidifies under atmospheric pressure;
- Low-pressure die casting (LPDC). Liquid metal is forced into the die cavity using air pressure typically below 0.5 MPa;
- High pressure die casting (HPDC). Liquid metal is forced inside a die cavity by a hydraulic pressure, above 7 MPa along with high velocities, ranging from 20 - 90 m/s. After the filling phase is complete, the solidifying metal is subjected to an intensifying pressure, ranging from 100 to 1000 Bar.

Figure 1 represents the differences between every metal casting processes in terms of process parameters and possible post casting procedures. As shown in Figure 1, the HPDC process when compared to other metal casting processes excels in terms of low cycle times, producing components with the highest surface quality and by being fully automated. As disadvantages, it requires a high investment cost, high lead times and produces parts that cannot be heat treated or welded, if entrapment air is present throughout the component.

<i>Property</i>	<i>Sand casting</i>	<i>Investment casting</i>	<i>Permanent mold casting</i>	<i>Low-pressure die casting</i>	<i>High-pressure die casting</i>
Cycle time	2	1	3	3	4
Investment cost	4	2	3	2	1
Lead time for prototype/design change	4	2	1	1	1
Process efficiency	1	1	2	4	3
Automation level	2-3	1	3	4	4
Post-casting heat treatment	4	4	4	4	1
Casting weldability	2-3	3	3	3	1
Quality surface	1	2	3	4	4

4: Excellent; 3: Good; 2: Fair; 1: Poor

Figure 1- Comparison of properties of different foundry processes [1].

Two important casting characteristics to determine the best suitable process to produce a certain product are the number of castings to be produced per year and the weight of component. This means that for the HPDC process, a high number of parts is needed to payoff initial costs. Also, this process is suitable for producing components up to 50 Kg. As shown in Figure 2, the sand casting process offers the highest weight for a casting and the high pressure die casting requires the highest number of casting per year to compensate the initial costs.

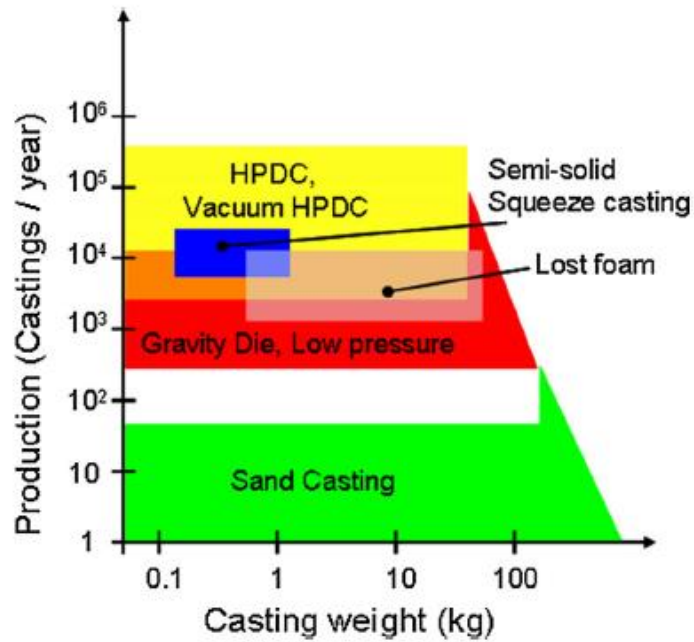


Figure 2- Manufacturing conveniences of different foundry processes as function of production rate and casting weight [2].

As shown in Figure 3, the high pressure die casting process is at the top end of parameters like molten metal injection velocity and injection pressure, comparing to other metal casting process. Among all processes, HPDC is the process that generates a higher quantity of gas related porosities due to the high injection velocity [3].

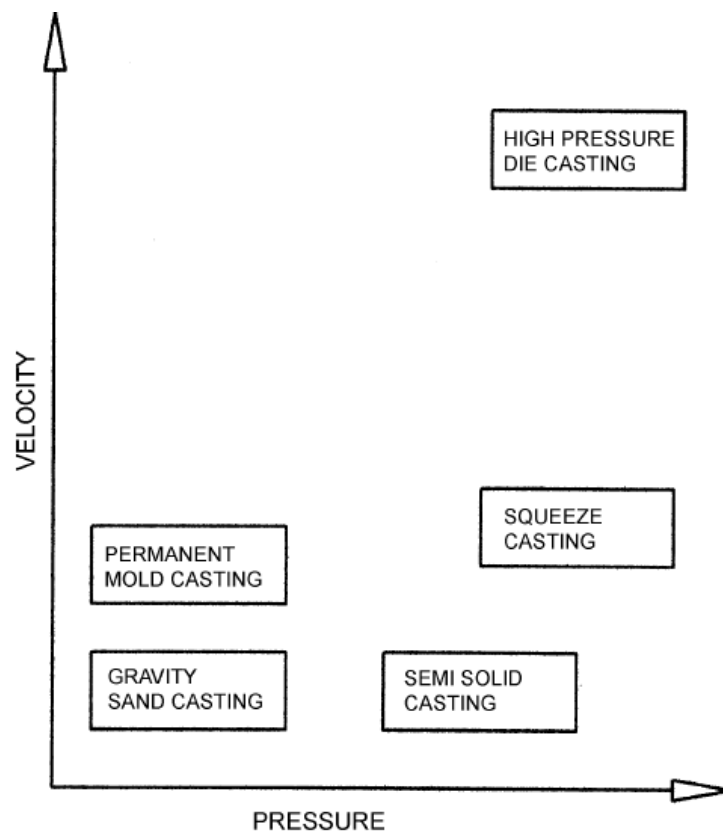


Figure 3- Representation of casting processes respecting velocity and pressure [3].



## 2.2 High pressure die casting

### 2.2.1 Historical review

Casting processes are believed to be amongst the oldest methods to manufacture metal components. Initially, only processes which the mould had to be destroyed to remove the solidified part existed. These processes are still heavily used in the present. Subsequently, it became clear that a reusable mould had to be manufactured to start increasing the production capacity [4].

In the middle age, the first reusable moulds were optimized and used to cast pewter components. Processes kept evolving and being optimized until Sturges in 1849 invented the first die casting machine, presented in Figure 4. This invention was developed due to the high demand of printing letters used in the printing process. This was a manually operated machine, primarily used for casting print type using led [5].

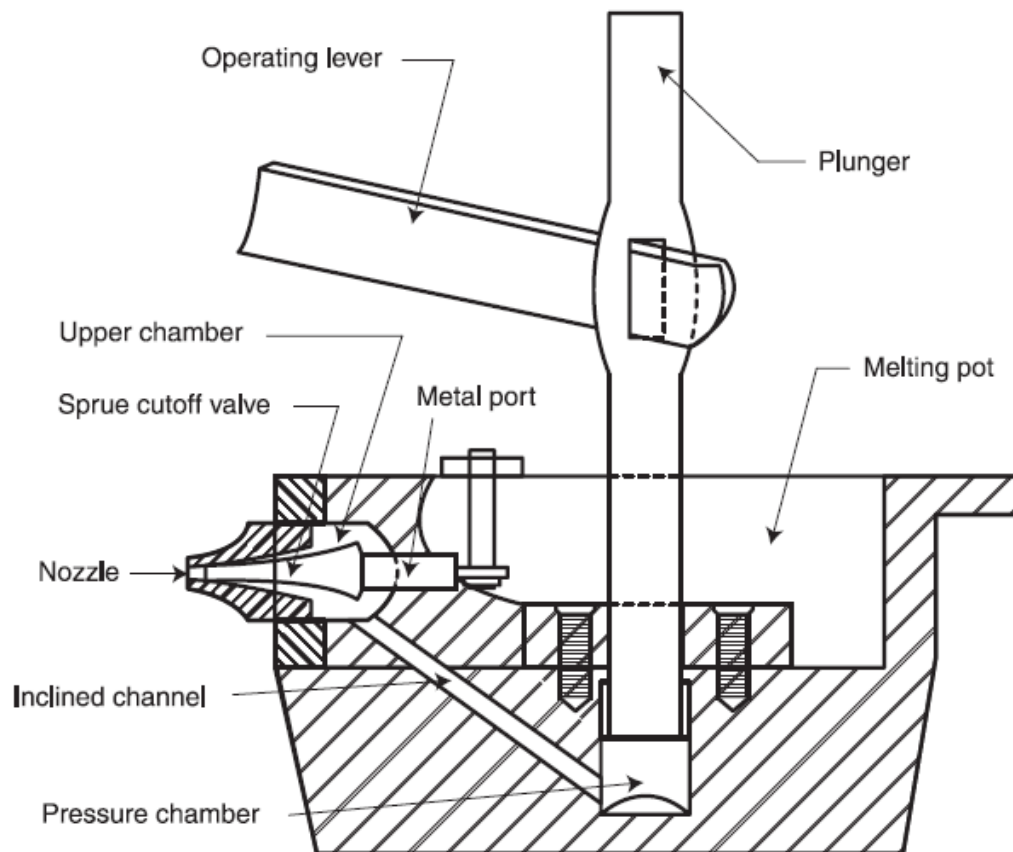


Figure 4- Sturges die casting machine patent [5].

In the late 19<sup>th</sup> century, due to a constant process development, processes were developed to inject metal into metal moulds. This process was better known for producing brass metallic letter moulds, also called as matrices. This progress resulted in the creation of the linotype machine by Ottmar Mergenthaler [4].

Other applications for phonograph parts required a different approach in terms of machinery since it required the combination of decorative and engineering features. This led to the development of a new machine (Figure 5) operated by two people, which required a 90-degree swing of the machine. By only using zinc, led and tin, parts such as cast magneto housings,

carburettors and other automotive parts were produced using this machine right up until 1915 [5].

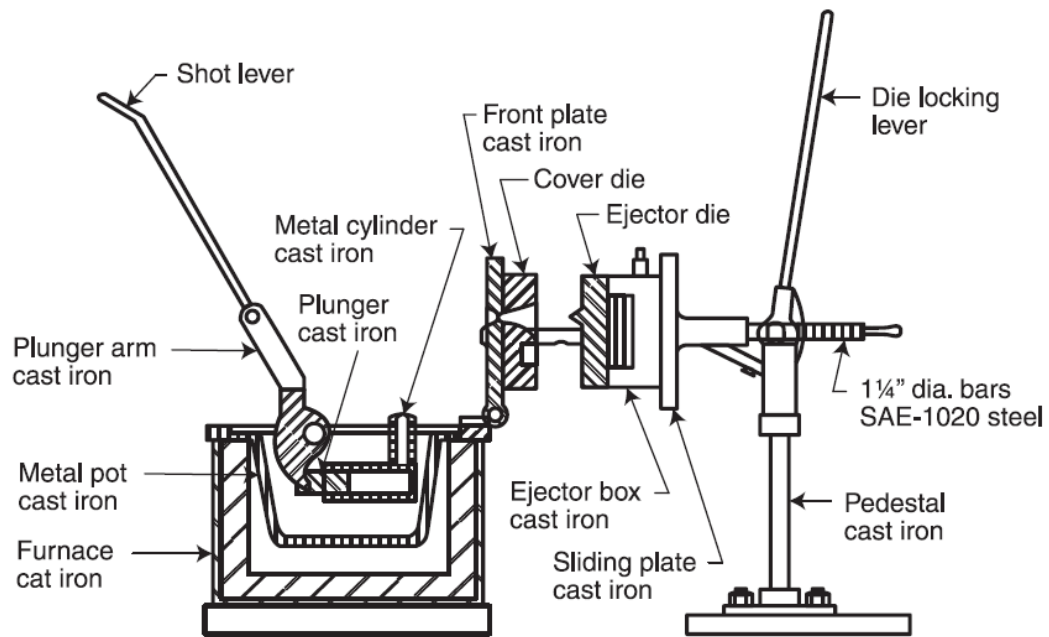


Figure 5- Early die casting machine that required two people to operate [5].

Later, a new machine, presented in Figure 6, was developed. This invention used pneumatics to push the piston and to open and close the dies. This resulted in a higher productivity and higher quality parts with thinner sections. In 1915, the first aluminium die casting machine was developed [5].

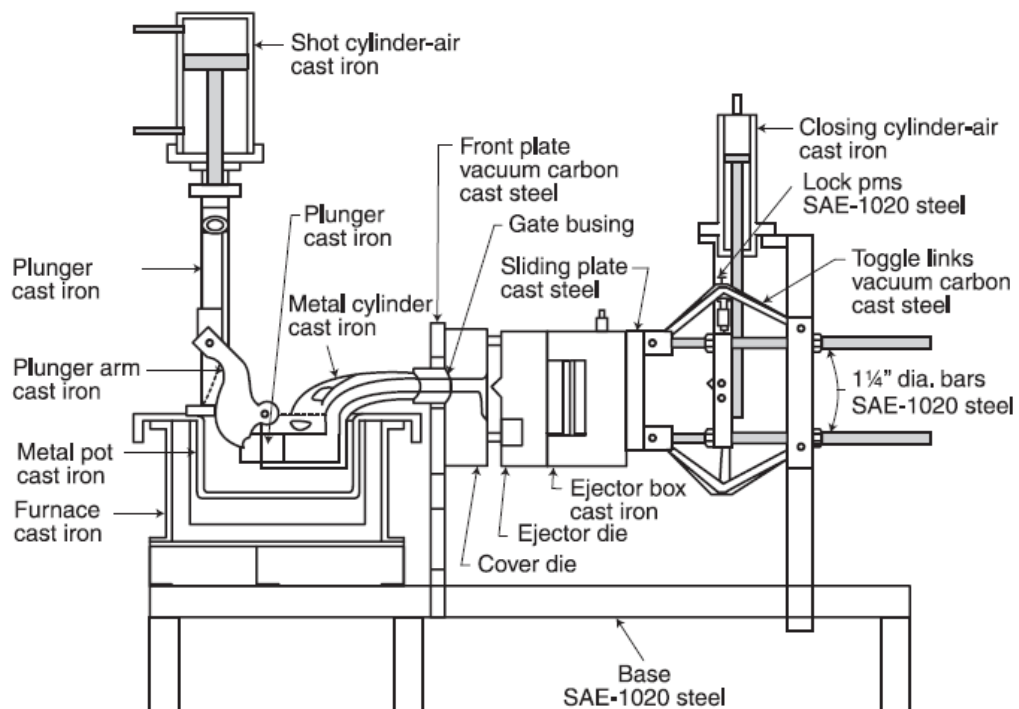


Figure 6- Pneumatic die casting machine [5].

### 2.2.2 High pressure die casting

High pressure die casting (HPDC), or simply die casting in the US [1], is an economical manufacturing process for mass production [6]. This process is used to produce nonferrous and low-melting point base alloys parts such as aluminium, zinc, lead, brass and tin. Also, a titanium alloy was successfully casted using the HPDC process [7]. These components can range from a few grams up to 25 kg [4]. By using high velocities along with high pressures to inject liquid metal into a die cavity, a reusable metallic mould, thin-walled products (as low as 0.25 mm) with high geometry complexity and surface hardness (SH) [8], near net shape, very good surface finish (by casting standards) are produced [9]. All these extreme conditions that the molten metal is submitted and the difficulty to maintain process parameters make HPDC a defect-generating process [2].

The high pressure die casting process can be used to replace assemblies of various parts, produced by different manufacturing processes. An example is presented in Figure 7. The production of just one component instead of various, results in the reduction of the overall process labour and production costs [4].



Figure 7- Left: Shock tower with an assembly of various sheet steel parts; Right: Same part with just a single part produced by aluminium die casting [10].

The main problem of this process, is the high porosity levels of the cast products. This is related to air entrapments during the highly turbulent filling process, among others that will be further described [6]. These defects limit the use of the HPDC process in components where higher mechanical properties, excellent surface finishing is required. In structural applications, porosities act as stress concentrator which leads to cracks initiations. Also, heat treatment rarely can be applied to parts that present porosities since they can emerge as surface defects known as blisters [4]. The most effective procedure to calculate the gas level of the castings is the vacuum fusion method. By heating a sectioned casted part until molten under vacuum, the pressure created by the gas release is measured [11]. There are several reported procedures to reduce porosity levels such as modifying the alloy constituents, that leads to a higher metal fluidity and therefore an injection speed reduction is possible; optimization of process

parameters such as metal injection velocity, applied casting pressure and molten metal temperature; applying vacuum to the die cavity and the use of other type of injection process such as squeeze casting or any semi-solid process. A viable alternative to reduce the size of gas pores is to set the intensification pressure as high as the machine can deliver. This leads a reduction of the volume percentage of the gas porosity [12].

An optimization of process parameters such as solidification time, molten temperature, die cavity filling time, plunger velocity and pressure is required to manufacture defect free components [13].

Figure 8 presents the typical steps involving the high pressure die casting process.

1. The cycle starts by closing the two die halves and injecting the liquid metal into the die cavity by the plunger (piston). Depending on the alloy, molten metal is injected into the steel die cavity with velocities between 30 m/s and 90 m/s;
2. The closed die is held under high compacting pressures until the material is solidified;
3. The die open's through the parting line and the part is extracted, either manually or automatically, by the ejector pins;
4. A blow stub cleans and cool's down the die cavity surface and lubricant is applied;
5. The die is closed by moving the clamping system and a new cycle starts [6].

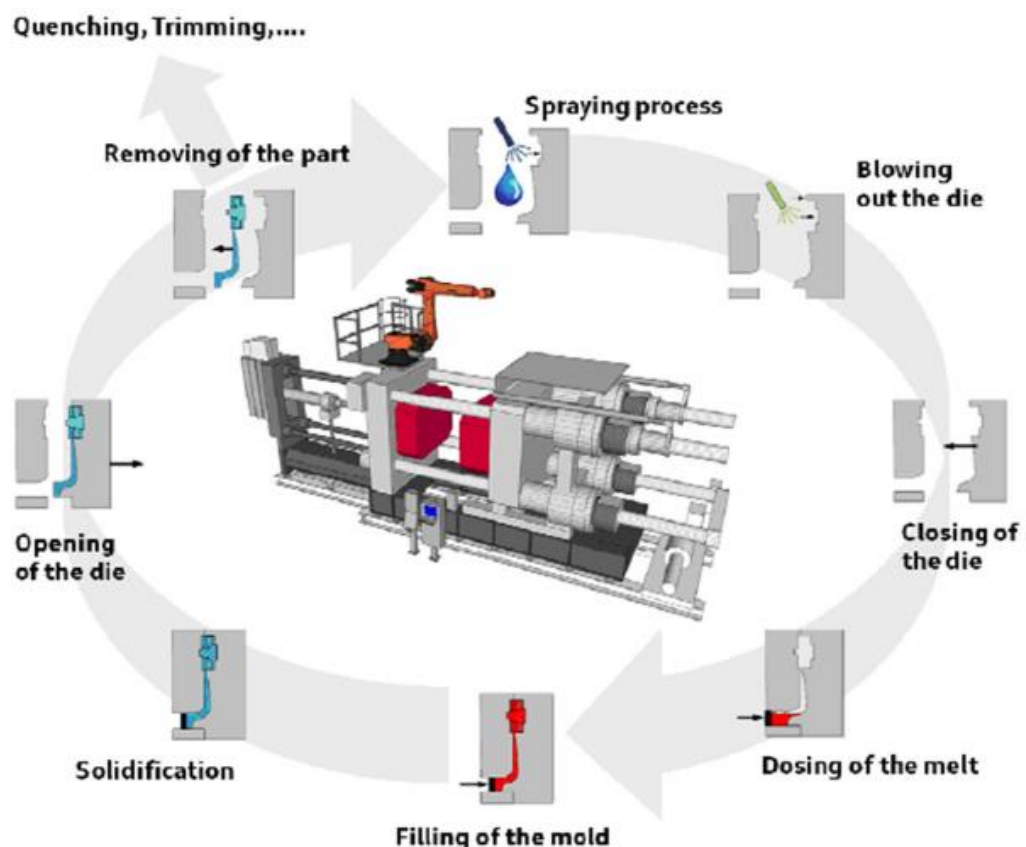


Figure 8- High pressure die casting process [2].

These steps translate the reality of the HPDC process in general, but there are two conventional varieties which depends on the alloy to be casted and differs from each other with respect of the metal injection design [4]. Alloys with low melting points, such as some zinc alloys and tin,

are cast using a hot chamber machine while a cold chamber machine is used to cast high melting points such as aluminum, some zinc alloys, brass. Magnesium alloys are also used in HPDC process and are cast in either hot and cold chamber machine, which depends on the required part size. Theoretical, alloys with lower melting points can be cast in the cold chamber machine but the other way around is not possible.

In the cold chamber machine (Figure 9), liquid metal is poured, manually or automatically, into a pouring hole located in a shot sleeve. This results in a short contact time between the molten liquid and machine components, that otherwise would damage them due to high metal melting point and the fact that aluminum aggressively attacks iron components. After the liquid metal is poured, the hydraulic plunger is displaced through the shot sleeve forcing the liquid metal into the die cavity. With a cold chamber machine, it's possible to produce larger and heavier parts, due to higher machine injection pressures and locking forces. A component produced by this process can be easily identified, since after solidification the component has a “biscuit” where the metal entered the die cavity, Figure 9. right [4].

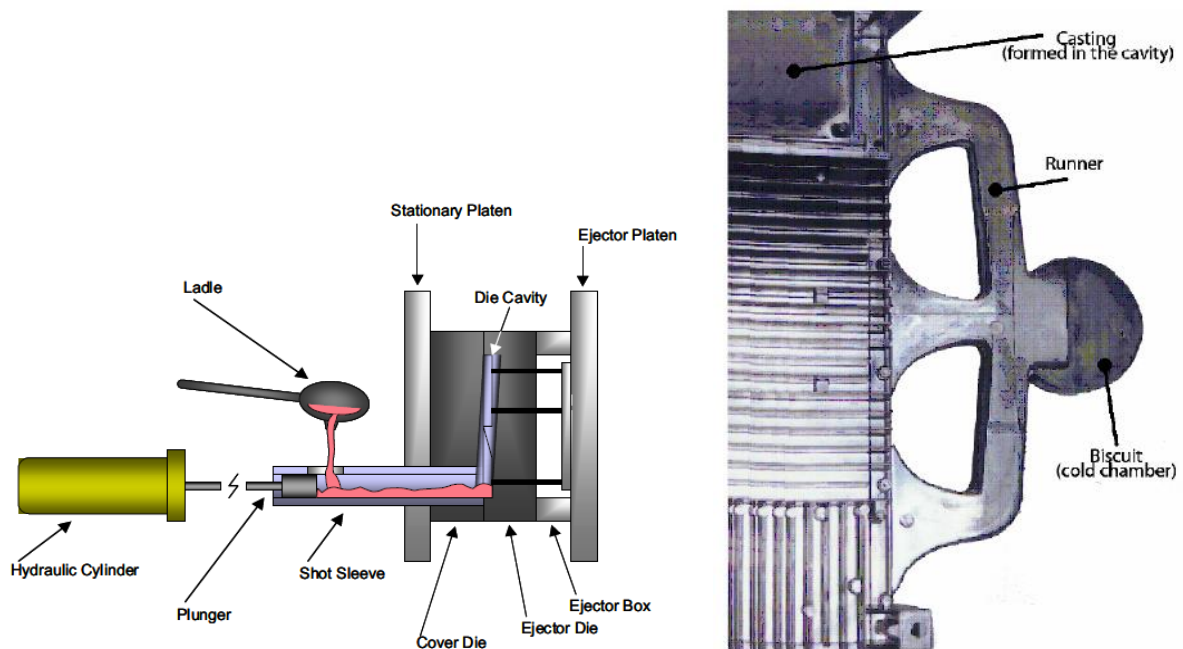


Figure 9- Left: Schematics of a conventional HPDC cold chamber machine [14]; Right: Typical layout of a component produced by a cold chamber machine [15].

### 2.2.3 Most common defects

There are nine different reported subclasses of defects and more than thirty specific types of defects that can be surface, internal or geometrical related. Figure 10 presents a resume of common defects with respect to their sources. Each defect is characterized by its morphology and origin and in some cases can be predicted using simulation tools [16]. Defects such as shrinkage, gas-related and filling-related are the most frequent in the HPDC process totalizing 20 %, 15 % and 35 % respectively [2], with porosity being the main defect, which can be gas porosity, shrinkage porosity or leaker [9]. Table 1 briefly describes some frequent defects, its causes and possible solutions.



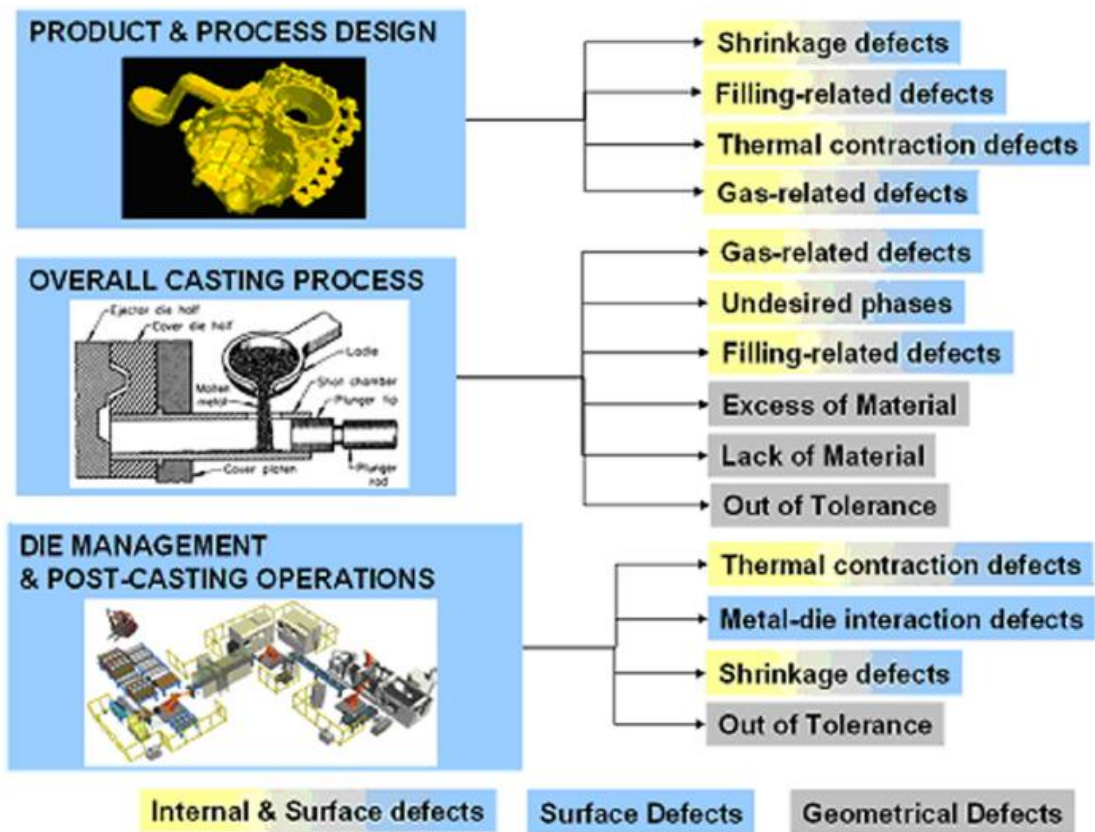
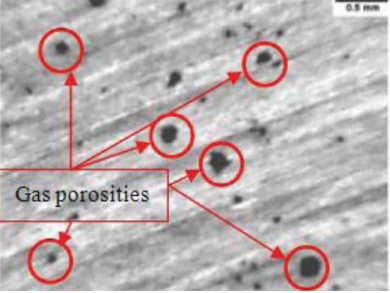
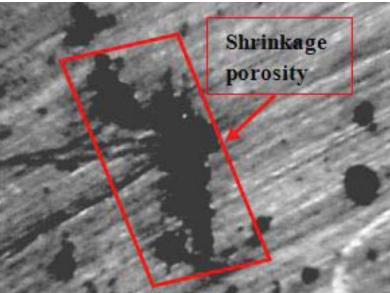




Figure 10- Classification of defects and their origins [16].

Table 1- Defects in HPDC [9; 17-21].

Defects	Causes	Possible solutions	Appearance
<b>Surface defects</b>  Cold flow, cold lap, chill, swirls	Leading edge of metal flow is too cold.	Increase local die temperature;  Lower filling time;  Improve filling pattern;  Increasing local die temperature.	
<b>Lamination</b> layers of metal inside or outside the casting	Poor metal flow control;  Poor die locking during filling.	Correct injection parameters;  Good flow pattern;  Ideal idea temperature.	

<b>Gas Porosity</b>	Air entrapment in the casting	Optimal Injection parameters; Higher venting and overflow function; Optimal gating and runner design; Vacuum.	
<b>Shrinkage Porosity</b>  Internal cracks in the casting	Thick walls in the casting;  Metal volume reduction during solidification;  Inability to feed shrinkage with more metal during solidification;  Hot spots	Cool hot spots or heat cold spots;  Higher intensification pressure;  Better filling patterns, especially on thicker zones.	
<b>Blister</b>	Gas entrapped under the surface during metal filling	Optimal injection parameters;  Optimized gating system;  Higher venting efficiency.	
<b>Flash</b>  Solidified molten metal around the die parting line	Insufficient machines locking force;  High metal liquid temperature;  Poor die fit.	Efficient die fitting;  Adequate machine locking force;  Better die and casting thermal conditions.	

## 2.3 Hot chamber machine

Zamak alloys are the most commonly used for a hot chamber machine. Others zinc alloys such as ZA8, AcuZink 5 and 10, EZAK™ are also used. Some magnesium alloys are used even though there're mostly used on a cold chamber machine.

Molten metal held in a steel holding pot, protected by a specific atmosphere, is injected with a plunger into a die cavity through a nozzle. The nozzle is connected with a channel, called the gooseneck which is immersed in the molten metal [14]. By keeping the gooseneck immersed, cycle times are kept at minimum since molten metal travels a short distance in each cycle [4].

Hot chamber machines are characterized by having very low filling times, 5 to 40 ms, and low cycles times. Parts with a few grams translates into a cycle time of about 1 s while parts with several kilograms can take around 30 s [4]. Figure 11 and 12 illustrate different components that integrate the hot chamber die casting machine.

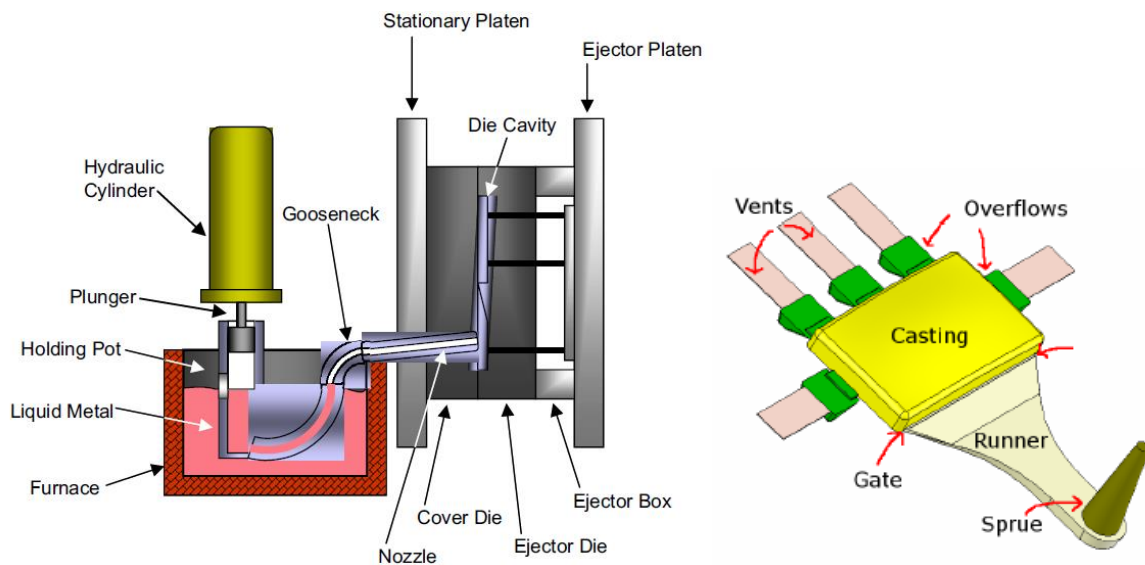


Figure 11- Left: Schematics of a conventional HPDC hot chamber machine [14]; Right: Components produced by a hot chamber machine [22].

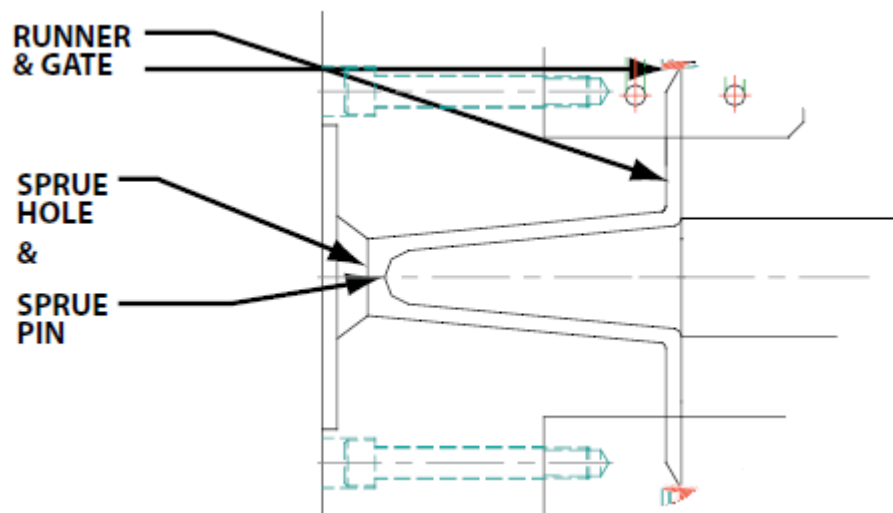


Figure 12- Passage connecting the nozzle to the die cavity of a hot chamber machine [23].

Every die casting machine is characterized by its clamping force. During the cavity fill and specially during the intensification phase, a high pressure is generated inside the die. The clamping force is the force responsible for resisting the opening of the die, and for a hot chamber machine ranges from 20 to 800 Ton.

The pressure built up inside the die generates a force which is proportional to the casting projected area. Considering the casting projected area of Figure 13, the generated force can be calculated by multiplying the projected area,  $1,49 \text{ dm}^2$ , by the intensification pressure, 200 Bar for example, resulting in a breaking force of 298 KN. This would require a machine clamping force of 29.8 Ton, but it is recommended that the actual clamping force should be 25 % higher than the calculated breaking force.



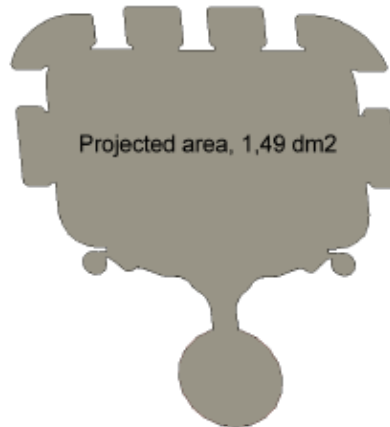


Figure 13- Projected area of casting which includes, die cavity, overflows, gating system, vacuum valves and runners [22].

As shown in Figure 14, this process can be divided into 3 phases, in terms of velocity and pressure. This also happens with a cold chamber machine:

- First phase - Molten metal enters the die through the gooseneck and nozzle, passing the gating system until it reaches the gate. This phase is characterized by a low plunger speed and hydraulic pressure. In some cases, a partial fill of about 10 to 15 % of the components die cavity to reduce gas porosity. This is usually applied for a wall thickness of about 4 mm and thick gates [24];
- Second phase- In this phase, the components die cavity is filled, including overflows. For zinc die casting alloys, typical cavity filling times, can range from 5 to 50 ms. The plunger injection speed increases to its maximum. Also, the hydraulic pressure generated by the plunger increases up until the third phase;
- Third phase - An intensification pressure of 100 to 400 bar is applied to the solidifying pressure. Solidification starts from the surface of the part towards its interior. Due to different solidification rates between the surface and the interior, generally different grained sized structures are formed.

During the entire injection process, the nozzle and the gooseneck is preheated to prevent a premature freezing of the molten metal. It is also kept full with molten metal in the middle of each shot in order which reduces cycle times [14].

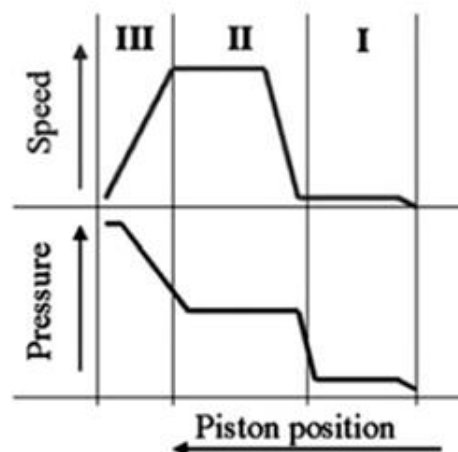


Figure 14- High pressure die casting process phases; representing piston speed and pressure as function of piston position [1].

A hot chamber machine presents the following advantages when compared to a cold chamber machine:

- By limiting the contact of the molten metal to air, the formation of oxides is greatly reduced or eliminated [14];
- Molten metal is kept in a sealed melting crucible until the injection process starts [14];
- Higher production cycles, from 150 per hour for large components and up to 2000 per hour for smaller components [25], due to the inexistent liquid metal ladling process;
- No cooling of the piston tip and the shot sleeve is required [15].

Also, it presents the following disadvantages:

- With low pressures generated by the hot chamber machines, ranging from 5 to 35 MPa, this process is limited to the production of small castings [14; 26];
- Limited to lower melting point alloys. primarily zinc and some magnesium alloys. In the hot chamber process, machine elements such as plunger tip and gooseneck are in constant contact with the molten metal. Higher melting point alloys would cause an excessive wear of these components. Since aluminium alloys aggressively corrodes iron, these alloys are excluded from this process.

### 2.3.1 Zamak alloys

It is believed that zinc started to be die casted in the early 1900's, replacing lead and tin die casting components. When compared to these alloys, zinc is considered a high strength, lightweight and low-cost. In the 60's, ZA (alloys with a wt.% of Al higher than 5) were developed and considered high strength alloys. Twenty years later, GM developed ACuZinc 5 & 10, that presents higher strength, wear performance and creep resistance due to higher wt.% of copper [27].

The two most common challenges concerning the zinc die casting are density (around 7.14 kg/dm<sup>3</sup>) and creep resistance, inherent properties of zinc. The ability to achieve thinner walls with higher fluidity zinc alloys, minimizes the negative impact of the density on the final part weight. To compete with lighter metals, ultra-thin walls and new processing technics are used.

Zamak alloys are a family of alloys, that includes Nr. 2,3,5 and 7, containing zinc, as its main element, and other alloying elements such as aluminium (3.7 - 4.3 %) copper (0.1 - 3.3 %) and magnesium (0.025 - 0.06 %). Other eventual elements are considered as impurities. Since pure zinc is known to be a low strength, low ductility and brittle fracture (due to coarse grains), adding these elements refines the microstructure and improve the strength. Zinc alloys are known for the following characteristics: good corrosion resistance, when plated; good sound damping properties; low melting temperature which translates into energy and cost savings; good castability; good casting dimensional tolerances; good machinability; high density alloy, which is a downside [28]. These alloys are used for several applications fashion and design applications, where an excellent surface quality is required [29]; key fob accessories; antennas; small decorative automotive parts; handles amongst many others. Typical Zamak components are illustrated in Figure 15.



Figure 15- Zamak components ( Courtesy of Dynacast) [30].

Aluminium is the alloying element present in the Zamak alloys, responsible for increasing strength by grain size reduction. Percentages above 4.3 wt.% reduces the impact strength, and below 3.7 wt.% softens the alloy. Intergranular corrosion on the Zamak alloys, exist due to the presence of aluminium and initiated by impurities. A Zinc-Aluminium alloy reaches its maximum castability at 5 wt.% of aluminium, but is extremely brittle [28]. The addition of copper increases the strength and hardness in the Zamak alloys since it allows a higher solubility of aluminium. As a consequence, alloys with higher copper contents are less dimensionally stable and also promotes stress concentrations, reducing the fatigue life and increasing the cracking tendency [31]. Also copper inclusions at the surface promotes galvanic corrosion with zinc and aluminium since these elements possess a more negative potential comparing to copper [32]. Magnesium is added to enhance the alloys corrosion resistance but lowers properties such as castability and elongation [33].

Zinc alloys are rarely used without any post surface treatment, since they are susceptible to corrosion in acidic, strong alkaline and industrial environments. For this reason, surface treatment, such as electroplating, of zinc components is a must to overcome these disadvantages. Also, electroplating zinc components is a very effective process due to their high-quality finishing characteristics [32].

After the component is solidified, the gating system is removed which usually reveals existing internal porosities. If these zones aren't properly sealed before electroplating, defects such as corrosion, blistering and coating delamination can occur [32].

An important pre-treatment step for plating is the grinding process, using abrasive chips, which are represented in Figure 16. Depending on their properties, they can be used for polishing, grinding or smoothing. By subjecting the cast components to ceramic or plastic bonded chips, called a grinding process, the above defects can be minimized without sacrificing too much microns from the material [32]. The plating process must be applied right after the grinding process ends, to avoid any possible contact with any moisture.



Figure 16- Left: Cast components being subjected to a grinding process; Right: abrasive chips [32].

A problem that affects zinc-aluminium alloys is the corrosion-induced cracking, initiated by humid conditions, that can cause swelling of the casting. Corrosion starts at the surface moving inwards, mainly along the  $\beta$  phase boundaries. Being an electrochemical process, it is caused by the presence of impurities such as lead, cadmium and tin and is initiated with the presence of moisture and accelerated with high temperatures [34].

Using high purity zinc along with its alloying elements (99,99 %), is an effective process to avoid the initiation of this problem. Other procedures to enhance the corrosion resistance of zinc-aluminium alloys are: chromium plating and adding a 0.03 wt. % of magnesium in the alloy, that forms a stable compound  $MgZn5$  [28].

Other countermeasure is a coating process based on a colorless polymer with a generic name “Parylene”, offering great resistance to solvents, acids and bases. It also has a low permeability to moisture and are stable up to 200 °C. During the coating process, moisture entrapped in cracks can be effectively pumped away since its applied by vapor condensation in a low-pressure (partial vacuum) environment. The downsides of this process are the high application costs and that it’s a highly specialized process [34].

It has been reported that the addition of small percentages of rare earth elements, transition metals (Ti, Mo and V) and binary alloys (Ti+B) on Zamak alloys can act as grain refiners. These fine structures, with higher grain boundary area, are better protected against the grain dislocation when compared to coarse grain materials. Alloys with finer grains means better mechanical properties (strength, hardness and wear resistance) compared to coarser grains [35].

Adding 0.10 wt. % of Hafnium (hf) to a Zamak 5 alloy has the following effects:

- Transformation of a dendritic structure to a new structure with finer equiaxed grains, presented in Figure 17;



Figure 17- Left: Zamak 5; Right: Zamak 5 + 0.10 wt.% hf. Both allots at 200x magnification [35].

- Increase by 2.5 % on the microhardness, from 99.5 HV to 102 HV;
- Slight enhancement of the yield strength and fracture stresses;
- Wear resistance behavior improvement by 42 %.

A new alloy trade marked as EZAC<sup>TM</sup> developed by Eastern Alloys, is a promising solution to overcome the characteristic creep resistance problem of zinc castings. Besides having the best creep resistance among the hot chamber zinc alloys, it is also the hardest and strongest alloy while maintaining excellent castability. With a low melting point, it can be easily cast in a hot chamber machine, without wearing the shot end components [27].

According to the values of Table 2, EZAC<sup>TM</sup> performs better in terms of mechanical properties when compared to existing alloys, in properties such as UTS (ultimate tensile strength), YS (yield strength) and hardness. In terms of elongation, EZAC<sup>TM</sup> has the lowest performance among all zinc alloys.

Table 2- Mechanical properties [27; 30].

<b>Alloy</b>	<b>UTS (MPa)</b>	<b>Yield Strength (MPa)</b>	<b>Strain (%)</b>	<b>Charpy Impact Strength (N-m)</b>	<b>Hardness (Hv)</b>
<b>EZAC<sup>TM</sup></b>	417	396	1	2,71	68
<b>ACuZinc5</b>	386	386	7	2,71	61
<b>Zamak 2</b>	330	278	4	4,06	57
<b>Zamak 3</b>	283	221	10	-	-
<b>Zamak 5</b>	328	269	7	-	-
<b>Zamak 7</b>	283	221	13	-	-

Table 3 presents the results of creep tests performed at 140 °C and 31 MPa. EZAC<sup>TM</sup> has by far the best creep performance compared to existing alloys, reaching up to 731 hours. This value is fourteen times higher than Zamak 2 and 3 times than ACuZinc5. To successfully perform creep tests, it is important that the tested parts are gas porosity and cold shuts free since their presence negatively affects the creep performance [27].

Table 3- Creep Results [27].

<b>Alloy</b>	<b>Time to Failure (hrs)</b>	<b>Minimum Creep Rate (mm/hr)</b>	<b>Elongation at failure (mm)</b>
<b>ACuZinc 5</b>	212	0.021	6.9
<b>EZAC™</b>	731	0.004	6.7
<b>Zamak 2</b>	52	0.152	9.1

A new high fluidity alloy (HF) was developed during the years of 2005-2014, which offers the possibility to produce parts as thin as 0.25 mm. Higher fluidity in zinc alloys is associated with higher aluminum content, with a maximum at the eutectic point at 5 % Al [36], and lower magnesium and copper content. With the lower percentage of magnesium, a higher control of impurities is required [37].

This alloy also undergoes ageing effects at room temperature in a similar way as the Zamak 3 after the casting is solidified. This happens since the solubility of alloying elements is much higher in the liquid melt than in the primary solid phase [37].

Like conventional hot chamber zinc die casting alloys, the following scenarios also occur on the HF alloy [38]:

- Section thickness has the greatest effect on tensile strength, meaning that lower section thickness translates in a higher tensile strength;
- Parts injected into lower die temperatures have higher tensile strength;
- Process parameters are less pronounced with thicker sections;
- Tensile strength decreases during natural and artificial ageing;
- An increase of the ingate velocity can generally increase the tensile strength.

There are several factors that must be considered during the choice of the most indicated alloy for a component. The capacity to deliver the required mechanical properties is crucial, but also each alloy present different production costs, which must be included during this process.

## 2.4 Die

A die is composed by two halves separated by a parting line. Each half is fastened to its respective platen on the die casting machine: the cover die, which may be machined in the solid die half or inserted, on a stationary platen that doesn't move during the injection cycle; ejector die on a movable platen of the machine. An example of a dies geometry is represented in Figure 18. The die cavity corresponds to the parts geometry and is formed by machining the die halves along with inserts or cores and movable slides. If the process is optimized, no metal should be soldered to the die cavity [39; 40].

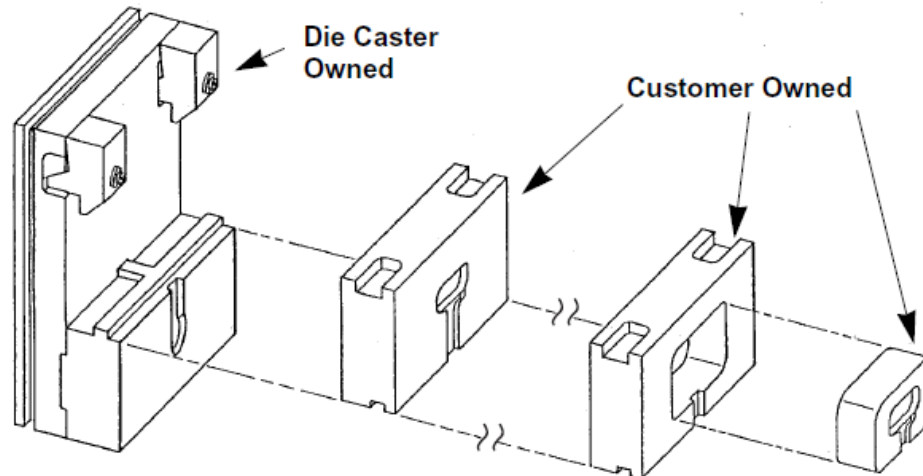


Figure 18- Components of a unit die assembly [23].

Certain aspects such as injection system, casting condition, gating system, cooling system must be considered during the die manufacturing process. This process, in some cases, is a try-and-error method based on a heuristic know-how, which lacks scientific calculation and analysis leading to an incorrect mold design [6; 40].

A CAE simulation technology will minimize incorrect die design, since it helps designers to generate, verify and validate and optimize the design solutions. It can be useful to identify the following situations [6; 41]:

- Possible defects that may occur during the injection process, by giving the possibility to optimize the gating system before manufacturing the mold. Defects such as internal porosity, caused by air entrapment and solidification shrinkage (occurring on thicker sections) can be predicted and reduced;
- Last areas to fill. This will define the location of the overflows, vents and chill vents;
- Areas of excessive heating in thick areas or excessive cooling in thin areas. These hot areas are the last to solidify, leading to shrinkage porosity or heat-shrinks. During the mold manufacturing, it is necessary to implement cooling system in these hot areas to present their related defects;
- Isolated areas, due to poor metal flow. Changing the direction of the flow that enter the ingate can help solving this problem;
- Generation of turbulence duo to fluid collision. This exists when two or more fluids coming from their respective gate/runner collide. Using simulation technics, it's possible to predict these collisions and therefore change the metal flow by optimizing the gating system [42].

Figure 19, represents a flow chart simulation process using ProCAST™ for the HPDC. The flow chart is divided into three stages: pre-processing, problem solving and date output. Generally, a CAD model of the component with its gating system is supplied by the client. After the CAD model is imported into the die casting simulator tool, a fully automatic 3-D tetrahedral mesh generator is called to generate surface mesh, the shell and the volume mesh. Then, the following conditions are defined: assigning materials, defining interface, setting boundary conditions, appointing process and selecting suitable running parameters. After this procedure, FEM calculations takes place, and the results can be visualized by ViewCast module.



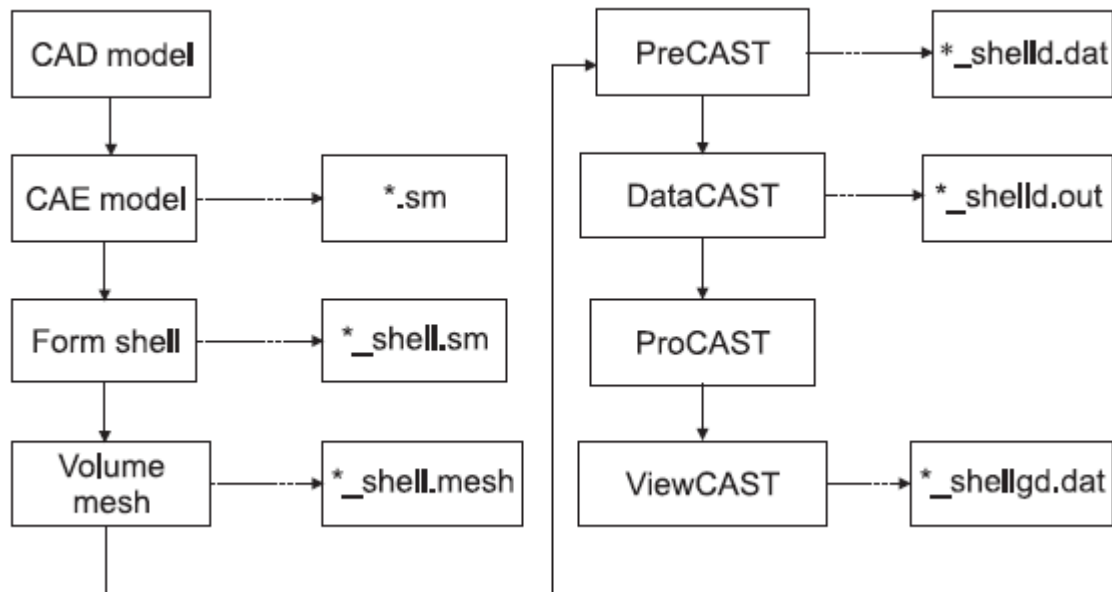


Figure 19- Flow chart of the simulation process based on ProCAST™ [43].

The most common material's to manufacture high pressure die casting molds are either hot work tool steel H11 or H13. The main problem on using these materials is that after the machining process of the die cavity, a heat treatment (quenching and tempering) must be applied, which may result in dimensional deviations [40].

The heat-checking phenomenon represents the most common die failure in high pressure die casting. By controlling parameters such as impact toughness, strength at elevated temperatures and thermal properties, it's possible to minimize the occurrence of this problem [40].

TOOLOX 44 is a pre-hardened tool steel with a hardness of 45 HRC, similar as the commonly used in die casting molds. Table 4 illustrates the composition of a common H13 alloy and the TOOLOX 44. TOOLOX 44 offers better mechanical properties when compared to the currently used such as improved Charpy-V impact toughness at room temperature and at elevated temperatures; better thermal conductivity which benefits the reduction of the heat-checking risk. Another great advantage by using a pre-hardened steel is that the die manufacturing time can be greatly reduced since no heat-treatment is required after machining of the die cavity. The absence of a heat-treatment means that no dimensional instability occurs during a die manufacturing [40].

Table 4- Typical composition for TOOLOX 44 and hot working steel (H13), all elements are given in wt.% [40].

Grade	C	Si	Mn	P	S	Cr	Mo	V
<b>TOOLOX 44</b>	0.32	1.1	0.8	Max 0.01	Max 0.003	1.35	0.8	0.14
<b>H13</b>	0.4	1.05	0.4	Max 0.03	Max 0.03	5.15	1.35	1



Figure 20 is an example of a die casting mold used to inject a Zamak alloy. Manufacturing time was reduced from 300 to 200 hours when the material was replaced from a H13 tool steel for a TOOLOX 44 [40].

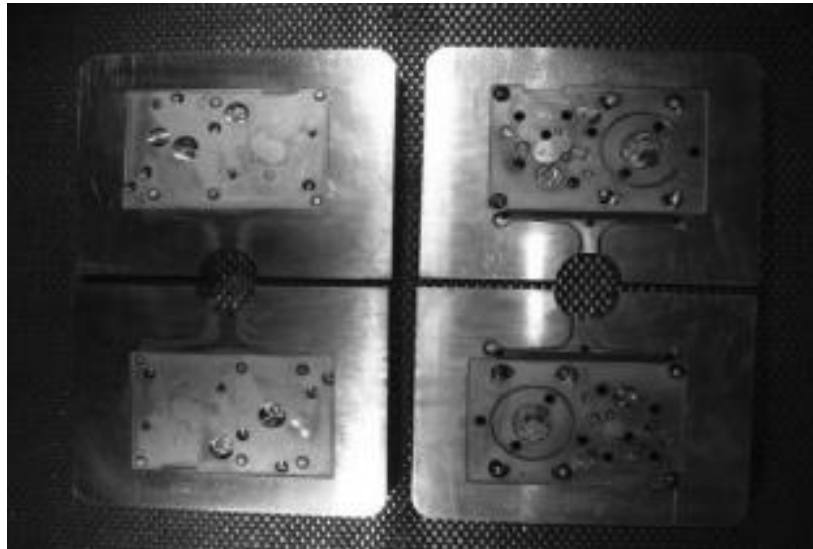


Figure 20- Die casting mold manufactured with TOOLOX 44 to inject Zamak [40].

The die represents a very expensive high pressure die casting component, with prices that can reach up to 100 000 €. Factors that contribute to the highly pricing are: high complexity; the die material which normally is a highly alloyed steel, stable mechanical properties at elevated temperatures; post machining treatments such as quenching, tempering and nitrating; and in some cases, a surface coating can be applied. Also, the surface die cavity must maintain dimensional accuracy and specific roughness during the injection process [44].

The most influential die wear mechanism is thermal fatigue. The die cavity surface suffers great oscillations of temperatures during the injection process. The high temperature variation is propitious of the development of surface cracks due to the constant contraction (during heating) and expansion (during cooling) of the die. Also, the die cavity surface must be resistant to erosion caused by high molten metal injection speed (up to 60 m/s) and process pressures that reach 120 MPa [44].

A lubricant is normally based on graphite, molybdenum disulphide or hexagonal boron nitride dispersed in a water solution. When applied to the die surface, acts as a physical barrier between the casting alloy and the die. Intermetallic compounds can appear where the lubricant is absent, especially in slower cooling areas and where the die has been repaired by welding [44].

Due to the high price of a die manufacturing, repairing is an option to prolong its life span and to quickly resume production. Dies can be repaired by welding, but this procedure is quite complex and difficult to apply. It can cost up to 10 % of the initial die cost and can be done more than once. A constant monitoring of the die surface is important to avoid part rejection. There are several die repairing processes with different characteristics such as [44]:

- TIG (tungsten inert gas welding) is the most common die repairing process since it gives the operator good control over the welding process. During this procedure, several problems can occur like distortion of thin parts, welding undercuts, oxidation, porosities and cracks;
- The laser beam welding (LBW) is an alternative process to TIG, which offers higher energy density, very narrow heat affected zone (HAZ), minimal post machining process

and has proved to double the life span of a die. This process has some limitations in terms of low productivity, expensive equipment and materials and highly qualified welders. Also, delivers the best results when repairing TIG weld undercuts;

- Plasma spraying method, metallization, can also be applied to repair dies. It offers lower mechanical properties than achieved by welding and this kind of coating has a low durability;
- The electro-spark deposition (ESD) is a coating process that uses a pulsed-arc micro welding that can be used on hard metals. The coats are fused to the surface with a low energy input that allows the base material to main an ambient temperature, eliminating the possible die distortion. Many studies conducted on a H13 alloy using this process proved that it has good resistance to wear mechanisms.

#### 2.4.1 Water-soluble salt cores

Since high pressure die casting is ideal to produce highly complex shapes, cores are very useful to produce features that cannot or are very difficult to be formed by two die halves. Currently most of these cores are manufactured with the same die material or with copper/beryllium alloy. The problem is that in very complex castings, removing them from areas that are hardly accessible for mechanical cleaning is very difficult [45].

Currently a good alternative to metal cores are disposable water-soluble salt cores [46], due to their high strength and surface quality. Figure 21 represents the application of a salt core to produce a cavity in a component. Also, they are easily removed by dissolution i.e. in hot water. These salt-cores require great impact resistance, since the density of zinc die casting alloys is about 2.5 times higher than aluminum alloys [45].

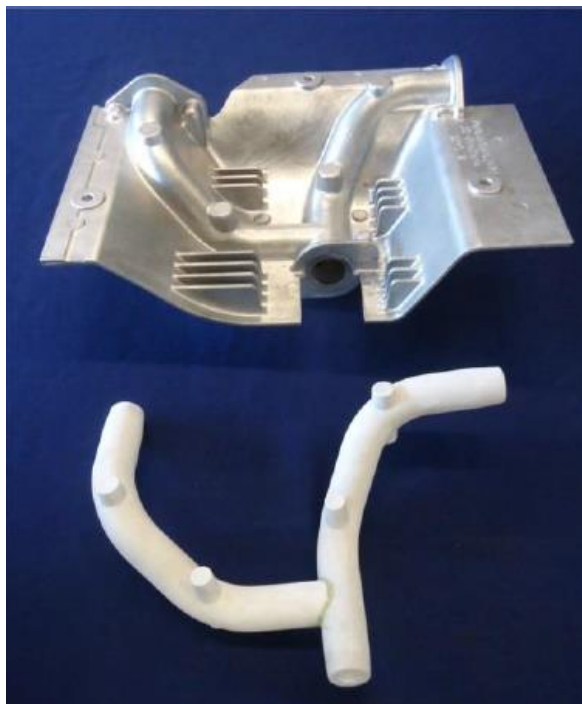


Figure 21- Salt core and die casting with cavity [47].

Cores can be manufactured by three processes: high-pressure squeezing; shooting (binder alkali silicate) and casting of molten salts with post pressing. The process that offers the best combination of advantages is the high-pressure squeezing. Cores manufactured with this process present better strength, and lower porosity levels when compared with other processes. The core porosity levels are particularly important for the high pressure die casting since it will affect the penetration of the molten metal into the cores. There're limited to simpler shapes since they present a low solubility in water and have a non-uniform degree of compaction, one-way pressing. Special thermal treatments can be applied to prevent the core destruction generated by residual stress [45; 48; 49].

Many cases of precast holes of complex shapes require gluing of cores in two ways: cores-cores and cores-metal. These bonds must guarantee: sufficient strength under elevated temperature; dimensional accuracy and easy removal of the cores during their dissolution. Currently, the available glues can deliver a range of shear strength of the core joints with salt-salt within 63 - 105 N/cm<sup>2</sup> (0.63 - 1.05 MPa) and salt-metal within 160 - 232 N/cm<sup>2</sup> (1.6 - 2.2 MPa) [45; 48].

For zinc high pressure die casting with a die temperature ranging from 125 - 150 °C, a salt A-KCl system is a suitable choice. It has the highest tensile strength among the system salt cores used in HPDC and has a melting point around 340 °C. Other major advantage comparing to other salt systems, is that it has no adverse effects on the surface of the zinc alloy casting during the core dissolution. By using ceramic and whiskers as reinforcing particles, it is possible to increase the mechanical strength, improve surface quality and reduce defects such as deformation, shrinkage and cracks. It was studied that the optimal composition for the reinforced salt cores was: 70 wt.% salts (92 wt.% of salt A, remaining 8 % of KCl) and 30 % of reinforcing particles (100 % of a layered material or a mixture of layered material with an acicular material with a 1:1 ratio. These “triplet” systems deliver 30 - 32 MPa of bending strength, can be recycled without a high decrease of bending strength and have good aging resistance. An example of a “triplet” system core inserted into a die cavity is represented in Figure 22 [45].



Figure 22- Left- “Triplet” salt core inserted in the die cavity; Right- Injected part of a zinc alloy [45].

Other water-soluble combinations using salt cores with reinforcing particles, such as 15 wt.% of bauxite powders with 15 wt.% glass fibers or 15 wt.% bauxite powders with 15 wt.% sericite powders (which is a type of mica), were tested. These combinations resulted in a bending

strength over 45 MPa. The first combination was used to cast a zinc alloy and resulted in a casting with a very smooth surface and was easily removed, presented in Figure 23 [50].

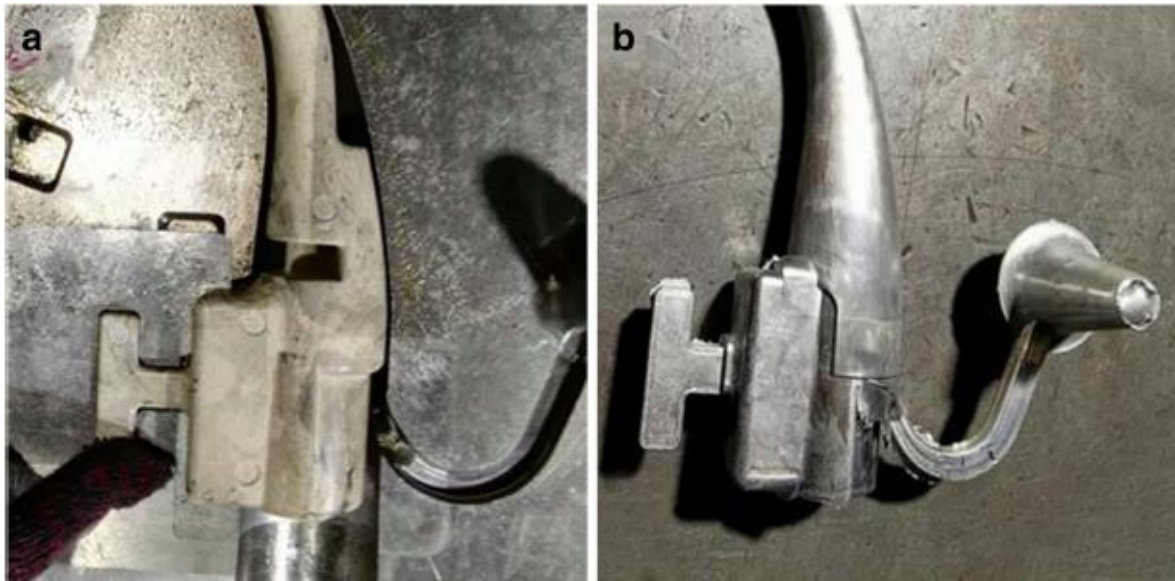


Figure 23- Water soluble salt core with bauxite powders and glass fibres for a zinc alloy casting [50].

#### 2.4.2 Lubricant

Results from a previous study [51] proves that a die and its cooling channels are responsible for absorbing about 80 % of the heat coming from the molten metal, 5 % is exchanged with the environment while the remaining 15 % is absorbed by the lubricant [52].

A lubricant is used in a die cavity for several reasons such as cooling the die, ensuring a temperature uniformity on the cavity surface; acting as a releasing agent for the casting, to prevent soldering and deformation; allows a correct cavity filling preventing surface laminations [52].

With an optimization of the lubricant process, it is possible to increase the lubricant absorption up to 50 % plus and additional overall cycle time reduction [52].

During the application of the lubricant in the die cavity, a layer of active parts is created and the water present in the solution is evaporated, cooling down the surface. A common problem that occurs during the injection of the molten metal, is a pyrolysis reaction, resulting in the blackening of the die surface. This happens due to the high die temperature and absence of oxygen that generates gases. The formed layer, normally lower than 10  $\mu\text{m}$ , should be consumed and restored during each casting to prevent the increase of die cavity surface thickness and to prevent machine downtime [52-54].

Figure 24 presents a clear example on how the application of lubricant influences the uniformity of the die temperature. The right image clearly shows a non-uniform distribution of the die surface temperature, which leads to local overheating. In addition to expected several surface or geometrical defects, the die will be subjected to aggressive thermal shocks [52].



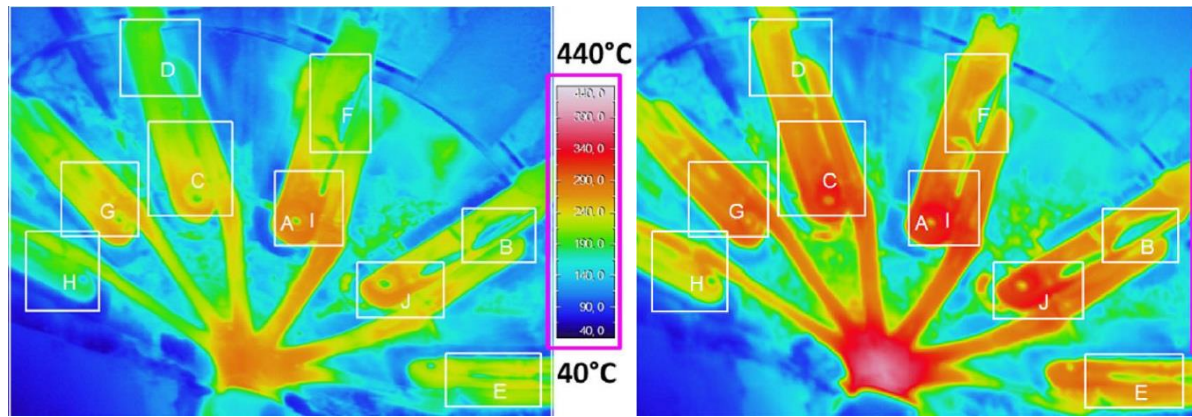


Figure 24- Thermal images of the die after spraying (left) with an average surface temperature of 180 °C, and before spraying (right) [52].

During the casting process, the die temperature should be monitored and controlled since it will affect the effectiveness of the lubricant. There's an optimal die temperature range, which depends on the metal to inject, to guarantee the quality of the casting. If the die temperature is below the range limit, the water in the lubricant solution may not evaporate, resulting in a low heat flux. Other consequences may appear such as the die goes through a violent thermal shock in contact with the molten metal; early solidification of the molten metal which leads to an incomplete filling of the die cavity; residual lubricant that can generate porosities. There's also consequences when the die temperature is above the optimal range. In this case, the lubricant may not be able to wet the die cavity surface due to the Leidenfrost effect. This happens when a liquid enters in contact with a solid with a temperature far superior of the liquids boiling point. This results in a layer of vapor that keeps the liquid from evaporating rapidly. If the heat flux is too low, the die can be subjected to soldering and thermal fatigue leading to scrap castings [52].

There's several defects related to an inefficient use of the lubricant such as pultrusion's due to surface lamination and soldering; and geometrical deformation.

Lamination is a surface defect, visible as protrusions and a thin metallic skin separated from the surface, that can also generate porosities due to air entrapment. Originated due to cold dies or when the injected molten metal solidifies with a higher cooling rate than its surroundings, causing premature solidification of the molten metal. This type of defect belongs to a filling-related defect and are represented in Figure 25 [52].

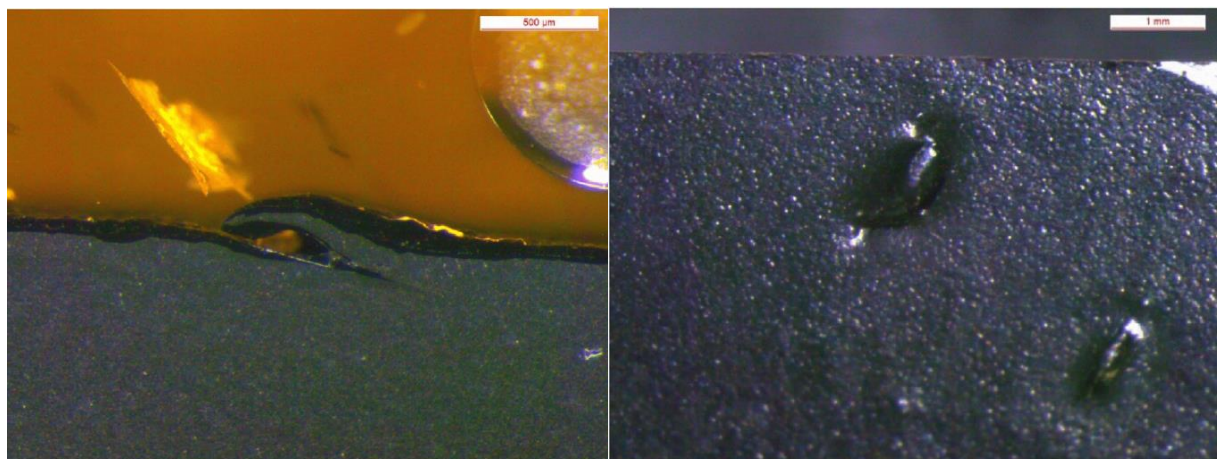


Figure 25- Protrusions related to lamination. Left: magnified 25 x; Right: magnified 10 x [52].

Deformation defect can be understood as when the casting part doesn't have the exact geometry, due to thermal contraction and soldering during solidification. Insufficient lubricant in the critical regions, internal stresses due to shrinkage of the casting and the geometry of the internal die cooling are the reasons why this type of defect appear. An example of this defect is represented in Figure 26 [52].



Figure 26- Deformation present on a manufactured part [52].

Soldering is a die/molten metal type of defect, characterized by the presence of intermetallic phases on the die caused by and ineffective layer of lubricant or a long overall cycle time. This defect compromises the surface quality, creating roughness (represented in Figure 27) or localized lacks of material normally identified through visual inspection [52].

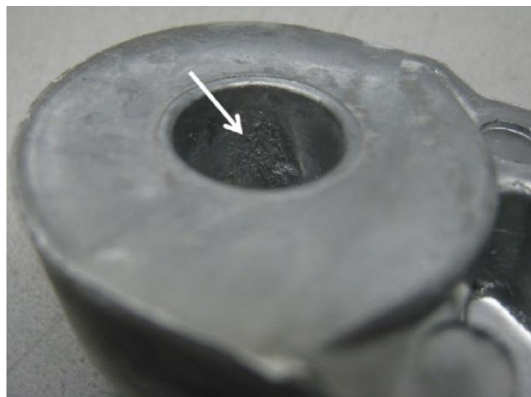


Figure 27- Surface roughness due to soldering [52].

## 2.5 Hollow structures

As mentioned before, using water-soluble salt cores instead of metal cores is feasible to produce three-dimensional hollow structures. These cores are then easily removed from the solidified part, with hot water for example [10].

A novel reported alternative to produce three-dimensional hollow structures and ribs is by using the gas injection technology, originally used in injection moulding of thermoplastics [55]. Up until 2014, this process was only used to cast zinc alloys on a cold chamber machine [56-58]. Posteriorly, this technology was successfully implemented on a hot chamber machine using a magnesium alloy [10].

With this technology, functional cavities are produced within the part by injecting high pressure nitrogen, flowing on predetermined gas channels that have been machined into the mould. The

gas injection happens immediately after the mould cavity is 100 % filled with liquid metal and the outer shell has solidified [58], resulting in a liquid metal displacement into an overflow cavity. Typical gas injection pressure can range from 20 to 50 bar with a maximum of 200 bar [10]. Examples of components with functional cavities produced by HPDC using the injection gas technology is represented in Figure 28.



Figure 28- Examples of components using the gas injection technology using a cold chamber [10].

This technology in the HPDC offers the following possibilities: production of parts with functional cavities which would be highly difficult or expensive using conventional metal cores; material loss reduction; high pressure-tightness of the castings; cost-efficient large series production; production of extremely low-weight parts; development of innovative HPDC parts like media-carrying pipes and low weight door handles made of zinc. Figure 29 represents two possible components that could be produced using this process [10].



Figure 29- Possible applications for gas injection technology in the high pressure die casting technology. Left: intake manifolds; Right: Hollow structures in clutch pedals [57].

There's several attributes of the original process, used for thermoplastics, when transferred to the high pressure die casting can cause major problems such as [10]:

- Increased wear on the steel injector. This happens since the original process deals with a melt temperature ranging, which a Polyamide 66, from 300 to 320 °C, and in high pressure die casting from 420 to 700 °C. Therefore, a new injector that can withstand uninterrupted service have to be developed. This problem is even worse when applied to aluminium since aluminium aggressively attacks iron;
- Gas injection must be faster, with valve switching times as low as a few milliseconds. Plastics are characterized by being a low thermal conductive material, which means that the gas injection can take place rather slowly. The same process in the HPDC must take place 10 times faster since metals transfer heat faster leading to a higher solidification rate, or a lower period available until the melt reaches a temperature at which the material cannot flow anymore. This leads to the necessity of a higher and more accurate process control and fast-acting gas flow control with shorter delay times;
- Incorrect/inefficient gas penetration. Premature solidification of the melt which results in an insufficient gas penetration;
- High process instability between the individual cycles;
- Clogging if the gas supply is delayed;
- A foamed zone on the casting near the gas injector is formed, due to turbulence resulting occurring during gas injection;
- The injected gas entering the hot chamber machine filled with liquid metal, via the nozzle and the shot sleeve. Therefore, the hot chamber machine must be linked to the gas injector plant and its control system to prevent this problem to occur, represented in Figure 30. With a safety vault, it's possible to release the nitrogen to the atmosphere in case of a malfunction of the gas valve.

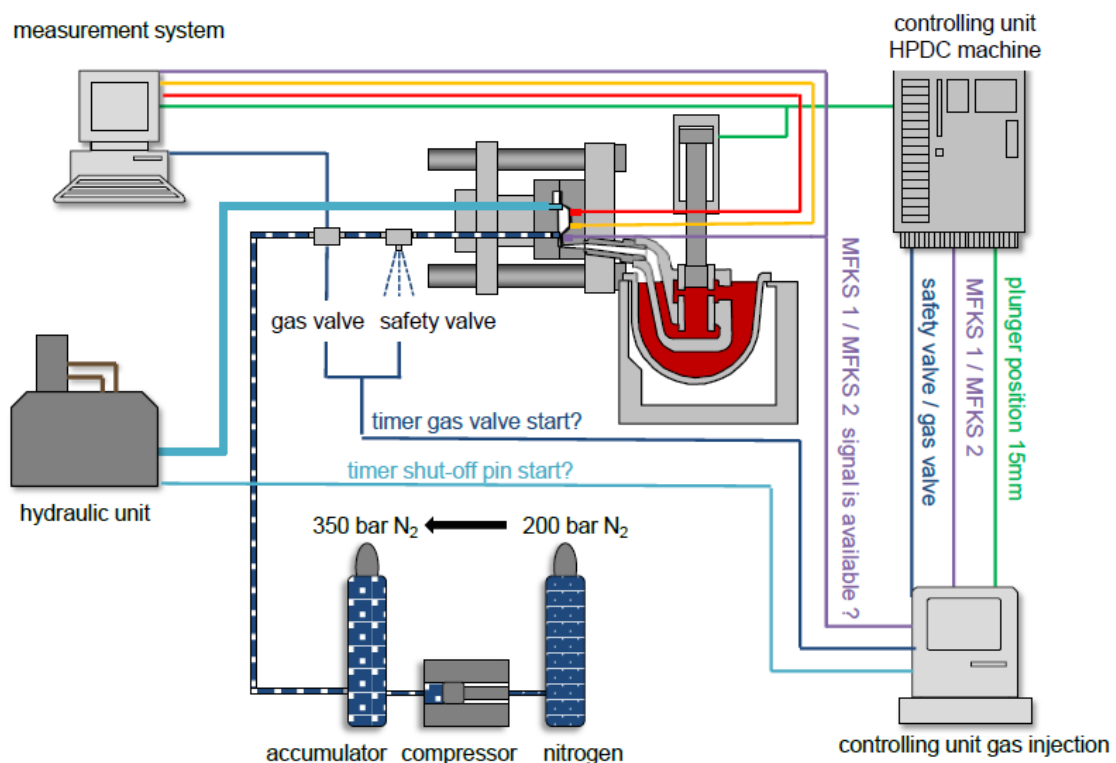
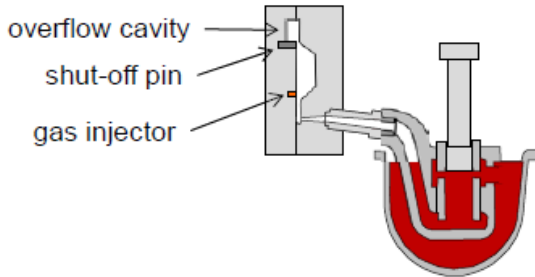


Figure 30- Control-related of the die casting machine and the gas unit [10].



As shown in Figure 31, the gas injection technology doesn't affect the home position and filling phase of a normal hot chamber process. This process requires additional components such as a gas injector, shut-off pin and an overflow cavity. During the filling phase, the cavity overflow is disconnected from the main cavity by a shut-off pin [10].

**Step 1: dosing / home position**



**Step 2: filling phase**

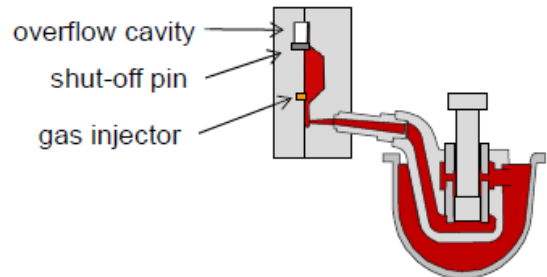
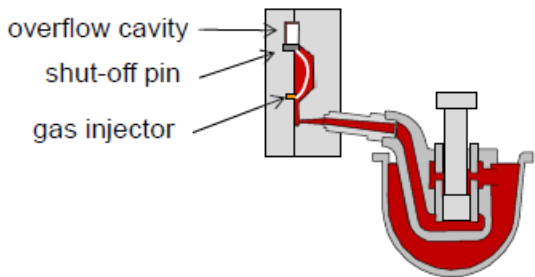


Figure 31- Home position and filling phase [10].

Figure 32 represents the last two steps on the high pressure die casting process moulded by the gas injection technology. As soon as the filling phase ends, high pressure nitrogen is introduced by the gas injector resulting in a liquid metal displacement into the now open overflow cavity. After the cast part is totally solidified, the gas pressure is released through the same place it was introduced [57].

**Step 3: gasinjection**



**Step 4: opening the overflow cavity**

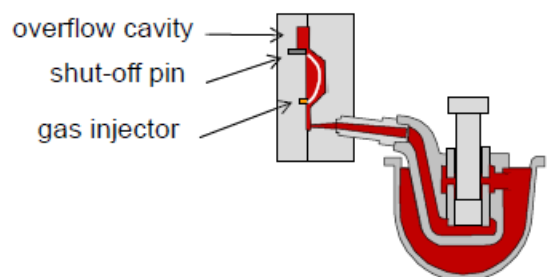


Figure 32- Gas injection and opening of the cavity overflow [10].

Figure 33 illustrates various process parameters during the injection process using the gas injection technology. Besides the typical HPDC process parameters such as plunger velocity, die temperature and internal pressure, the gas pressure is also displayed. The gas is injected into the die cavity after the intensification pressure phase. This leads to a higher compensation of shrinkage and pressure tightness of the cast component.

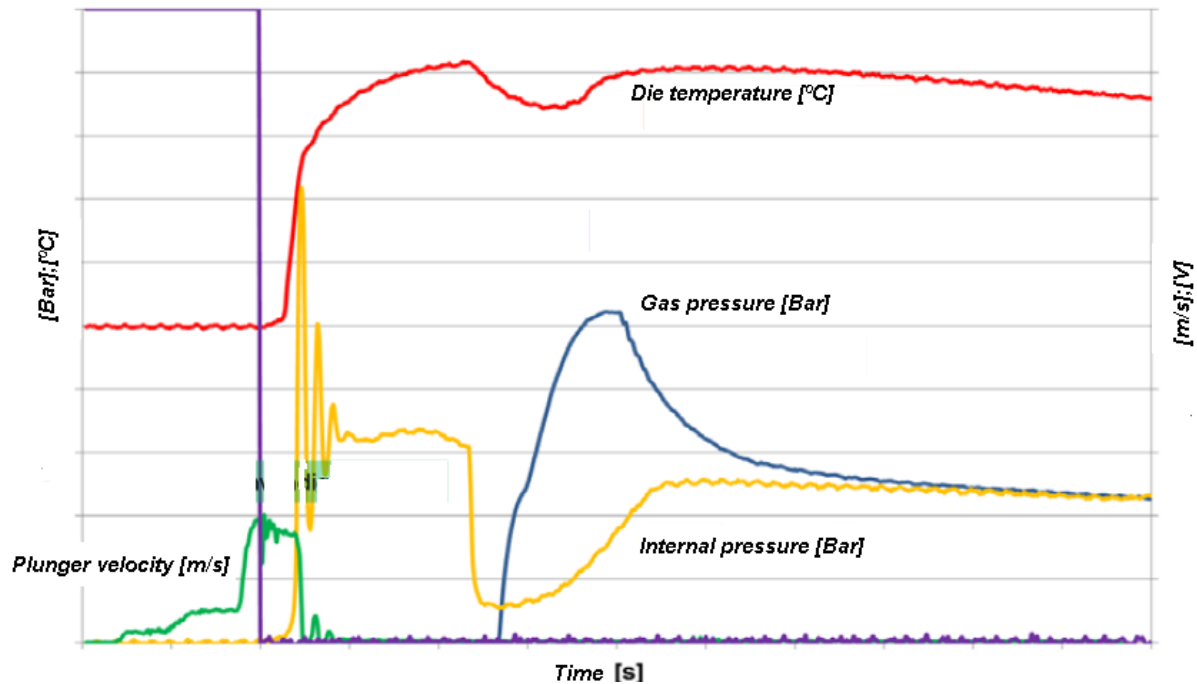


Figure 33- Shot curve with different process parameters [10].

Recent studies [57; 58] demonstrate how critical is the optimization of the gating system. It was proven that the location of the ingate contributes to the effectiveness using the gas injection process in the HPDC. As shown in Figure 34.a, the zone opposite to the gas injector is filled first and therefore is the first zone to cool down. In this situation, the gas won't be able to penetrate the solidifying casting since it has already solidified. An optimized solution presented in Figure 34.b, results in the top part solidifying last and therefore the gas correctly penetrates the solidifying part.

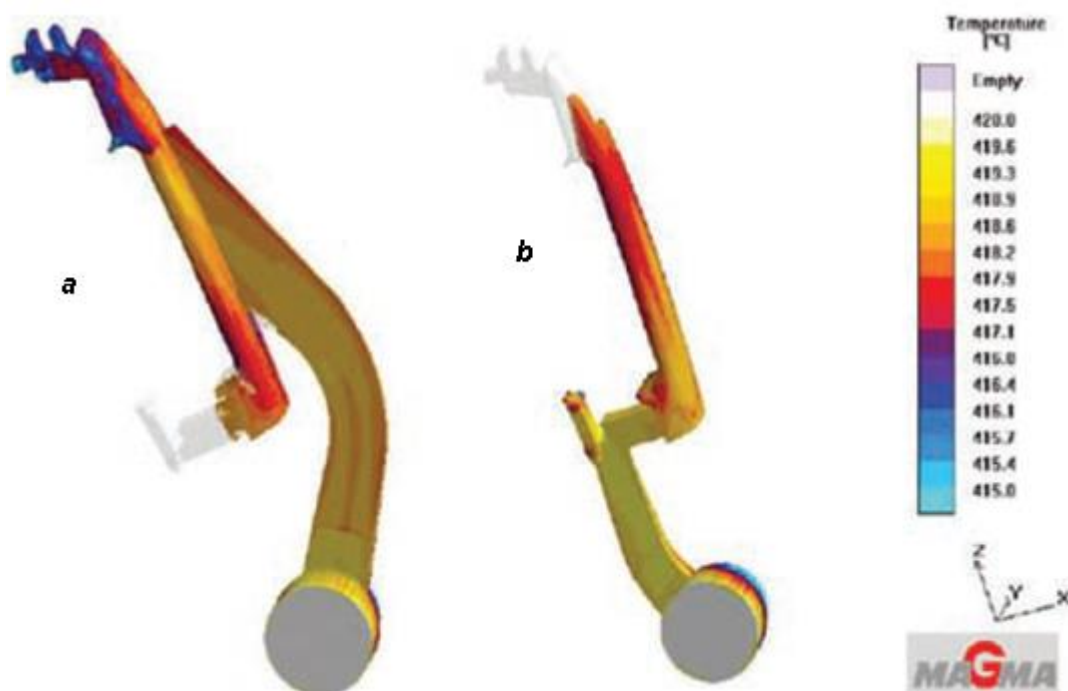


Figure 34- Simulation of die fill indicating cold metal near the gas injector for Gating [57].

Figure 35 presents the layout of a high pressure die casting tool for a 200 ton cold chamber machine used for the first gas injection in HPDC experiments. The required additional components can be clearly seen, and the two different gating systems used [57].



Figure 35- Pressure die casting tool for gas injection and a 200 ton cold chamber casting machine. 1- Overflow Cavity; 2- Locking Pin; 3-Injector; 4- runner; 5-Runner 2 [57].

The first successful high pressure die casted part moulded with the gas injection process was a zinc alloy, represented in Figure 36. In this case a cold chamber machine was used with the tool mentioned above. It was possible to produce a component with a smooth surface of the cavity. The characteristic problem of this process, which is a foamed zone near the gas injector, can also be clearly identified [58].



Figure 36- Zinc high pressure die casting with a cavity completely produced by gas injection [58].

## 2.6 Hot chamber semi-solid casting process

As mentioned before, the main problem affecting the HPDC process are porosity related defects. It becomes more serious for walls with thicknesses above 2.5 mm, whereas for thin-wall sections,  $< 2.5$  mm, with fine-grained and pore-free skins it becomes less relevant. Changing the original process may be beneficial to produce castings with less porosity, which enables post heat treatment, and better mechanical properties. This may reduce productivity along with higher costs. Their called high integrity die casting processes and are divided into: vacuum die casting, squeeze casting; semi-solid casting and novel partial squeeze and vacuum die casting process [59]. Even though these processes have different denominations, they use the same principles of the high pressure die casting process [14].

With squeeze casting, liquid metal is fed vertically into the die cavity with a speed of about 0.4 m/s after being poured into the injection sleeve. After the cavity is 100 % filled, an intensification pressure ranging from 490 to 1079 Bar is applied.

In the semi-solid die casting (SSC) process, a partially solidified metal, 30 to 60 %, is injected into a die cavity, producing castings with a refined globular microstructure. During the die cavity filling, due to a higher viscosity of the metal, a progressive flow front is generated. This results in a reduction of inclusions, oxidations, air entrapments and shrinkage when compared to the turbulent flow generated in the conventional HPDC process. These differences are highlighted in Figure 37. More importantly, due to a laminar flow, generation of air entrapments during the filling is greatly reduced. Components produced with this process, have enhanced ductility, toughness; strength; high dimensional stability and are near net-shape. Despite these numerous advantages, components manufactured by SSC are too expensive for highly competitive industries, such as the automotive industry [60; 61].

There are two different semi-solid processes, the thixo-forming and rheo-die casting process. The main difference between these two processes is the preparation process of the solid-liquid mixture before the injection process begins. In the thixo-forming process, a billet is prepared by solidifying an alloy by stirring, which is preheated later to form a solid-liquid mixture. This billet preparation is highly costly to make. In the rheo-die casting process, no billet preparation is needed. Instead, the desired solid-liquid mixture is achieved before the injection process, by pouring liquid alloy into the injection sleeve equipped with an electromagnetic stirrer [60; 61].

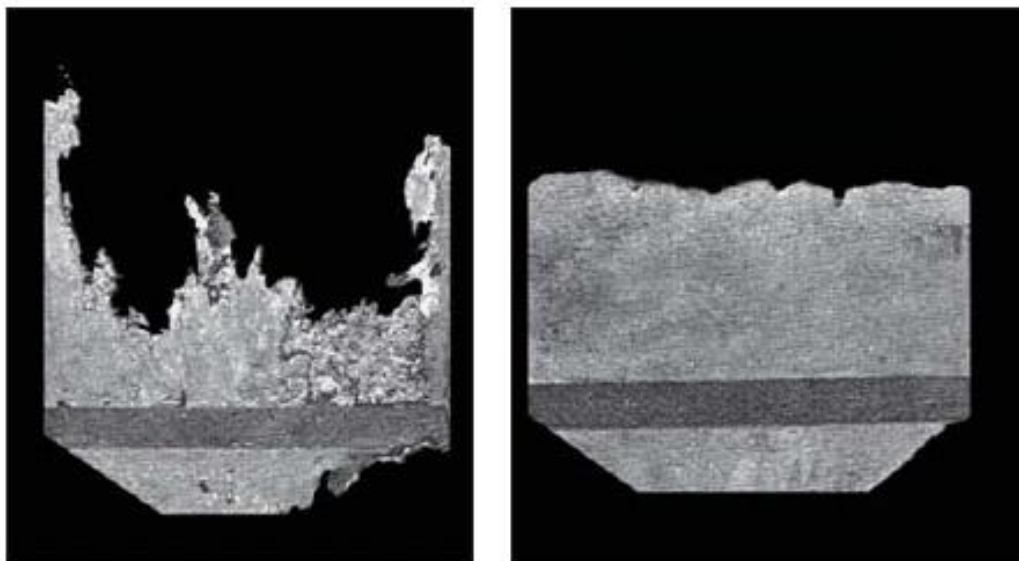


Figure 37- Left: Non plana filling; Right: planar filing [60].

One alternative to overcome the highly turbulent metal flow of the hot chamber HPDC process, is a novel variant of a semi-solid process (S2P), the hot chamber rheo-diecasting process [62].

This process was successfully implemented on a hot chamber machine to inject a AZ91D magnesium alloy. It requires no additional processing equipment, no molten metal control and no additional cycling time. It offers the following advantages such as reduced or absence of porosity, lower cycle times, lower processing temperatures and longer life. Apart from a traditional hot-chamber machine, this process only requires the addition of a magnetic field around the nozzle as observed in Figure 38 [62].

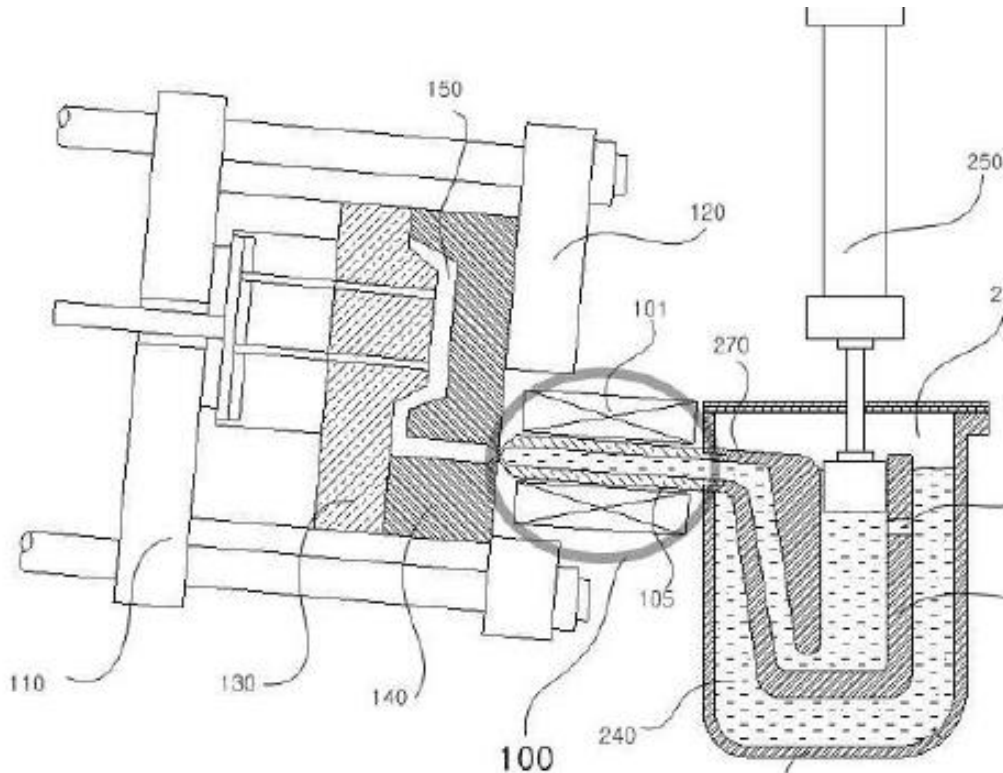


Figure 38- Hot chamber rheo-diecasting machine. The circle indicates de magnetic field around the nozzle [62].

As shown in Figure 39, the as cast microstructure is improved comparing to a conventional high pressure die casting pressure. Fine globular solid particles, that were uniformly distributed, replaced a dendritic structure, typically produced by the conventional die casting process. This evidences the fact that a lamellar filling of the slurry flow is achieved by this process, resulting in an absence of gas porosity [62].



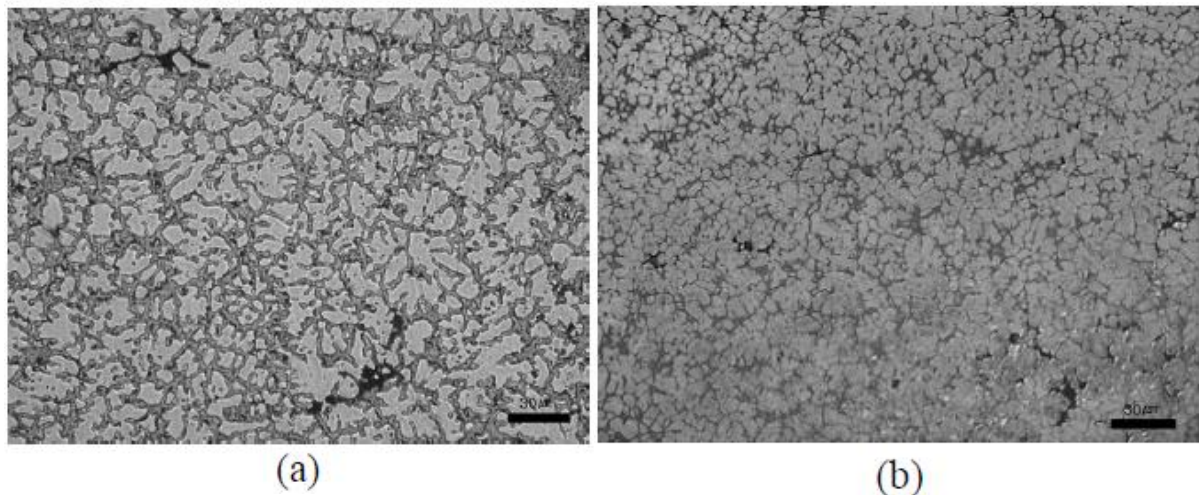


Figure 39- Microstructure of a magnesium alloy, AZ91D. Left: conventional high pressure die casting, Right: hot chamber rheo-die casting [62].

A similar study on a Zamak alloy would be interesting to analyze these effects on a different alloy using a hot chamber machine.

## 2.7 Heat treatments

Heat treatments are usually applied to HPDC die casting to enhance the components tensile properties [63]. There are also highly appreciated for the production of aluminum and magnesium structural components. These components are characterized by requiring exceptional mechanical properties and a rigorous control of defects.

The success for applying a heat treatment to a HPDC component highly depends on the porosity levels of the casting. Porosity levels are minimized by optimizing process parameters, the gating system and by using the vacuum die casting process [64]. Each heat treatment has different negative consequences on the residual air expansion due to different process temperatures [65].

The most common heat treatment applied to HPDC components are the precipitation heat treatments, with and without prior solution heat treatment. The temperature of the casting immediately it's extracted is considered a critical parameter to determine the viability of a heat treatment. If a heat treatment requires a temperature above this parameter, any residual air in the casting could make it non-treatable, due to air blistering problems. A solution treatment requires heating a casting close to its solidus temperature while a precipitation heat treatment occurs below the casting extraction temperature, which air porosity in the low-stress zones of the casting. With a solution treatment, higher mechanical properties are achieved but problems such as dimensional distortion, air blistering and high costs are associated. A precipitation heat treatment without a solution treatment minimizes problems related to air blistering, but it is less effective on increasing the components mechanical properties [65].

There are 10 conventional “T temper” heat treatments, which are listed below. Only T1, T2, T5 and T10 don't require a solution heat treatment. Heat treatments from T4 to T7 are the ones used for components manufactured by vacuum high pressure die casting [64-66]:

- **T1:** “Cooled from an elevated temperature shaping process and naturally aged to a substantially stable condition”;

- **T2:** “Cooled from an elevated temperature shaping process, cold worked, and naturally aged to a substantially stable condition”;
- **T3:** “Solution heat treated, cold worked, and natural aged to a substantially stable condition”;
- **T4:** “Solution heat treated, and naturally aged to a substantially stable condition”;
- **T5:** “Cooled from an elevated temperature shaping process then artificially aged”;
- **T6:** “Solution heat treated then artificially aged”;
- **T7:** “Solution heat treated then overaged/stabilized”;
- **T8:** “Solution heat treated, cold worked, and then artificially aged”;
- **T9:** “Solution heat treated, artificially aged, then cold worked”;
- **T10:** “Cooled from an elevated temperature shaping process, cold worked, then artificially aged”.

While heat-treatments from, T4 to T6, are reserved for zinc alloys with high wt.% of aluminium, ranging from ZA15 to ZA27 either manufactured by sand casting or permanent mould casting [67]. For Zamak alloys, only artificial ageing treatments are used [38; 68]. Heat treatments are more effective on components manufactured by gravity casting since this process produces less air entrapments during casting when compared to the HPDC process.

Numerous studies were conducted the binary Zn-Al alloys ranging from ZA20 and ZA27 to determine the influence of heat treatments such as T4 and T6 on mechanical and tribological properties and even on corrosion resistance. These heat treatments were carried for a wide variety of testing conditions of temperature and duration. Typical conditions used for a solution heat treatment are: temperatures from 300 to 400 °C with a duration from 3 to 10 hours. Prior to an artificial ageing (T6 - 370 °C for 1 - 24 hours) or natural ageing (T4) heat treatment, the solution heat treated component is water quenched. Every study led to the same conclusions: heat treatments led to a moderate increase of ductility at the cost of a tensile strength and hardness reduction. Also, it was found that heat treating ZA27 leads to an improvement of its tribological properties, from the aspect of wear and friction [69], and a T4 heat treatment leads to a slight increase of the alloys corrosion resistance [70]. These changes happen throughout the duration of the artificial ageing heat treatment and are accentuated at higher temperatures [71-74]. These studies may suggest that the same heat treatments would have the same consequences if applied to the Zamak alloys.

A problem that affects zinc high pressure die casting alloys is the mechanical properties change during natural ageing at room temperature. This happens due to a high amount of diffusion at room temperature which is enhanced by the alloys low melting point. Currently, an artificial ageing heat treatment is an optimal solution to deal with these changes. This heat treatment is interesting in the way that normally heat treatments are used to enhance mechanical properties, but in this case, it deteriorates during the artificial ageing. This process basically accelerates the natural ageing process which stabilizes the alloys mechanical properties by finishing the diffusion process [38; 68].

Every alloy within the Zamak family, Zamak 2,3 and 5 reacts the same way regarding tensile strength, yield strength, hardness, Young's modules loss and elongations increase during natural and artificial ageing. Temperatures between -35 °C and 85 °C are used for component testing since these are typical conditions for automotive applications. There are many existing studies regarding this subject for different alloys, but in this case only Zamak 5 will be considered since it's the most used alloy in Europe [38].

As shown in Figure 40, a decrease of a components tensile strength occurs for longer natural ageing times, higher components testing temperature and higher wall thickness. For every Zamak alloy, natural ageing is completed roughly after 1 year and the tensile strength reduction during both natural and artificial ageing differs among the alloys as well as the testing temperature and wall thickness. This reduction can be around 15 % when compared to as cast condition [38].

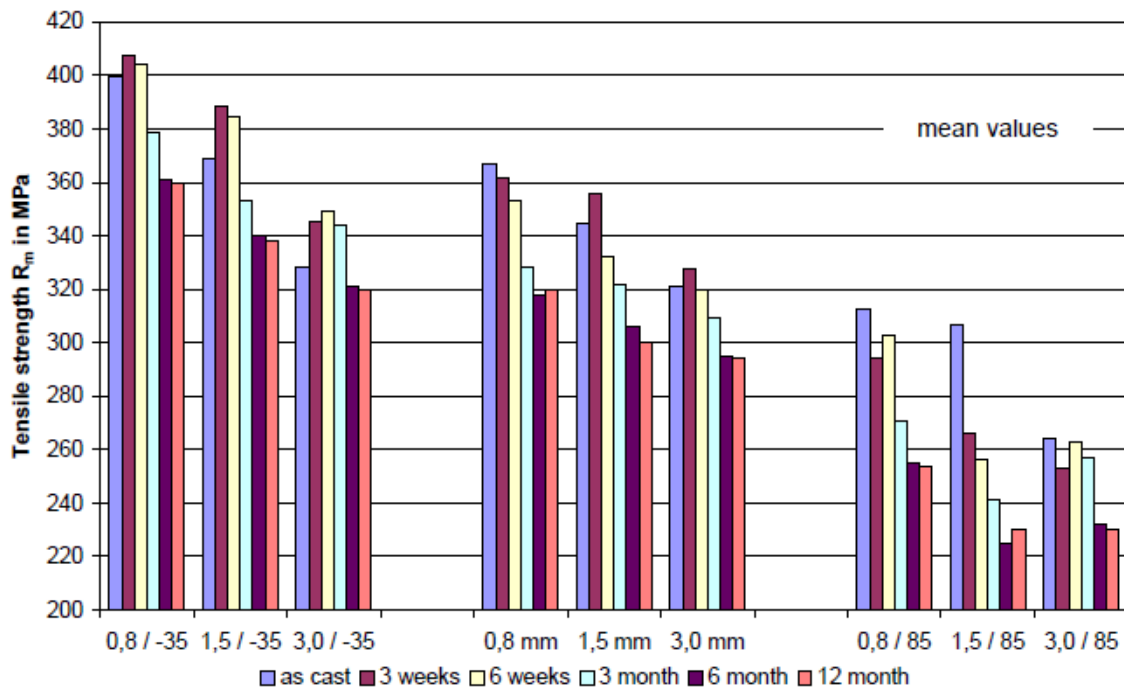


Figure 40- Effect of test temperature (-35, 23,85 °C) and wall thickness on the tensile strength of Zamak 5 during different natural ageing durations [38].

As shown in Figure 41, an average of 10 % hardness reduction occurs during the natural ageing process, for a Zamak 5 alloy. It was also proven that the gate velocity has no influence on this parameter while a colder die, higher wall thickness and higher copper content has a positive influence. Also, a higher copper content helps decreasing the ageing behavior [68].

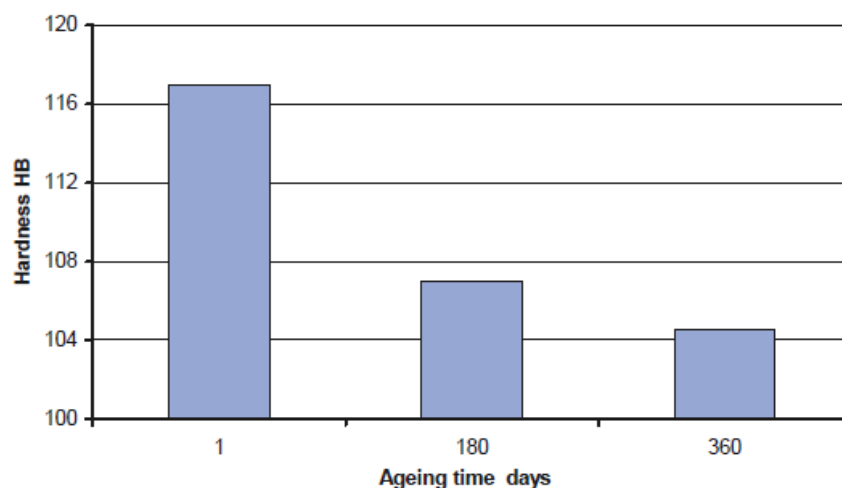


Figure 41- Hardness evolution of a Zamak 5 alloy during 1 year natural ageing [38].



Figure 42 presents information regarding the equivalent natural ageing times required to achieve the artificial ageing results. This means that for example, a 3 mm wall thickness component, an artificial ageing heat treatment of 105 °C for 24 hours is equivalent of 1 year of natural ageing [38].

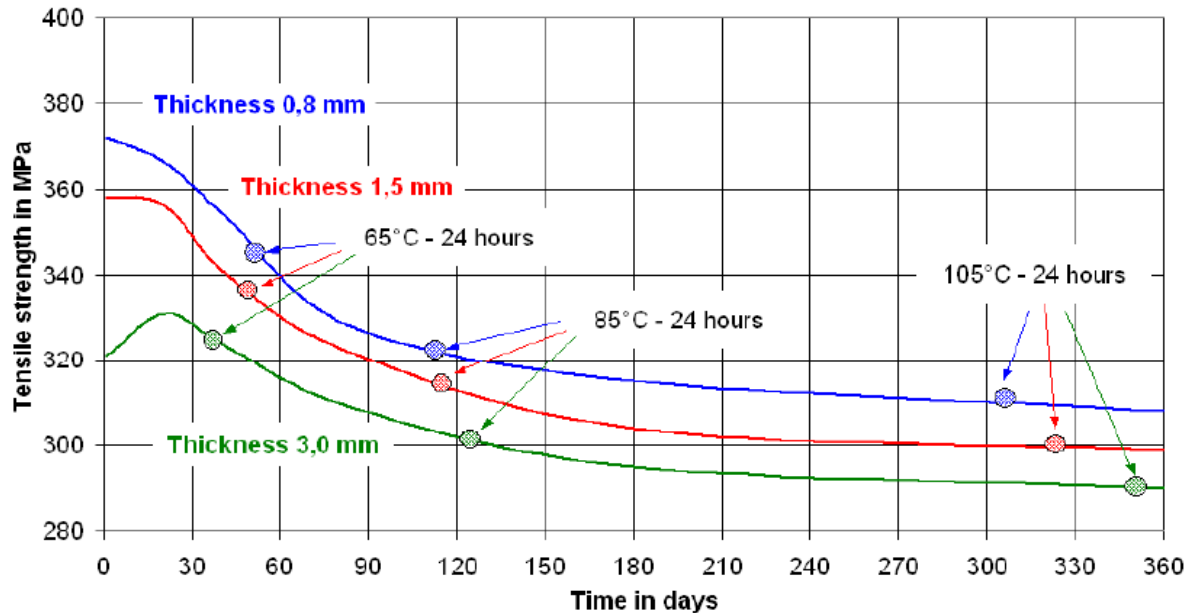


Figure 42- Artificial ageing of Zamak 5 alloy for 25 hours for 3 different temperatures [38].

In this section, a brief explanation of relevant topics, regarding the high pressure die casting process, was made in order to proceed with more detailed topics. During this section, the basic principles of this process was explained. Also, an investigation of novel methods/process was conducted. In this process, it was discussed the application of water-soluble salt cores for the industry, which gives the possibility to produce even more complex shaped castings; new zinc alloys, that helps minimizing typical problems with high creep rates and density; new mould repair technologies; a new die material, which saves time during the cavity machining process; a novel semi-solid hot chamber process, which is an alternative when a lower porosity content is required; application of the gas injection technology in the HPDC process, to produce functional cavities, which is extremely difficult to produce using a conventional process.

The next section will focus on topics related to the design of gating systems, with the presentation of a real case study.



### 3 Design and analysis of high pressure die casting components for zamak alloys

---

#### 3.1 Gating system

The gating system is a group of channels, machined into the die, responsible for leading the molten metal that enters the die into the components cavity. It is composed by various elements such as a sprue (just for the hot chamber machine), runners, gate-runner, overflows and vents, located in the parting line. Generally, there are no major differences between a gating system of a cold and a hot chamber machine in terms of form. The only element that's different is where the metal enters the die. For a cold chamber machine, the first component where the molten metal enters the die is called a "biscuit" while in a hot chamber machine is called a sprue. The total volume of the gating system is proportional to the components volume. Which means that a bigger component requires a bigger gating system. For both processes, the molten metal after entering the die, passes through the runner system and enters the components cavity through the gate [24].

The function of the gating system is to ensure a complete, smooth, and uniform filling to prevent defects such as misruns, cold shut, gas entrapment, gas porosity, inclusions and nonuniform mechanical properties. To avoid the occurrence of these defects the gating system must be optimized, which refers to an optimal design of each of its elements. The gating system design is a major task because it not only affects the manufacturing of the die but also the quality and cost of the produced components [75]. This process heavily depends on the designer's experience but also on technical knowledge. Usually, this process requires a number of iterations which results in a longer lead time and increased die cost [39].

Depending on the size of the casting, it may be necessary to use more than one gate and runner to achieve better productivity or to prevent defects mentioned above. This means that while in a simple casting a single runner and gate might be sufficient, a larger casting might require multiple runners and gates [76].

#### 3.2 Elements of a gating system

##### Gate

Figure 43 shows an example of a gating system, with each of its different elements identified.

The gate is the connection between the components cavity and the gate-runner, generally with a rectangular form. It represents the smallest section in the molten metal flow path to the die cavity. When designing the gating system, this is the first parameter to be dimensioned [39].

##### Runners

Is a branch structure composed of channels, that connects the metal-receiving hole of the die to the gate. These channels have a trapezoidal cross section and are machined entirely in the ejector half and the cover half forms the flat side of the runner [39].

After the gate is dimensioned, the shape of the gate-runner is chosen between a fan or a tangential and is based on the desired flow. The cross-sectional area of every runner section must converge, starting from the sprue until the gate. Each turn from a branch-runner to a main

runner or “Y” junctions, requires an immediate increase of the total cross-section area, of around 5 %, when working towards the sprue [24; 39].

A runner is composed by 3 sections:

- Main-Runner: Is the channel that connects the sprue to the branch-runner;
- Branch-Runner: Channel that connects the main-runner to the gate-runner;
- Gate-Runner: Channel that connects the branch-runner to the gate.

### Overflows

Overflows are reservoirs, located at the last filling spots in the components die cavity, that has the function of receiving the first molten metal that enters the die cavity. The first metal that enters the die cavity is considered a low-quality metal, since it contains oxides and other impurities. It also serves as a passage for residual air to be evacuated during the injection process.

Strategically placing the overflows helps to compensate metal shrinkage during solidification and also adding heat to a cold area in the die. [77].

Associated to overflows, there's always vents that allows the air to be evacuated from the die throughout the injection process.

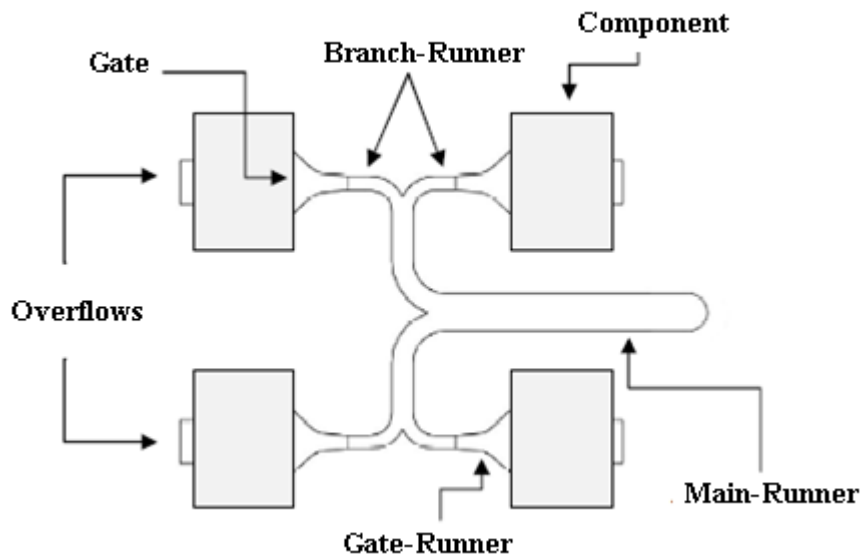


Figure 43- Elements of a gating system [75].

### 3.3 Gating system design

The gating system design in most cases, follows a traditional method based on the designer's experience. This method often leads to incorrect designs leading to a high percentage of components rejection rate.

Figure 44 describes a gating system design method with a more accurate approach when compared to the traditional method. There are a number of steps to dimension every element of the gating system. In this project, NADCA's gating manual will be considered which divides

this process into 6 steps, that will be described in detail. A resume of the NADCA's manual will be made, that will be sufficient for further gating design considerations.

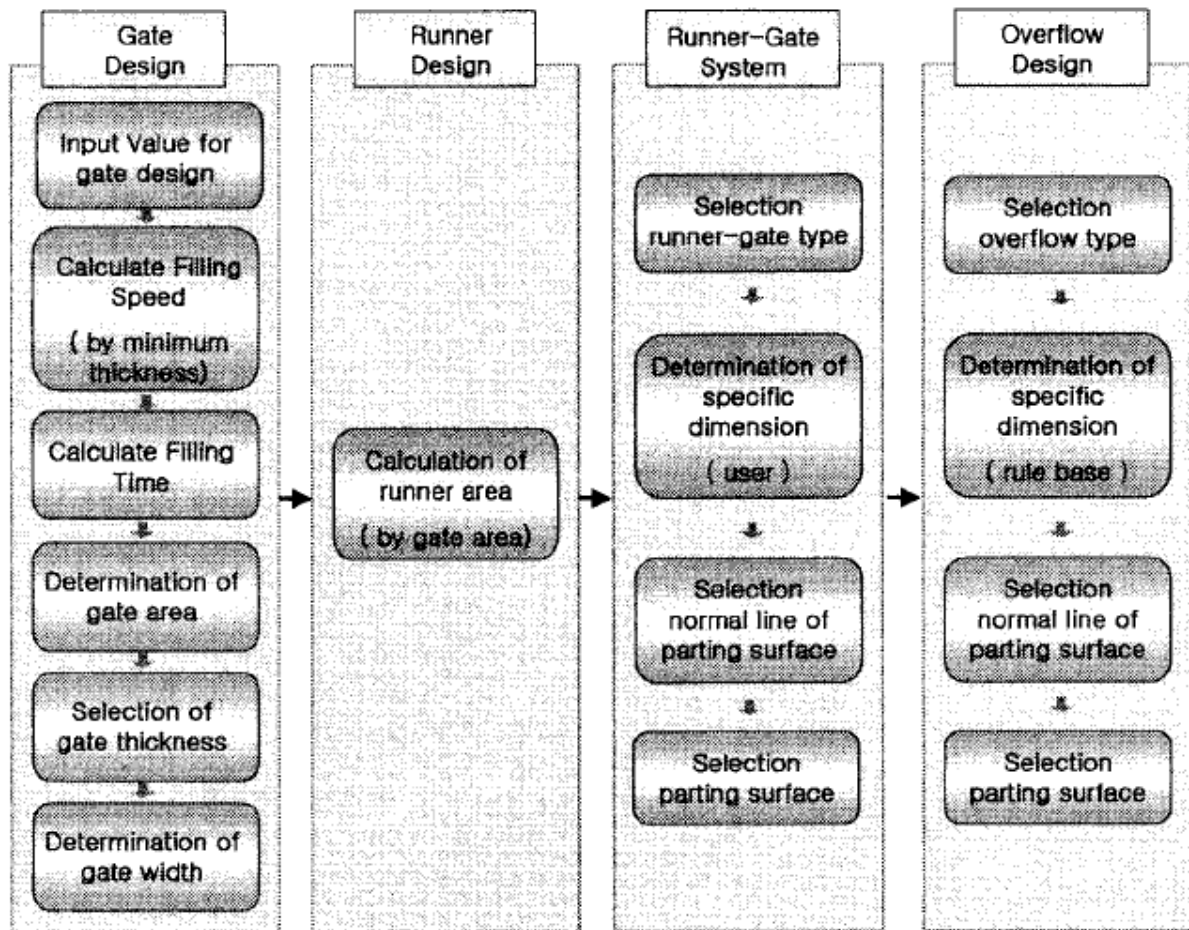


Figure 44- Flow chart for die layout design [39].

### 3.3.1 Casting quality requirements

The first step in the gating system design is to determine the required casting quality. This means that the designer needs to understand what specific attributes the customer needs for its component as for: admissible porosity content and post finishing procedures. A higher quality component means a very low porosity content and the possibility to apply a plating coating without post machining, which requires an excellent surface finish. There are some gating design factors that directly affects this quality parameter that will be further discussed such as flow pattern, cavity fill time, ingate velocity and overflow size. Table 5 briefly describes some gating design parameters affecting each level of surface finish quality requirements [24].

Table 5- Surface finish in function to fill time and flow pattern design [24].

<b>Surface Finish Quality requirements</b>	<b>Guidance for selections used during fill time calculation</b>	<b>General considerations in flow pattern design</b>
Average (some minor cold flow permissible)	Middle to high end values of fill time	Some minor lines and swirls
Good (no visible cold flow)	Middle values of fill time	Minimum swirls, minimum flow lines
Excellent (painting or plating grade finish)	Shortest possible fill time	No swirls, no flow lines, even in small areas

### 3.3.2 Required flow pattern and ingate and outgate location

After determining the casting quality, now is the moment to define where and how the liquid metal enters the die cavity through the gate. Also, it is also necessary to determine the best location for the outgates, which connects the die cavity to the overflows. Even though this step is heavily dependent on the designer's experience, there's some technical rules that must be respected to achieve an optimized filling pattern, by locating the ingate correctly:

1. By using as much parting line as possible, the flow should be distributed as long as possible, respecting a minimum gate thickness of 0.3 to 0.5 mm for a zinc alloy. Fan and tangential runners are commonly used to obtain a distributed flow, unlike for a chisel runner that causes swirls, entrapped air and poor filling. Small jet gates are used for local porosity control;
2. The flow should be directed right to areas that requires higher surface finishes or even where defects might appear. Also, an atomized flow should be maintained throughout its path to ensure a good finish;
3. The gate should be placed where the flow has to travel the shortest distance from the ingate to the outgate;
4. The flow should travel through the natural shape of the casting;
5. Injecting the liquid metal directly into walls or cores should be avoided, since besides erosion problems, it results in more air entrapments;
6. Thicker part sections should be fed first;
7. Certain difficult and complex areas might need to be fed by two flows, otherwise a poor surface finish will be obtained;
8. For an oval or round die cavity, its centre should be fed first;
9. For a multi cavity die, each cavity should have the same filling pattern and cavity filling time;
10. Runner gate should be placed far away from the most critical components decorative zone;
11. Dividing the cavity into segments ensures that critical areas are fed correctly. Each segment is associated to a unique ingate, and usually 2 to 4 is necessary to ensure an

optimal filling pattern. Each segment is feed by unique ingates with different dimensions, but filling times must be the same for each segment. Segments are created based on: different wall thickness; different local casting quality; areas that are subjected to filling defects and natural flow paths. Basically, each segment is treated as a unique casting during the gating design analysis. The best way to determine each segment volume, is by using a CAD software. In each segment volume, the associated overflow (if necessary) must be included.

### 3.3.3 Cavity fill time and flow rates

#### Cavity fill time

The cavity fill time is defined as the time that the molten metal takes from entering the die cavity until its 100 % full, which is controlled by the second injection phase. The die cavity must be fully filled before the molten metal reaches a point that it no longer flows, due to heat losses. An incorrect filling time is responsible for numerous casting defects, and normally it's better to error on the side of a fast filling. It has major influence on surface finish and in theory, a shorter filling time may be beneficial to reduce porosities since air has more time to be evacuated. For a multi cavity die, each cavity must be filled at the same time.

An easy approach to calculate this parameter is by using NADCA's fill time equation. Each of the values presented are related only for the Zamak alloys:

$$t = K \left\langle \frac{T_i - T_f + SZ}{T_f - T_d} \right\rangle T \quad (3.1)$$

Where:

t- Filling time expressed in s or ms (ranges from 15 ms to 150 ms);

K- Empirically derived constant related to the die steel ( $K = 0.0346 \text{ s/mm}$ );

$T_i$ - Metal temperature at the ingate ( $T_i = 405 \text{ }^\circ\text{C}$ );

$T_f$ - Minimum flow temperature of the metal alloy ( $T_f = 382 \text{ }^\circ\text{C}$ );

$T_d$ - Die surface temperature just before the metal arrives ( $T_d = 230 \text{ }^\circ\text{C}$ );

T- Wall thickness of the casting (can be either the thinnest or average wall section);

Z- Solids units conversion factor ( $Z = 2.5 \text{ }^\circ\text{C}/\%$ );

S- Percent solids at the end of fill.

Table 6- Recommended amount of Solidified material, S [24].

Wall thickness [mm]	S [%]
< 0.8	5- 15
0.8 - 1,25	10- 20
1,25 - 2	15- 30
2 - 3	30-35

### Flow rates

With segment volumes and die cavity filling time calculated, flow rates for each segment are calculated using Equation 3.2:

$$Q_i = \frac{V_i}{t} \quad (3.2)$$

Where:

$Q_i$ - Flow rate for segment i ( $\text{m}^3/\text{s}$ );

$V_i$ - Volume of segment i, ( $\text{mm}^3$ );

$t$ - Cavity fill time (s);

$Q = \sum Q_i$ - Flow rate for entire casting ( $\text{m}^3/\text{s}$ ).

### 3.3.4 Ingate parameters

With previous parameters calculated, the apparent ingate area,  $A_{\text{appi}}$ , is calculated using the following Equation:

$$A_{\text{appi}} = \frac{Q_i}{V_g} \quad (3.3)$$

Where:

$A_{\text{appi}}$ - Apparent ingate area of a segment ( $\text{mm}^2$ );

$Q_i$ - Flow rate of a segment volume ( $\text{m}^3/\text{s}$ );

$V_g$ - Ingate velocity (m/s).

The ingate velocity is an important process parameter that directly affects the components mechanical properties and surface quality. Generally, a higher ingate velocity is necessary for a better quality surface finish and mechanical properties. Regarding the zinc alloys, the ingate velocity depends on the desired quality finish: for decorative parts, 30 m/s; for engineering parts, 40 m/s; and for pressure tight parts, 50 m/s. The velocity must be sufficient so that an atomized flow is produced off the ingate.

The minimum value of ingate velocity to obtain an atomized flow, which is represented in Figure 45, can be calculated using the following Equation:

$$V_g^{1.71} = T_g * \rho \geq J \quad (3.4)$$

Where:

$V_g$ - Ingate velocity (m/s);

$T_g$ - Ingate thickness (mm);

$\rho$ - Density of the metal ( $\text{Kg}/\text{m}^3$ );

$J$ - Atomized factor ( $J = 475$  for a zinc alloy).



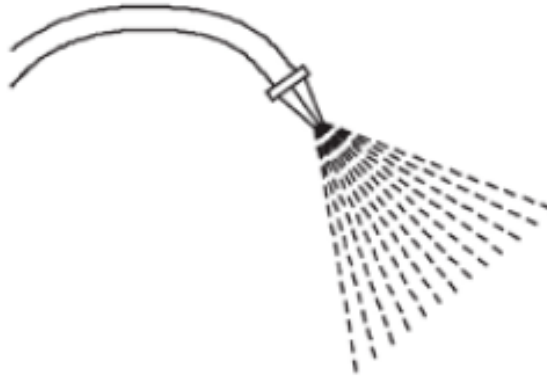


Figure 45- Atomized flow [24].

After calculating the ingate area for each segment, either the ingate length or thickness can be calculated. Usually values for ingate thickness for the Zamak alloys can range from (0.3 - 0.5 mm) not exceeding 75 %, of the wall thickness of the part, and therefore the ingate length can be calculated. Also, depending on the situation the ingate length can be previously known and therefore the ingate thickness is calculated.

$$L_{gi} = \frac{A_{gi}}{T_{di}} \quad (3.5)$$

Where:

$L_{gi}$ - Segment ingate length (mm);

$T_{gi}$ - Segment thickness (mm).

### 3.3.5 PQ<sup>2</sup> analysis

In in this stage, a PQ<sup>2</sup> analysis verifies the compatibility of a specific die casting machine to a gating system, with respect to its plunger hydraulic system. Two parameters are considered: P for metal pressure and V<sub>g</sub> for metal flow rate. A higher ingate velocity requires a higher metal pressure. The necessary metal pressure to achieve a desired metal flow can be calculated from the equation 2.6:

$$P_m = \frac{\rho}{2 * g} * \left( \frac{V_g}{C_d} \right)^2 \quad (3.6)$$

Where:

$P_m$ - Metal pressure (MPa);

$\rho$ - Metal density (Kg/m<sup>3</sup>);

$g$ - Gravitational constant ( $g = 9.81 \text{ m/s}^2$ );

$V_g$ - Ingate velocity (m/s);

$C_d$ - Discharge coefficient, Hot chamber machine: ( $C_d = 0.55 - 0.65$ ).

### 3.3.6 Gate-runner design

Runner systems are designed starting from the ingate, working off to the sprue. The trapezoidal cross-sectional area of the runner system decreases continuously from the sprue until the ingate, to ensure a correct die filling. For zinc alloys, the runner size ratio is often 1.05 to 1.15 times the gate area.

Two common gate-runner designs are the fan, Figure 46, 47 and 48, and tangential runner, Figure 49. Each design is used depending on the components complexity. An important parameter when considering which fan-runner to be used is the desired flow angle that the liquid metal goes off into the die cavity. The angle is measured relative to a normal line to the gate. This value for a fan gate-runner can range from 0 to 45 ° while for a tangential gate-runner 26 to 45 °.

#### Fan gate-runner

Fan gate-runners generate a strong centre line which is useful to feed metal into critical areas. As disadvantages, a high heat loss occurs and there's a high potential of air entrapment if poorly dimensioned. There are two types of fan gates: straight and curve sided. When compared to a curved sided fan, the straight sided fan, provides accurate information regarding the flow angle and is easier to trim when solidified but is harder to machine into the die.

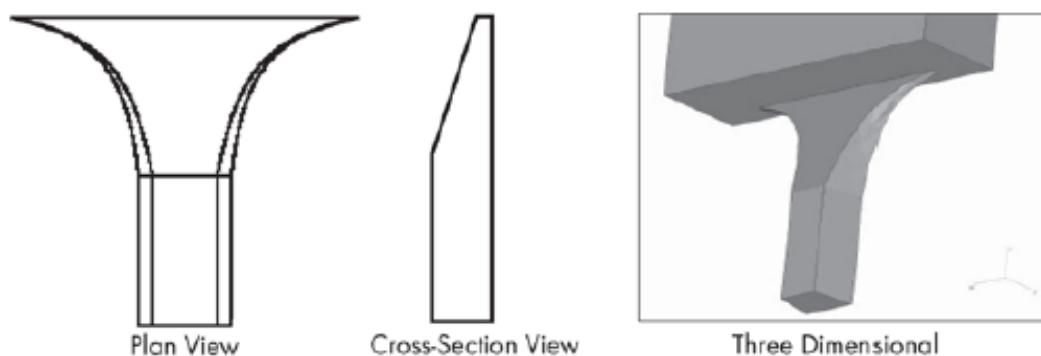


Figure 46- Curve sided fan runner-gate [24].

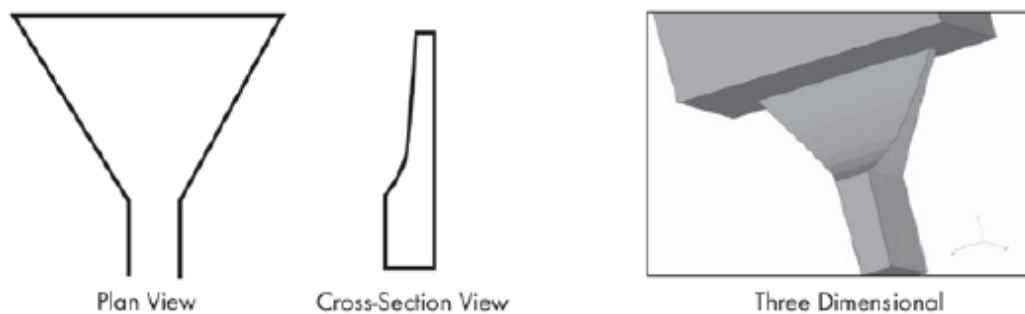


Figure 47- Straight sided fan runner-gate [24].

The designing process of a fan runner-gate starts by dividing it up to 9 sections up to the main runner spaced equally from each other. Then various parameters from each section can be calculated using the following Equations.

$$h = \frac{\text{Area}}{\text{depth}} \quad (3.7)$$

$$\text{Average width} = \frac{\text{Area}}{h} \quad (3.8)$$

$$b = \text{Average width} + c \quad (3.9)$$

$$t = \text{Average width} - c \quad (3.10)$$

$$c = 0.176 * h \quad (3.11)$$

$$d = 0.176 * h \quad (3.12)$$

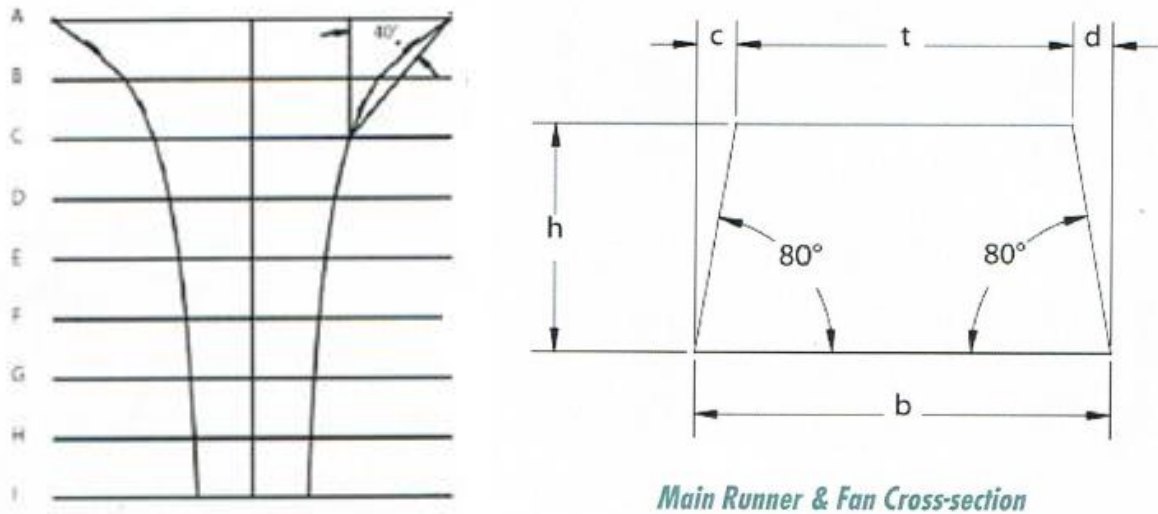


Figure 48- Left: Top view of a curved sided fan divided into 9 sections; Right: Cross sectional view of a fan gate-runner and main runner [24].

### Tangential gate-runner

This type of gate-runner runs along the side of the cavity, where the gate is located. When compared to a fan gate-runner, it offers the following advantages: more compact that can be kept to the casting; the flow direction is better controlled and the heat present in the liquid metal is better distributed over a longer distance. In a single tangential gate-runner, it is possible to have different flow angles which ensures a correct feed of metal in problematic areas, presented in Figure 48. As a disadvantage, the runner becomes too large when smaller flow angles are required. Other important aspect regarding this type of gate-runner, is the fact that the metal sees a smaller gate area comparing to what is actually cut into the die [24].

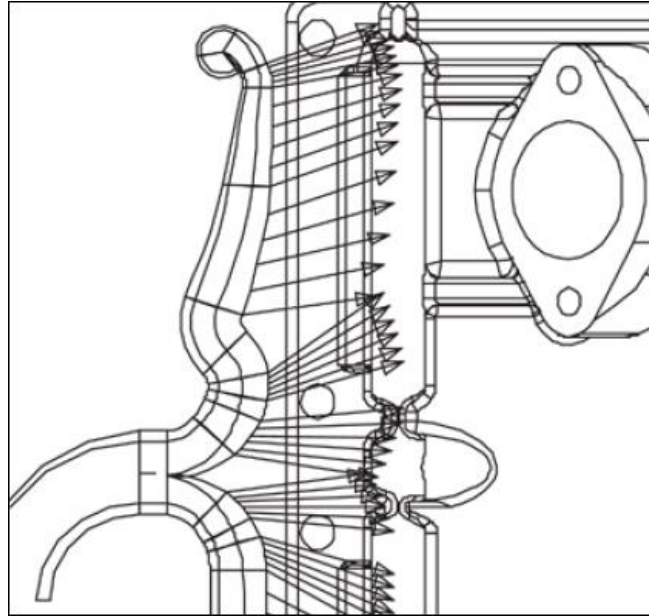


Figure 49- Tapered tangential gate-runner that illustrates different flow angles [24].

### 3.3.7 Overflows and vents design

The first step in order to design an overflow is to determine the correspondent outgate area and dimensions, such as width and length. The total outgate area is 50 % of the ingate and the minimum recommended thickness for Zamak ranges from 0.15 - 0.3 mm.

An overflow is located far away from the ingate or at the last filling point, which can be identified through CAE. The size and number of overflows is highly dependent on the required components quality and metal flow behaviour. The overflow size is directly dependent upon the desired components quality, illustrated in Figure 50.

Typical Overflow Sizes			
Thickness of Segment - in. (mm)	Cavity Fill Time - sec.	Overflow size as percent of adjacent cavity segment	
		Hardware Quality Surface Finish - %	Some Cold Shut Allowed - %
0.035 (0.90)	0.012 - 0.021	150	75
0.050 (1.30)	0.017 - 0.029	100	50
0.075 (1.80)	0.026 - 0.044	50	25
0.100 (2.50)	0.035 - 0.059	25	25
0.120 (3.20)	0.042 - 0.071	----	----

Figure 50- Typical overflow sizes [24].

With the volume of the overflows defined, its dimensions, presented in Figure 51, are calculated depending on the available space on the die.

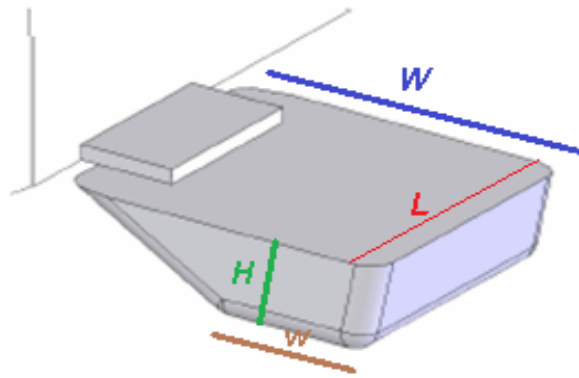


Figure 51- Overflow.

Vents are narrow channels connecting the overflows with the exterior, represented in Figure 52. Venting area can be calculated by dividing the ingate area by 4.

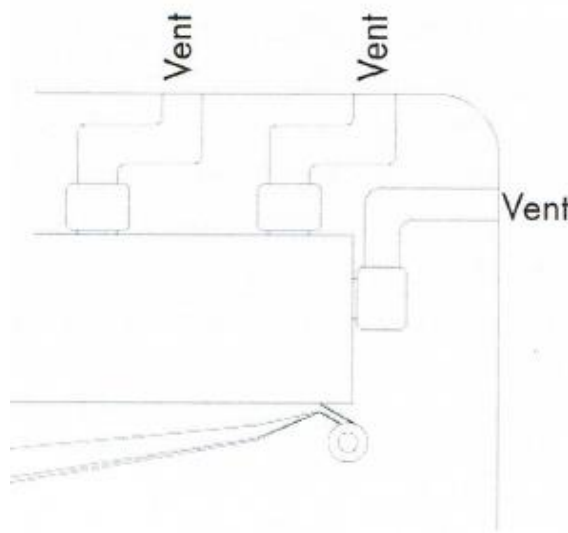


Figure 52- Location of vents on the die [24].

### 3.4 Case study

The case study consists of a Zamak 5 component that was manufactured with the high pressure die casting process. After the component is manufactured, a painting process that can reach up to 200 °C is applied. During this process, the components surface starts to develop blisters and pin holes, represented in Figure 53. As a result, this component has a rejection rate of over 35 %. As previously mentioned, blistering occurs due to the expansion of air under high pressure below the components surface, which in this case study occurs during the painting process. Air entrapments are known to be related to the turbulence of the filling process. While this is a characteristic problem of the high pressure die casting process, an optimized gating system and optimal injection parameters such as temperature of the molten metal, plunger injection speed and pressure are known to minimize these problems.



Figure 53- Left: Blistering; Right: Pin holes.

### 3.4.1 Iteration 1

Figure 54 illustrates the CAD model of the gating system that leads to a rejection rate of over 35 %. This gating system was designed based on the designer's experience, which lacks accurate calculations. It consists of feeding the die cavity using a frontal and 2 side fan gate-runners, with one overflow at each side.

As shown in Table 7, the total volume of the overflows is around 7 % the components volume. Along the section 3.3.7 it was presented that according to NADCA's gating manual, the minimum value for the overflows volume should be at least 25 % the components volume. This value depends on the sections thickness and required surface quality. The size of the overflows, with this gating system design, may be insufficient to ensure a high-quality component, with a low content of filling related defects.

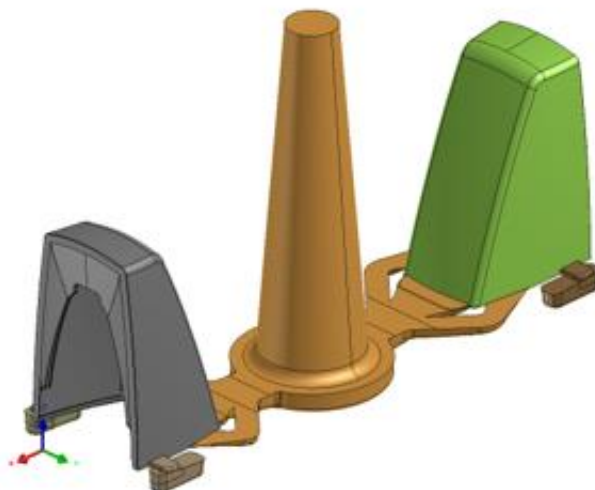


Figure 54- CAD model for a gating system which was responsible of a rejection rate of over 35 %.

As shown in Figure 55, independently of the type of gate-runner used, the molten metal will hit the components die cavity surface immediately after passing through the gate. As previously discussed, this event is a known cause of air entrapments.

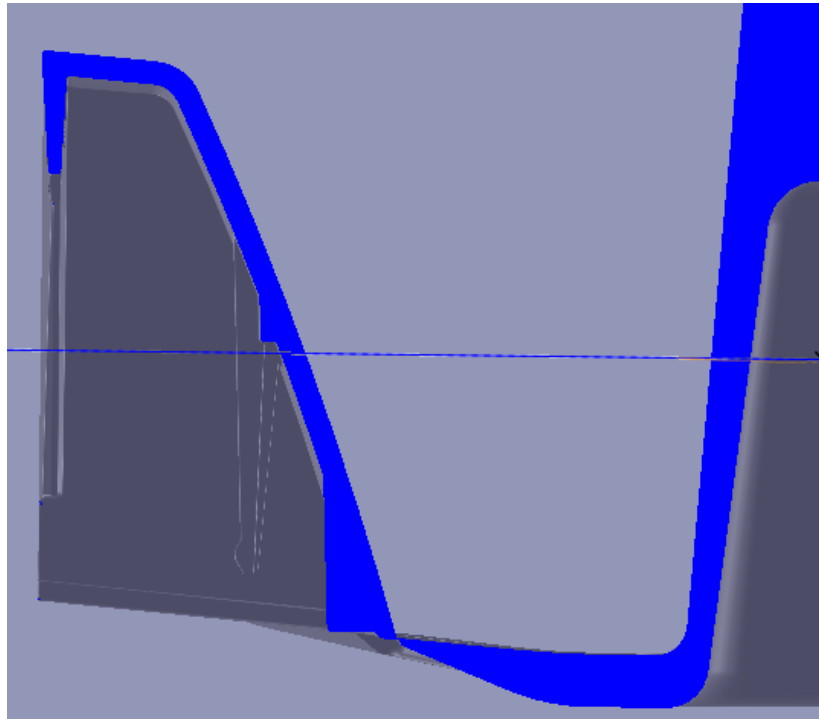


Figure 55- Cross section of the die cavity for iteration 1.

In order to analyze more possible causes of air entrapments during the filling process, two different analysis are discussed. The first is based on the discussion of parameters related to the design of the gating system, using the CAD model. For the second analysis, a die casting simulator, ProCAST<sup>TM</sup>, will be used to analyze the filling pattern.

### Analysis 1

In the first analysis, the convergence of the gating system will be discussed. In order to analyze the convergence of a gating system, a chart which plots the cross-sectional area in each zone was created. This analysis starts from the entrance of the sprue up until the gate, due to the convergence rule mentioned during section 3.3. The entrance section of the sprue is the highest cross-sectional area among all the gating system elements, while the gate is the lowest.

Using a CAD software, each cross-section area is easily identified and calculated, represented in Figure 56. As shown in Figure 56, the cross-sectional area doesn't converge from the sprue to the gate, which goes against a good gating system design. Constant changes of molten metal velocity leads to air entrapments. In this case, the company started to design a non-optimal sprue, since its area considerably increases until it connects the main runner. Therefore, even with an optimized runner, the gating system doesn't converge. In this case, if the gating system is maintained, the entrance area of the sprue has to increase from 59 mm<sup>2</sup> (8.7 mm in diameter) to at least 240 mm<sup>2</sup> (17.5 mm in diameter), so that it converges until the main runner. Other alternative, is to reduce the cross-sectional area of the entrance of the main runner, so that a considerable increase of the diameter of the sprue isn't required.

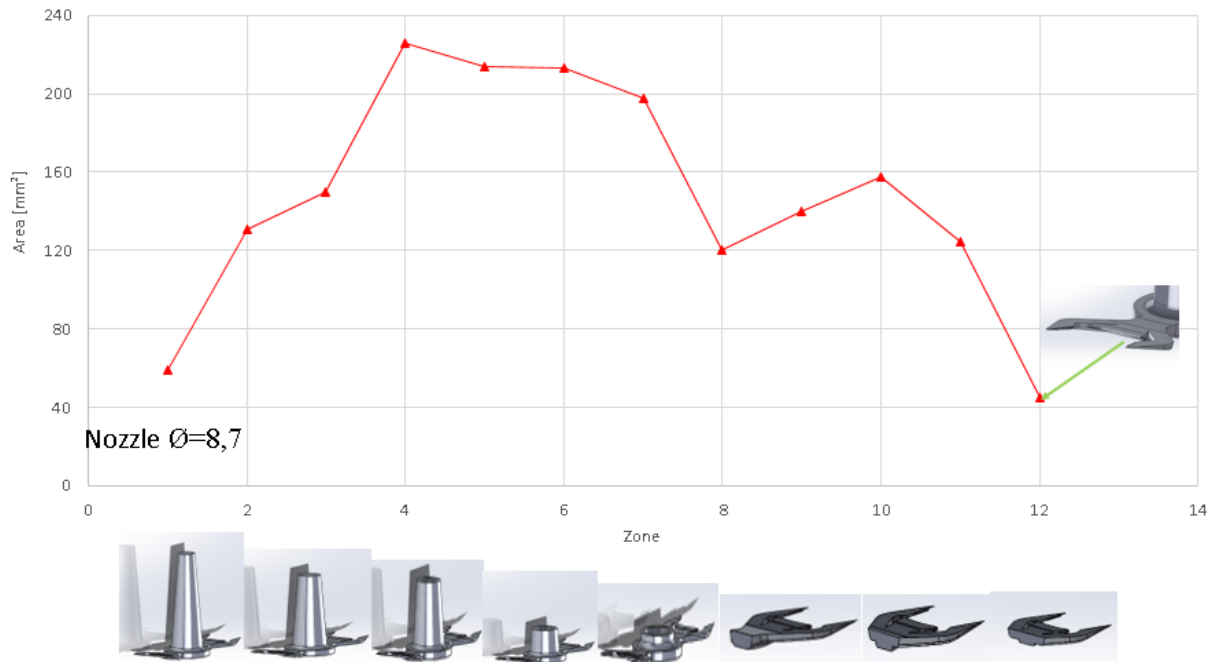


Figure 56- Analysis of the cross-sectional area of the gating system.

Other important parameter to consider during the design of a gating system, is the metallurgical efficiency. This parameter is calculated by dividing the components volume with its gating system volume, which affects the components final cost and the production cycles. Ideally it should be set as high as possible. In practice, a lower metallurgical efficiency translates into a higher volume gating system, which results in higher production costs. These costs are related to a higher remelting process and higher production cycles. Also, the available space in the die to machine the gating system will affect the metallurgical efficiency.

The metallurgical efficiency for iteration is calculated using Equation 3.13.

$$\text{Metallurgical efficiency} = \frac{20453 \text{ [mm}^3\text{]}}{26706.8 \text{ [mm}^3\text{]}} = 0.766 \quad (3.13)$$

## Analysis 2

In this analysis, a die casting simulator, ProCAST™, will be used to visualize the flow path during the injection process.

The use of simulation tools intends to support process and/or gating optimization to improve the rejection rate. The proposed CAD model of the gating system is imported into the ProCAST™ software. A finite element mesh was generated, and material properties, temperatures and initial interface conditions were assigned. These steps are represented in Figure 57.



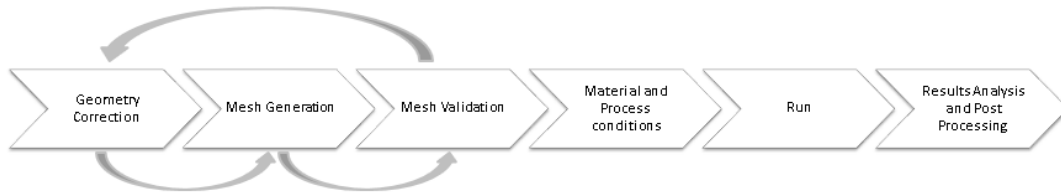


Figure 57- Overview of the work flow for a simulation tool.

## Model information

Table 7- Model bodies of the CAD model supplied by STA.

Name	Treated As	Volumetric Properties (per part)	Material	Temperature (°C)
<b>Part</b>	Solid	Mass=0.066 Kg Volume=10226.52 mm <sup>3</sup>	Zamak 5	420
<b>Overflows</b>	Solid	Mass=0,02 Kg Volume= 375.97 mm <sup>3</sup>	Zamak 5	420
<b>Gate</b>	Solid	Mass=0.164 Kg Volume=25175.90 mm <sup>3</sup>	Zamak 5	420
<b>Die</b>	Virtual Mould	-	Steel 1.24344 MG 50	130

Table 8- Input parameters supplied by STA.

Alloy	ZAMAK 5
<b>Alloy Temperature (°C)</b>	420
<b>Die Temperature (°C)</b>	130
<b>Ø Piston (mm)</b>	60
<b>Ø Nozzle (mm)</b>	8,7

Table 9- Input and mesh information.

<b>2D Elements</b>	430855
<b>3D Elements</b>	2821238
<b>Total</b>	3252093
<b>Minimum Side Length</b>	0,03 mm

One of the features that is possible to analyze from the simulation, is the liquid metal velocity profile evolution. Normally when this parameter isn't correctly optimized, it can cause air entrapment during the filling process.

Figure 58 represents the molten metal velocity profile throughout the injection process. As shown, the filling pattern of the injection process isn't optimized, because the feeding of the die cavity process starts before the sprue is totally filled. This results in a non-constant filling velocity profile through the gate during the second injection phase. An optimized gating system design, should ensure a metal velocity profile variation in a linear way, as described previously.

Other problem that arises from this gating system, is that the front fan gate-runner starts to feed the components die cavity before the two fan-gate runners, located at each side of the components die cavity.

The velocity profile of the molten metal at each gate function to the cavity filling time is represented in Figure 59. When the sprue is 100 % filled, an increase of the molten metal velocity is observed. The non-uniform metal velocity profile can be related the non-convergence gating system problem that was discussed previously.

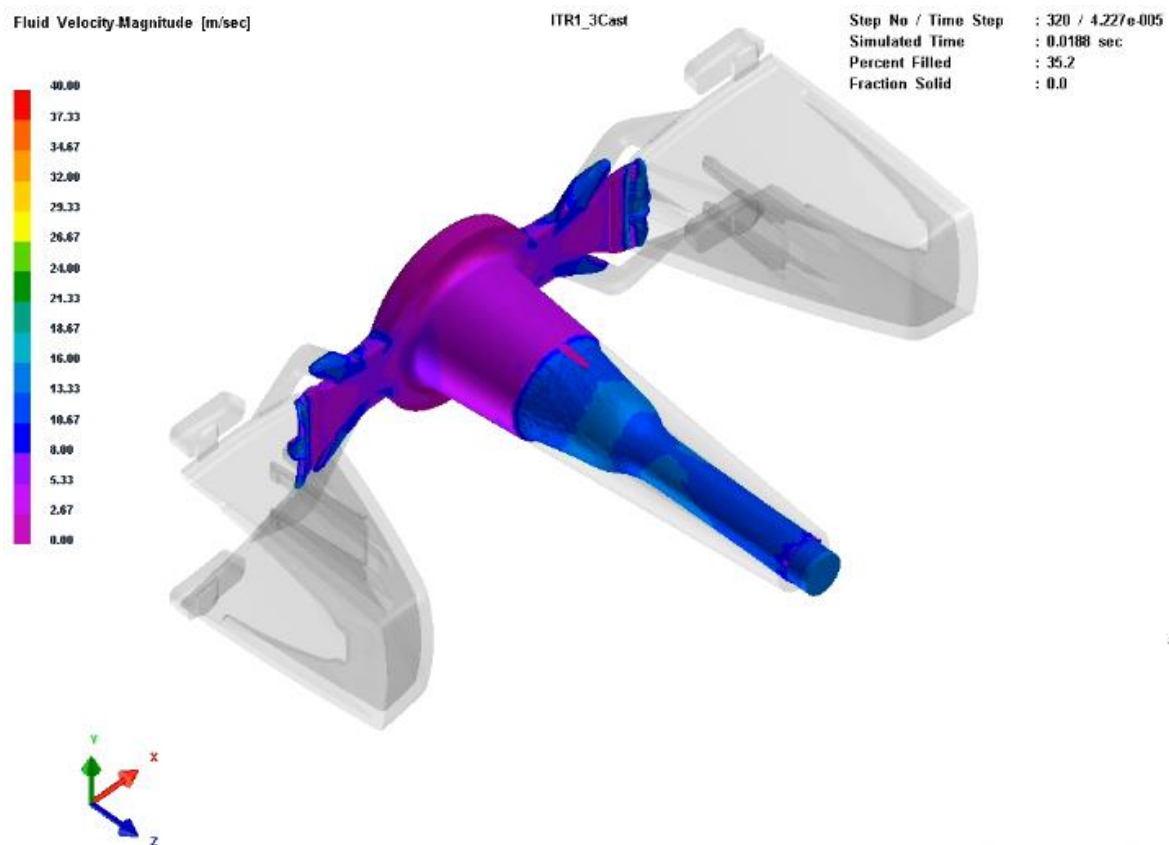


Figure 58- Velocity evolution at t=16.8ms and 35.2% filled.

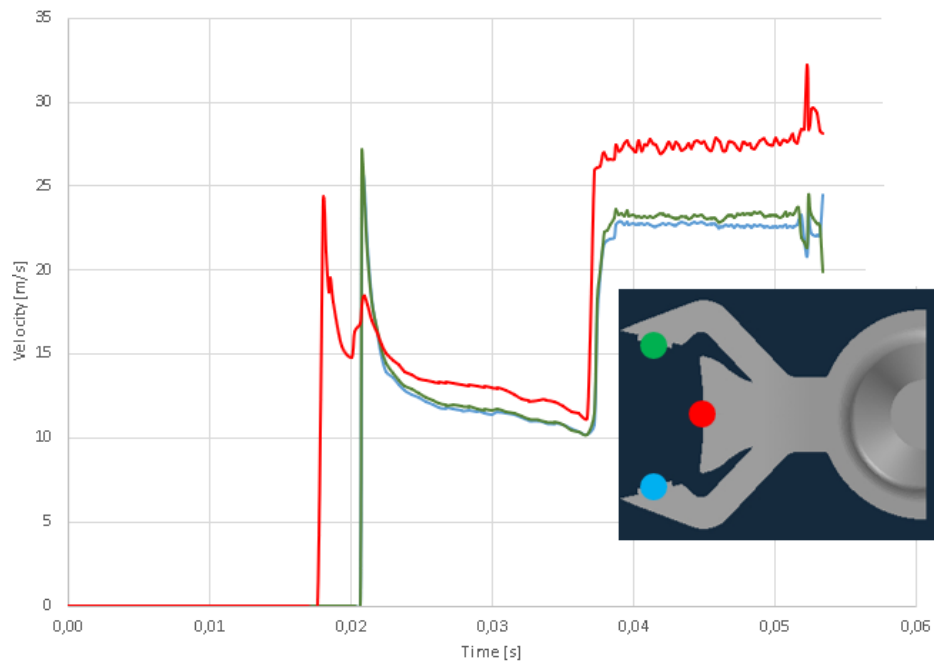


Figure 59- Velocity evolution at each ingate.

The metal velocity profile in the components die cavity is represented in Figure 60. During the components die cavity filling, other events such as generation of air pockets and collisions of metal fronts are predicted to occur. These events are a sign of bad gating system design which is can cause air entrapments. Normally air entrapments from air pockets can be effectively pushed into the overflows if they occur near them. In this case, air pockets occur far away from the overflows which doesn't allow the elimination of air from the components die cavity. In this case, an increase of the overflows volume could be a solution to remove these air entrapments generated during the second injection phase.

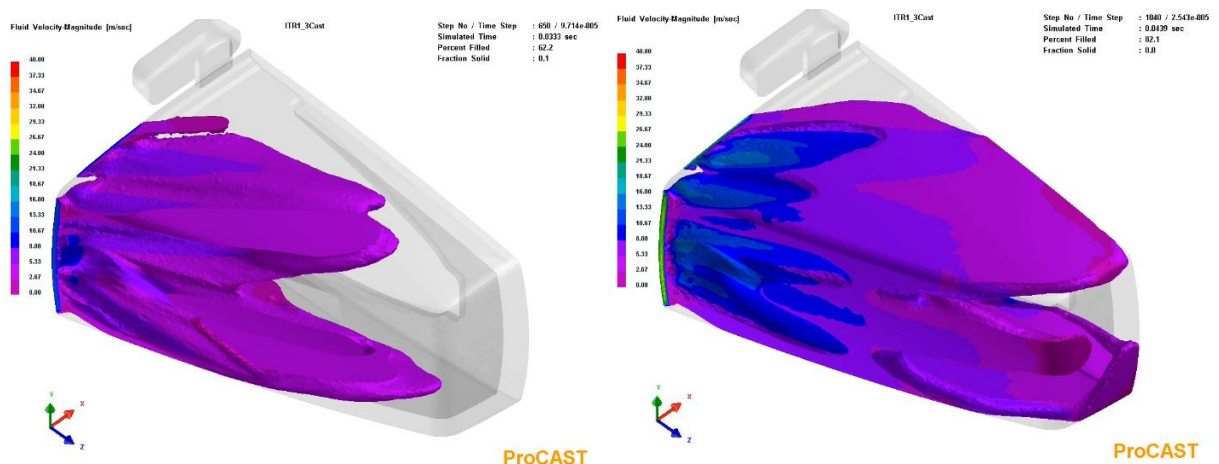


Figure 60- Velocity profile and representation of the metal front collision and creation of air pockets.

As mentioned before, this gating system design, produces components with a 35 % rejection rate due to air entrapment during the filling process. These defects can also be predicted using the simulation tool. Figure 61 is the result of the air entrapment prediction, plotting the density of air entrapment ( $\text{g/cm}^3$ ) for various sections of the component. Even though the overflows are full of air, which is a sign that the overflows are performing well, the simulation predicts several

air masses throughout the die cavity, that will expand and form blisters during the painting process.

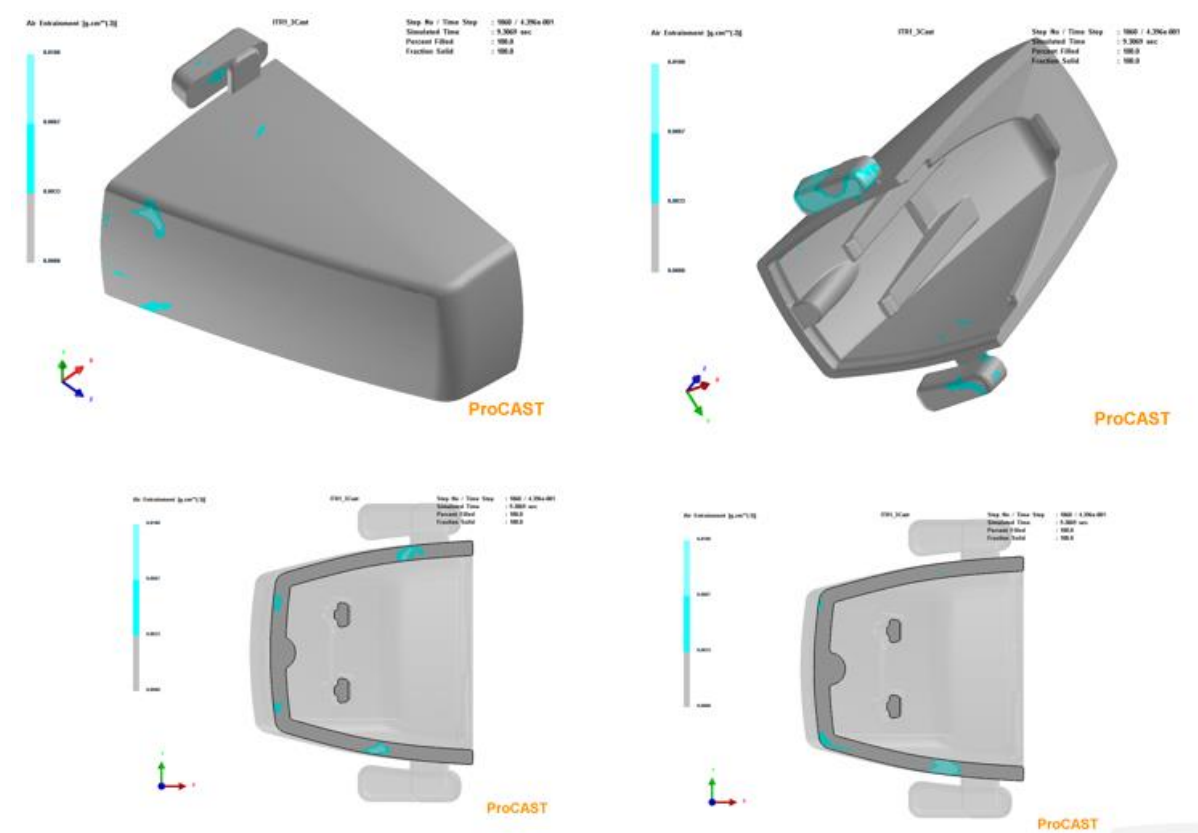


Figure 62 represents the results of a RX analysis of the component after the painting process. This analysis reveals air masses throughout the component, which serves as an experimental validation of the simulated filling process.

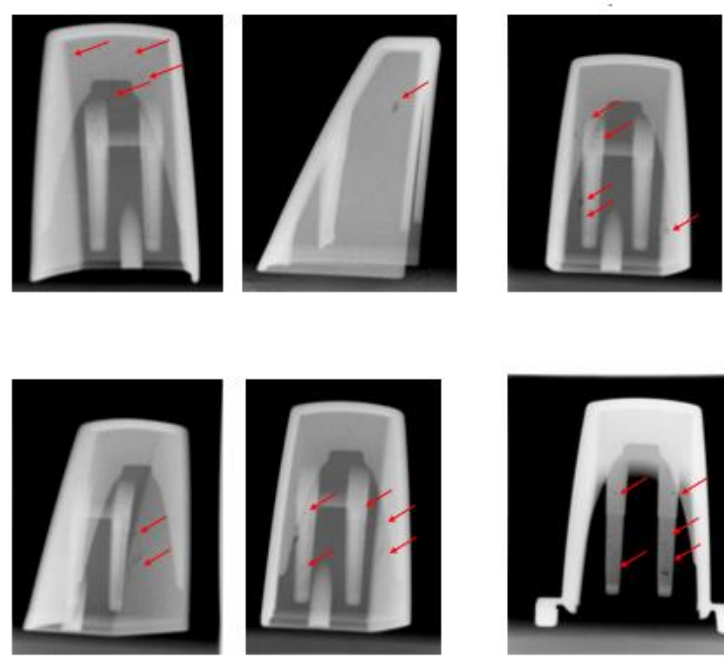


Figure 62- Rx analysis after painting process.

This gating system design leads to blistering, during the painting process, because air is being entrapped during the injection process. Even though air entrapment during the injection process of the high pressure die casting process is hardly unavoidable, a non-optimized gating system design increases the occurrence of this problem. In this case, no scientific rule was followed for the gating system design. Even with this gating system, increasing the overflows volume could be considered a solution to minimize filling related defects.

Since an optimized gating system is required to reduce the components rejection rate, a new iteration is made using a scientific method previously explained in section 3.3. The only element of the gating system that won't change is the sprue, because its supplied by the company.

### 3.4.2 Iteration 2

Iteration 2 is an attempt to feed the die cavity differently, by using NADCA's gating manual explained in section 3.3, to minimize air entrapments during the filling process. For this case, a single fan gate-runner will feed the frontal side of the die cavity with 2 overflows at each side at the last filling points, represented in Figure 63. This design was considered an attempt to minimize metal front collisions and air pockets.

This is considered an ideal design, because the available space to machine the gating system in the die isn't taken into account. If this gating system would be implemented in practice, this parameter would have to be considered due to space restrictions in the die.

For the design of the gating system, it was developed an excel spreadsheet that calculates every dimension of each component. This tool solves two problems mentioned previously: the non-convergent gating system and non-metal velocity profile. Since the sprue is the same as used previously, in this section the cross-sectional area isn't converging to the main runner. This method represents a great starting point for the gating system design procedure. The equations behind this spreadsheet are the ones explained in chapter 3.3.

Table 10- Cavity filling time.

<b>t- max filling time, s</b>	0,0361	[s]
<b>K - thermal constant of a die steel</b>	0,0346	[s/mm]
<b>T - characteristic thickness (average or minimum)</b>	1,8	[mm]
<b>Tf - liquidus temperature</b>	382	[°C]
<b>Ti - metal temperature in the gate</b>	420	[°C]
<b>Td - die temperature before the shot</b>	230	[°C]
<b>S- percent solids before at the end</b>	20	[%]
<b>Z- solids units conversion</b>	2,5	[°C/%]

Table 11- Flow rates.

Segment		#1	Total
t- cavity fill time	[s]	0,036	
Vg- volume of a segment	[mm <sup>3</sup> ]	10206,70	
Vo - volume of overflow segment	[mm <sup>3</sup> ]	5103,35	<b>50% of Vg</b>
Vi-total segment volume	[mm <sup>3</sup> ]	15310,05	
Gate velocity	[m/s]	40	<b>range [30-60] m/s</b>
Qi - Volumetric flow rate of each segment	[m <sup>3</sup> /s]	0,00043	
Q- $\sum Q_i$ - Volumetric flow rate for the entire casting	[m <sup>3</sup> /s]		0,00043
Ai-Ingate area of segment	[mm <sup>2</sup> ]	10,62	
A - Total Ingate area	[mm <sup>2</sup> ]		10,62

The metallurgical efficiency in this case is calculated using Equation 3.14:

$$\text{Metallurgical efficiency} = \frac{20453 \text{ [mm}^3\text{]}}{35225.8 \text{ [mm}^3\text{]}} = 0.58 \quad (3.14)$$

By increasing the overflows volume, the metallurgical efficiency decreases 24.282 %. This reduction translates into higher production costs, due to the increase of tooling costs and higher cycle times.

Table 12- Curved sided fan gate-runner and main runner dimension.

Gate Land Length [mm]	2								
	Flow angle = 40 degrees								
<u>Section</u>	A	B	C	D	E	F	G	H	I
Area [mm <sup>2</sup> ]	11,68	13,14	14,60	16,06	17,52	18,97	20,43	21,89	23,35
Distance [mm]	0,00	2,50	5,00	7,50	10,00	12,50	15,00	17,50	20
Depth (h) [mm]	0,61	0,78	0,95	1,13	1,30	1,48	1,65	1,83	2,00
Average Width [mm]	19,30	16,85	15,30	14,23	13,45	12,85	12,38	11,99	11,68
Base (b) [mm]	19,41	16,99	15,47	14,43	13,68	13,11	12,67	12,31	12,03
Top (t) [mm]	19,19	16,72	15,14	14,03	13,22	12,59	12,08	11,67	11,32
Side (c) [mm]	0,11	0,14	0,17	0,20	0,23	0,26	0,29	0,32	0,35
Side (d) [mm]	0,11	0,14	0,17	0,20	0,23	0,26	0,29	0,32	0,35

Table 13- Main runner dimensions.

<u>Section</u>	<u>Main Runner after Section I</u>
Area [mm <sup>2</sup> ]	35,03
Distance [mm]	45
Depth (h) [mm]	5
Average Width [mm]	7,01
Base (b) [mm]	7,89
Top (t) [mm]	6,13
Side (c) [mm]	0,88
Side (d) [mm]	0,88

Table 14- Outgate dimensions.

<b>Outgate data</b>	<b>#1</b>	<b>#2</b>
<b>Total Outgate Area [mm<sup>2</sup>]</b>	5,31	
<b>Number of Outgates</b>	2	
<b>Outgate Area [mm<sup>2</sup>]</b>	2,65	2,65
<b>Outgate thickness, C [mm]</b>	0,28	0,28
<b>Outgate width [mm]</b>	9,65	9,65

Table 15- Overflow dimensions.

<b>Overflow data</b>	<b>#1</b>	<b>#2</b>
<b>Number of overflows</b>	2	
<b>Total Overflow volume [mm<sup>3</sup>]</b>	5103,35	
<b>Outgate overflow length, B [mm]</b>	6,50	<b>Range [6-8 mm]</b>
<b>Land length, A [mm]</b>	2,50	<b>Range [2-5 mm]</b>
<b>Volume [mm<sup>3</sup>]</b>	2551,67	2551,67
<b>Overflow length, L [mm]</b>	32,56	32,56
<b>Overflow height, H [mm]</b>	5	5
<b>Overflow upper side length, W [mm]</b>	20	20
<b>Overflow lower side length, w [mm]</b>	11,33	11,33

Table 16- Vent dimensions.

<b>Vent data</b>	<b>#1</b>	<b>#2</b>
<b>Total Vent area [mm<sup>2</sup>]</b>	2,65	
<b>Number of vents</b>	2	
<b>Vent thickness [mm]</b>	0,25	0,25
<b>Vent area [mm<sup>2</sup>]</b>	1,33	1,33
<b>Vent width [mm]</b>	5,22	5,22
<b>Vent length [mm]</b>	<b>Function of the gate thickness</b>	50,80

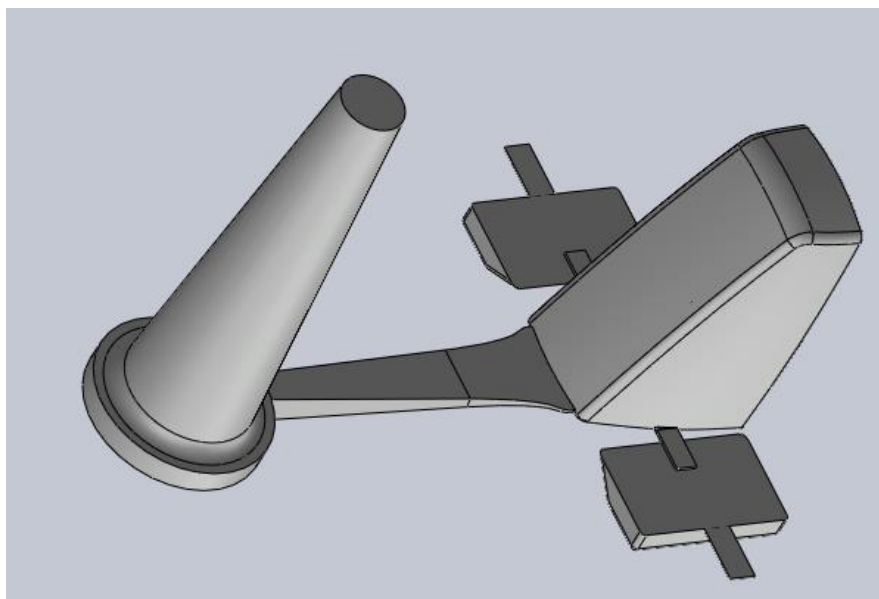


Figure 63- Optimized gating system for iteration 2.

Analysis

Figure 64 represents the molten metal velocity profile during the injection process. This iteration results in a better distribution of the metal flow inside the components die cavity when compared to iteration 1.

As expected, air entrappings are generated at the gates entrance as the second phase starts. This can be predicted even without simulation because the molten metal encounters a surface just as it enters the die cavity at high velocity. Other reason is the highly turbulent flow that is generated in the gate region, due to high metal flow velocities.

Air pockets are also generated right at the end of the components die cavity filling process. This isn't a critical problem because as the generated air pockets are near the outgate, they can effectively be pushed into the overflow. Even though there are two additional sources of air generation (besides the air generated by the natural turbulent flow) predicted during the injection process, the overflows volume is sufficient to receive a significant amount of molten metal with air.

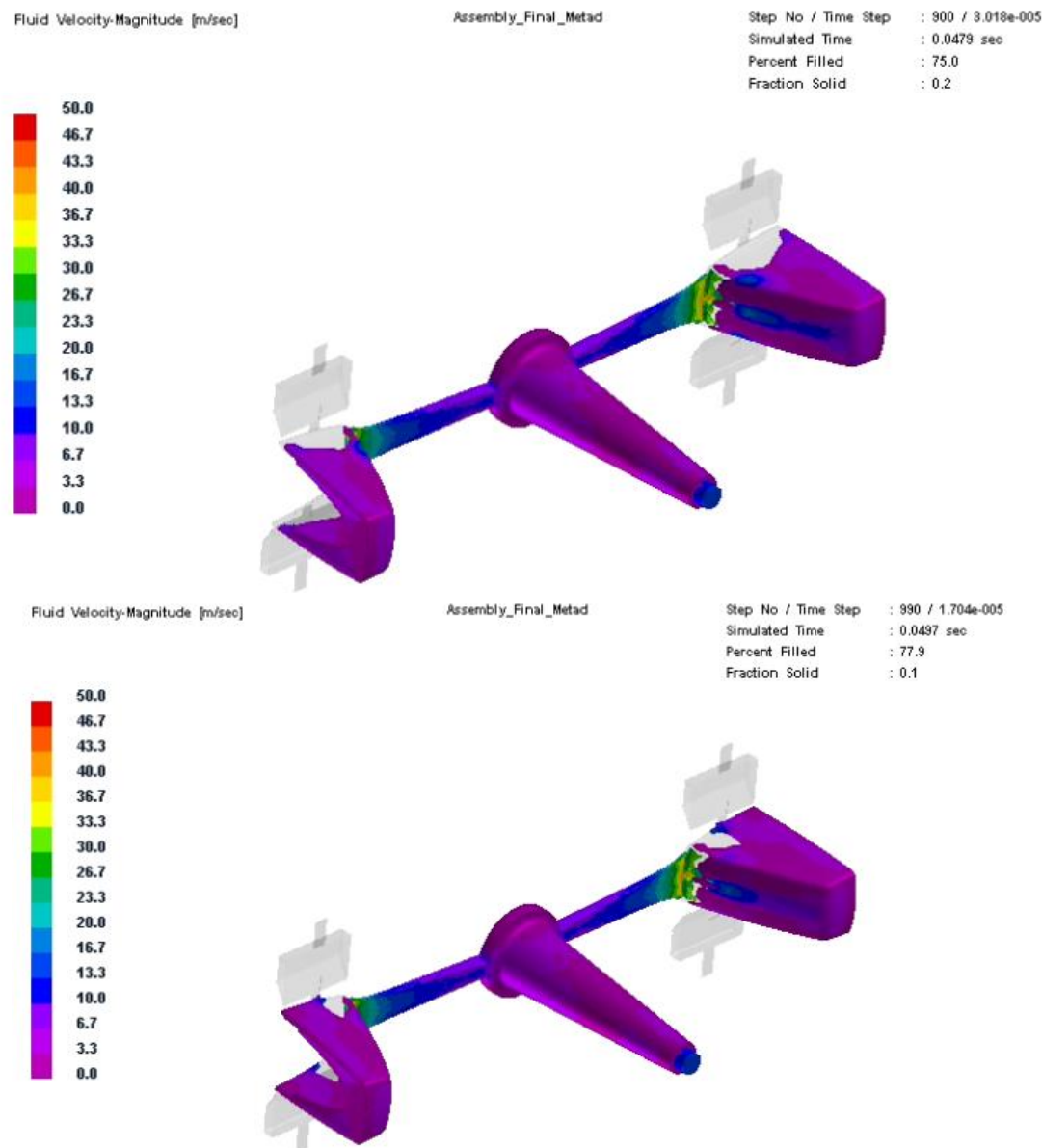


Figure 64- Simulation results of the entire component and gating system.



Figure 65 represents the molten metal velocity profile in 3 points, which are represented in Figure 66, function to the cavity filling time. Even though the incorrect filling of the sprue still occurs in this case, the liquid metal velocity at the ingate is constant, which represents an improvement comparing to iteration 1.

An unexpected problem that occurs using this design, is the high molten metal velocity profile when it hits the overflows. This problem can be explained by the high resistance that the molten metal encounters when it reaches the overflows, due to a very low outgate area. Even though this area was calculated using NADCA's gating manual, this can be increased in order to promote a better evacuation of the molten metal into the overflows.

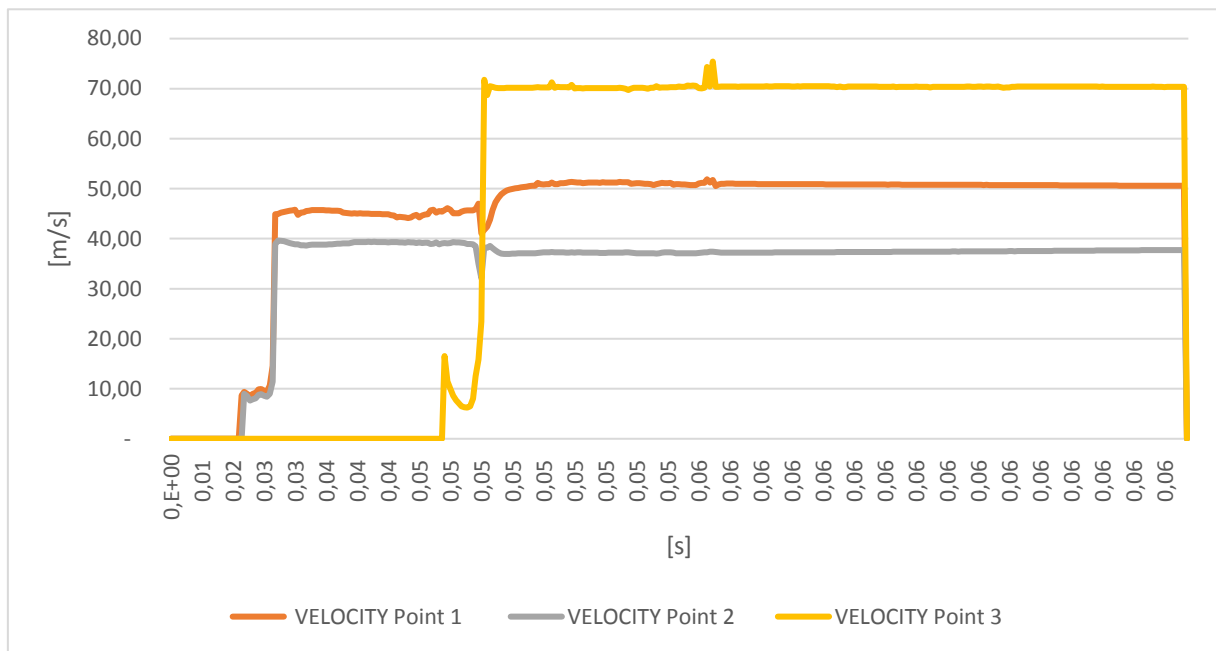


Figure 65- Molten metal velocity in function of die cavity filling time at 3 points.

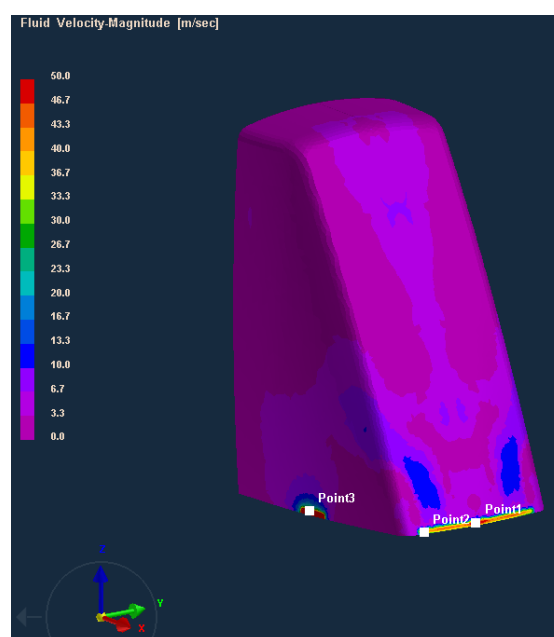


Figure 66- Molten velocity profile representing 3 different points.

The optimized gating system using NADCA’s manual resulted in a very positive prediction of air entrapments, presented in Figure 67. Analysing 3 different side views, it’s possible to observe that there’s a low quantity of air masses throughout the component, even on the overflows. This means that just by optimizing the gate-runner and main runner, the metal flow generated a low quantity of air during its path, and therefore smaller overflows would be as effective as the current ones. Reducing the overflows size will improve the metallurgical efficiency and therefore should be considered if this solution would be to implement in practice.

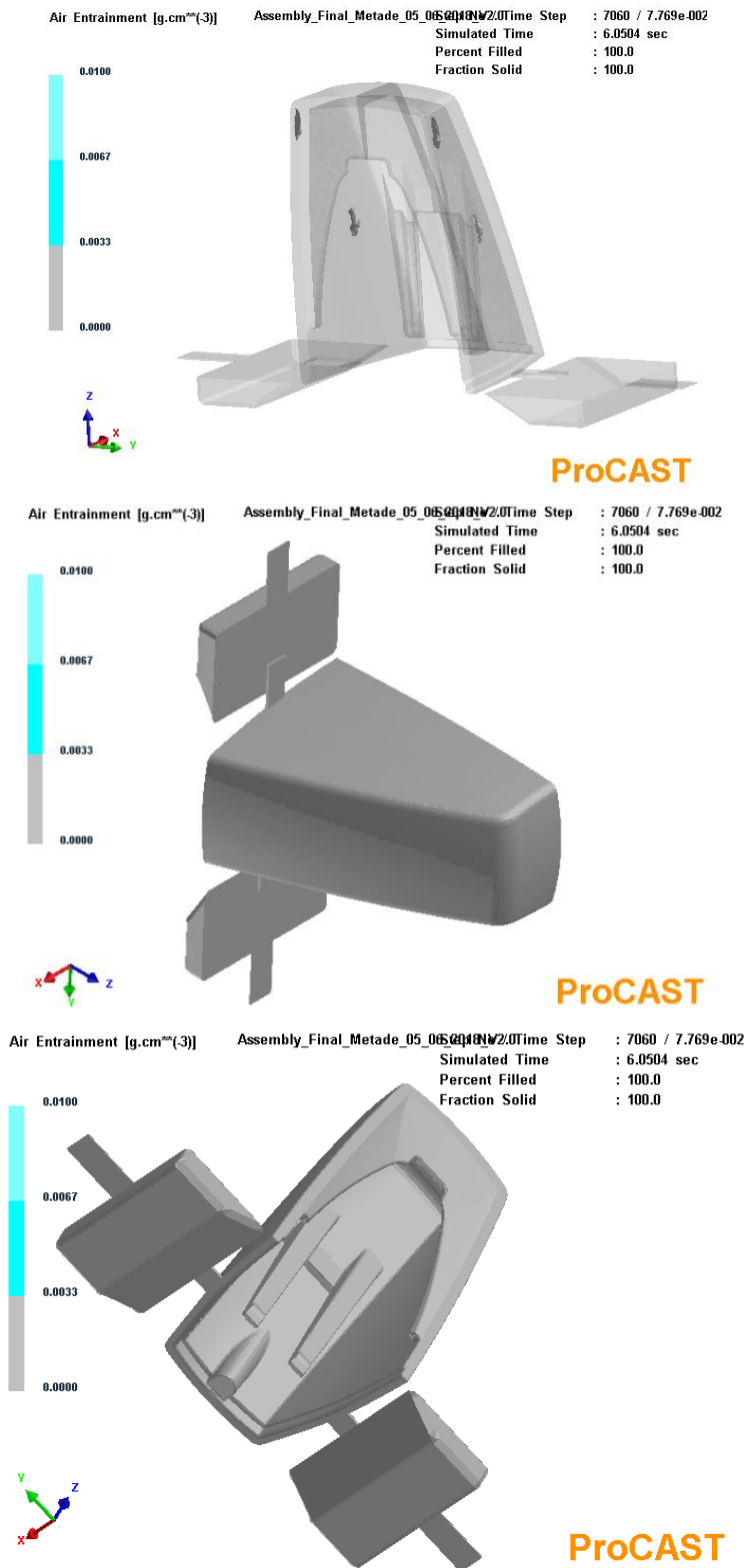


Figure 67- Air entrapment prediction using ProCAST™.

The purpose of iteration 2 was to analyse the difference between a gating system designed based on experience with another based on empirical rules. It was shown that a gating system designed using empirical rules resulted in less defects related to the filling process. For this reason, while experience plays an important role into gating system designs, empirical rules/calculations must be used.

In parallel to iteration 2, a new CAD model was developed by the company in order to take advantage of the existing die. The new gating system was designed so that the design from iteration 1 could be used. By changing the location of the overflow and increasing the side fan gate-runners length, the existing gating system machined into the die could be used. This procedure translates into a considerable cost reduction.

### 3.4.3 Iteration 3

Iteration 3 is a non-conventional gating system, since in general overflows are located adjacent to the dies parting line, for a posterior easy trimming. In this case, the die cavity is fed using every available space along the parting line with fan gate-runners, in attempt to minimize the occurrence of air pockets and metal front collisions. No empirical rules were used in the designing process. The CAD model is represented in Figure 68.

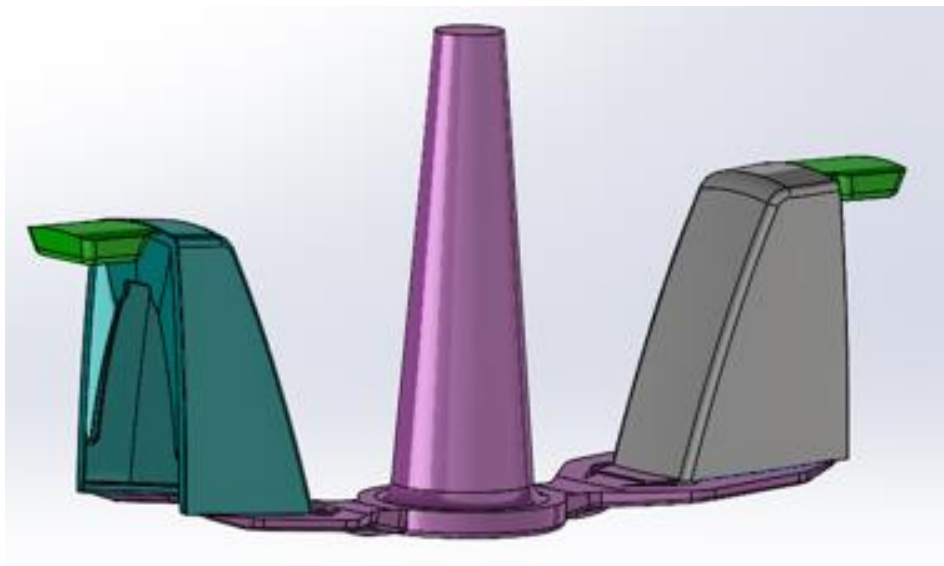


Figure 68- CAD model of iteration 3.

For this iteration, the same sprue from iteration 1 and 2 was used. For this reason, as shown in Figure 69, this element produces a non-uniform metal velocity profile. Other problem presented in Figure 69, is that the molten metal doesn't enter both gates at the same time. This can cause different solidification rates along different areas of the components, resulting in different solidified structures.

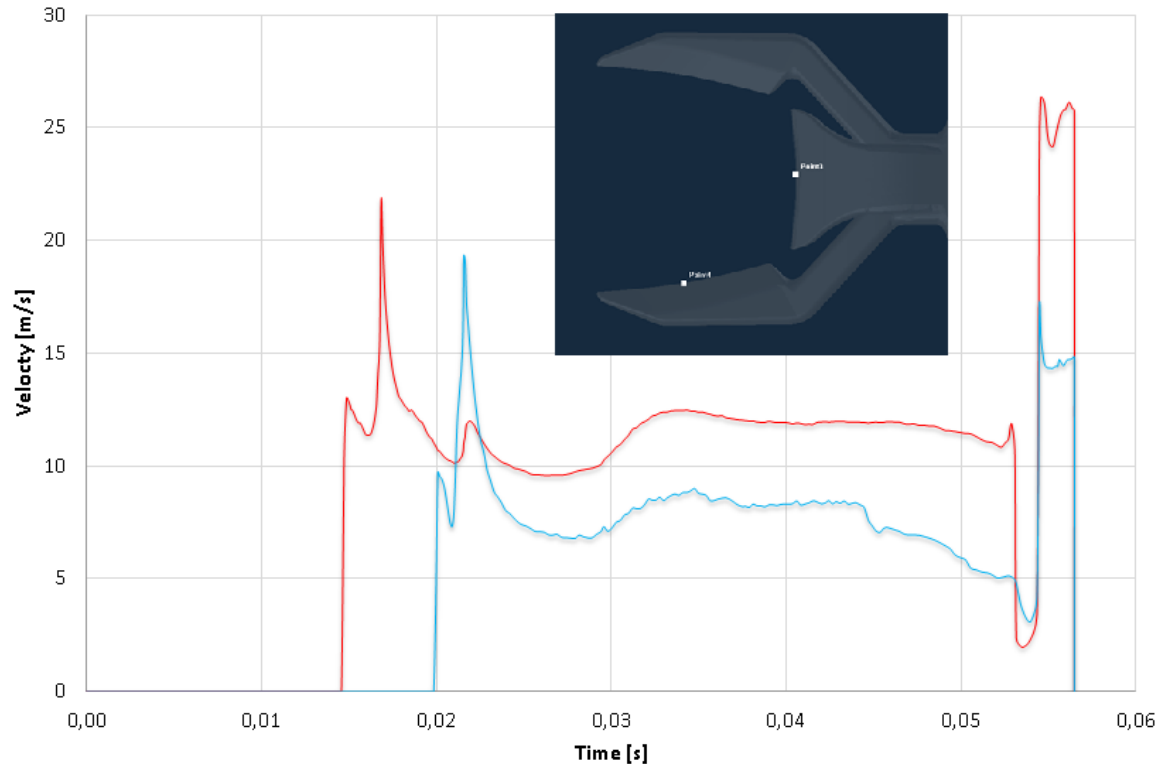


Figure 69- Molten metal velocity profile function to cavity filling time.

Figure 70 presents the metal flow velocity profile during the first injection phase. This system produces positive results, since a low amount of air pockets were generated and no aggressive metal flow front collisions occurred during the injection process. The ones that were created, were successfully pushed into the overflows. Also, the liquid metal has a flow path with no obstructions during the entire injection process.

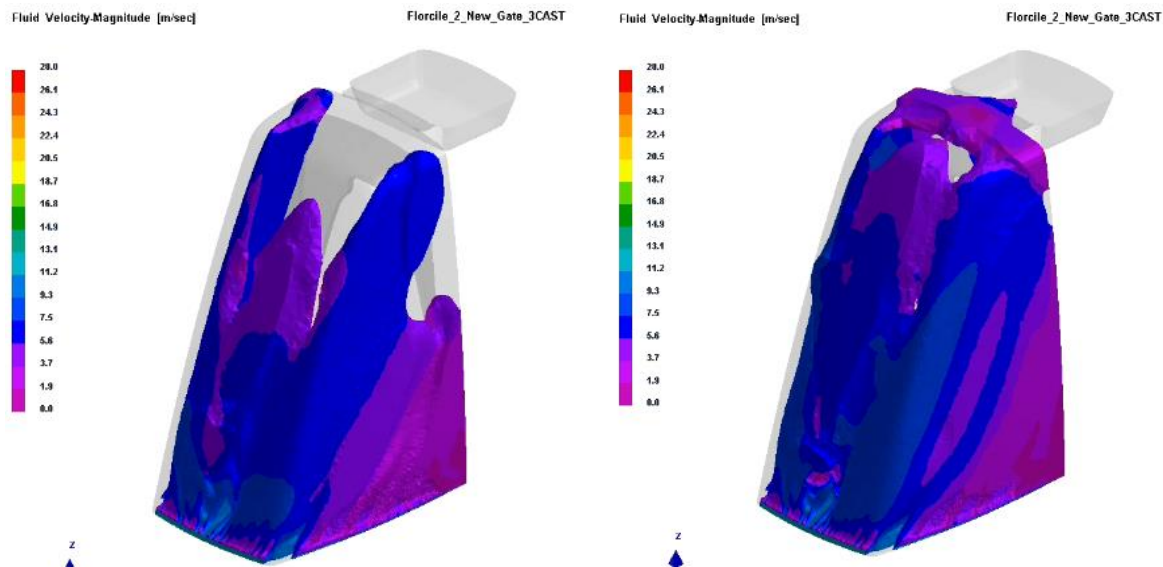


Figure 70- Metal flow in the components die cavity, representing the occurrence of air pockets during the injection process.

As shown in Figure 71, the air mass content throughout the component at the end of the injection phase suffered a great reduction when compared to iteration 1. This is a direct result from the overflow location and runner system modification.

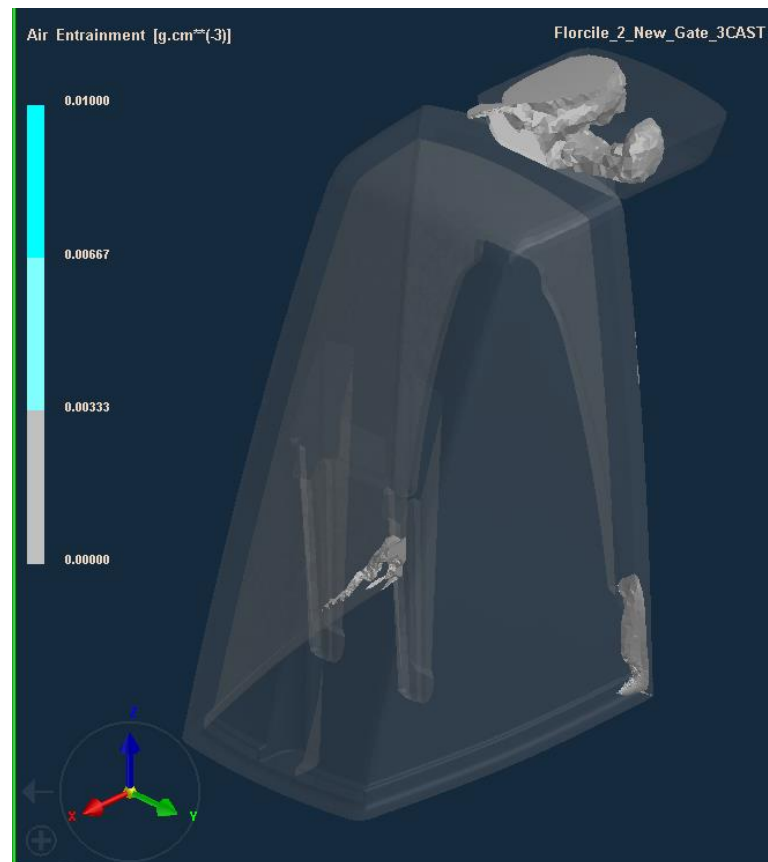


Figure 71- Prevision of air entrapments using simulation.

In this section, a different gating system design was presented. It consisted of changing the overflows location and increasing the side fan gate-runners length. Even though this solution still lacks an empirical designing approach, it is predicted that it generates less air masses throughout the component, due to less metal front collisions and air pockets.

This gating system was machined into the die, previously used in iteration 1, which allows for manufacturing cost savings. It was also implemented in a real production line, which led to first batches with a rejection rate of 5 %. Comparing to iteration 1, the components rejection rate decreased 30 %. These results are important, since the analyses made based on the simulation were validated experimental, which proves that the simulation software is somewhat accurate in the defect prediction.

#### 3.4.4 Conclusions

A total of 3 different gating systems were presented in this case study. Iterations 1 and 3 were designed by the company and iteration 2 by the author. Using the ProCAST™ software, parameters such as metal velocity profile; filling pattern; occurrence of air pockets; air entrapments; influence of the overflows were analyzed.

For each iteration, the same sprue was used. Since it doesn't converge from its entrance to the main runner, a non-uniform metal velocity profile will occur between the sprue and the main runner. Ultimately, the cross-sectional area of the entrance of the sprue has to increase so that the remaining gating system cross-sectional area can uniformly decrease until the gate.

During the analysis of the solution presented in iteration 1, typical problems emerged due to a non-optimized gating system: a non-converging gating system; non-uniform molten metal velocity profile and generation of air pockets and molten metal collisions during the filling process. Ultimately, these events result in air masses throughout the component. In the present study, these defects are highlighted during the painting process since these air masses expand, forming surface blisters. A possible solution to minimize these defects, while maintaining the gating system, is to increase the overflow volume.

Iteration 2 surges from the need of an optimized gating system, that minimizes the defects discussed above. The designing process followed empirical rules and calculations presented in section 3.3. Comparing to iteration 1, this optimized gating system resulted in a considerable reduction of air masses throughout the component. This highlights the importance of empirical calculations/rules in the designing process of gating systems. It is also important to state that even with a structured designing method, the designer's experience plays an important role to achieve an optimized gating system. Even though this solution benefits the reduction of filling related defects, in practice it results in higher production costs. Among the 3 iterations, iteration 2 has the lowest metallurgical efficiency, mainly due to overflow volume. It was also observed that the overflow volume could be reduced, while maintaining the porosity levels of the component.

An improved solution of iteration 1 was presented, which is predicted to cause less air entrapments during the filling process. This solution results in a similar mass content, comparing to iteration 2. Usually, the optimization of gating system based entirely on the designer's experiences, leads to a high number of incorrect die designs. For this reason, empirical rules/calculations for the designing process along with a simulation tool is the most optimal option for the optimization process of gating systems.

Even with optimized gating systems, the required porosity levels may not be achieved. In these situations, the application of the vacuum technology to the high pressure die casting process might be the solution. This process will be discussed in the next chapter.

## 4 Vacuum high pressure die casting

### 4.1 Vacuum die casting

Vacuum die casting process started being used for mass production in 1983 in Japan. In 1995, the Ultra high vacuum die casting process developed in Europe, to manufacture large and thin automotive parts such as pillars and space frames [78].

Even though there are no reported literature regarding vacuum die casting on zamak alloys, there are companies that already successfully performed this process. There are several reports addressing this topic mainly on aluminum and magnesium cold chamber die casting machine. Figure 72 represents two components manufactured with a zinc alloy using a hot chamber machine. The following solidified components are clearly represented: a sprue, where the metal entered the die cavity; runners and gate-runners, channels that lead the liquid metal from the sprue into the die cavity; component; vacuum runners attached to each overflow, connecting it to a mechanical valve solidified cavity.

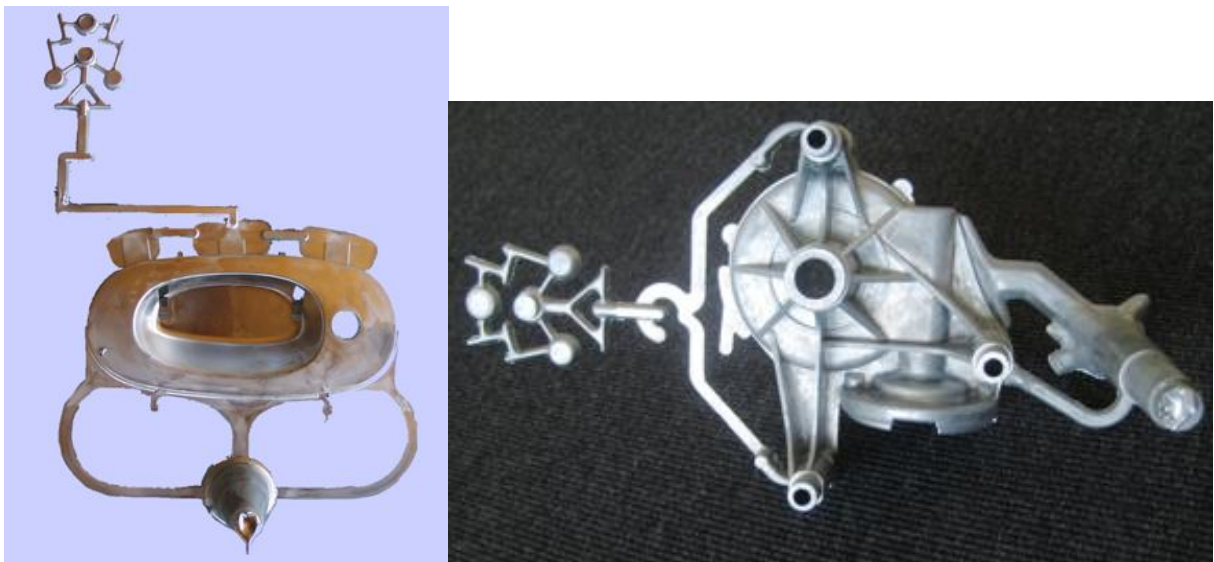


Figure 72- Two examples of Zinc alloy components produced by vacuum high pressure die casting (Courtesy of Fondarex) [79].

With this process, air is removed from the cavity during the injection process, resulting in parts with air porosity levels as low as 1 % [80]; higher pressure tightness; higher quality and surface finish [81] and higher mechanical properties when compared to a conventional high pressure die casting process. By removing air from inside the die cavity, the pressure drops from a typical 1013 mBar, atmospheric pressure, to 60-300 mbar for a vacuum assisted HPDC and < 60 mBar for a super-vacuum die casting. Die cavity vacuum levels or vacuum pressure as low as 5 KPa or 50 mBar have been reported to be achieved [82].

Figure 73 represents the differences between the conventional HPDC process with two variants of the vacuum die casting process.

The higher costs related to the additional vacuum system costs are justified since certain components, like structural and components that require post heat-treatment, cannot be manufactured by conventional high pressure die casting. Vacuum technology when applied to



HPDC, allows the cast components to be heat treated, which is a critical parameter for structural components or components with high mechanical property requirement, and welded [83; 84].

Process	Conventional HPDC	Vacuum-assisted HPDC	Super-vacuum die casting
Vacuum level	None	60–300 mbar	<60 mbar
Advanced vacuum monitoring and controls	No	No	Yes
Sealed die surfaces	No	Yes	Yes
Susceptibility to gas porosity	High	Low	Very low
Heat treatable	No	Yes	Yes

Figure 73- Comparison of conventional HPDC, vacuum-assisted HPDC and super-vacuum die casting [1].

Reports have shown that lowering the internal die cavity absolute pressure, by applying vacuum, has a positive effect on lowering the components porosity levels; reducing the pore size; better grain uniformization; improving mechanical properties such as ultimate tensile strength, yield strength and elongation; increasing components density and the microstructure of the cast component [82; 84-90]. Sharp pores negatively affects the mechanical properties since it acts as a stress concentrator while round pores minimizes this affect. Also it helps improving casting castability which is an important parameter when casting thin-walled components [91]. Reducing the die cavity pressure, by applying vacuum, promotes a better filling pattern and a higher injection velocity due vacuum suction forces [92].

Figure 74 represents the internal pressure and air mass evolution throughout a vacuum HPDC process. In this case, vacuum is applied at  $t = 0.2$  s after the first phase starts and the second phase starts at  $t = 1$  s. During both phases, an air mass reduction occurs while for the internal pressure the same occurs only at the first phase. This happens because at  $t = 1$  s, a rapid compression of the air volume takes place, which increases the internal air pressure. For this reason, the internal air pressure doesn't represent the existing gas in the internal die cavity [93]. Even though every die element should be perfectly sealed, a leakage area should be considered since it's impossible to guarantee a 100 % sealed die. A leakage area has major effects on the venting efficiency. As shown in Figure 74, it's possible to verify that by considering a leakage area, the minimum die cavity pressure is about 20 KPa, compared to the 10 KPa when not considering a leakage area. This can be explained by the fact that when an internal pressure of 20 KPa is achieved, the air evacuated from the evacuation device is roughly the same as the air that is drawn into the die cavity [93].



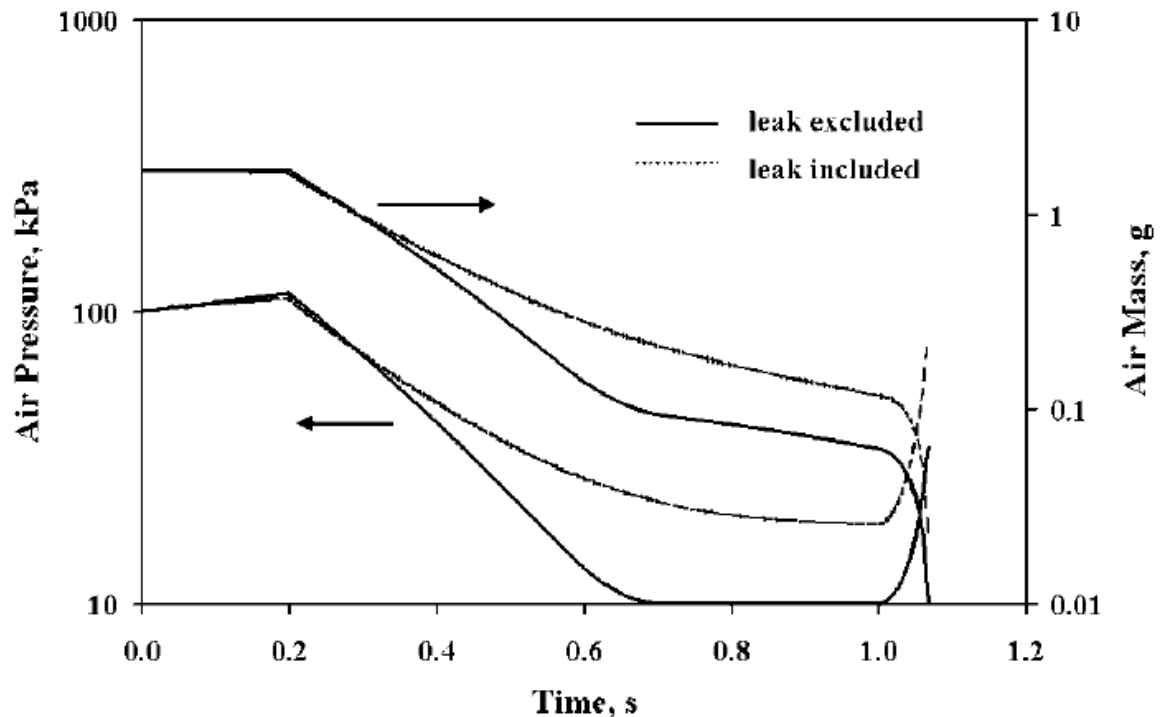


Figure 74- Case study presenting the internal die cavity pressure and air mass for a HPDC vacuum process including and excluding a leakage area [93].

A recent study evidences the possibility to further reduce the formation of gas porosities by controlling the plungers velocity in the first injection phase [94]. The slow shot speed effects the vacuum pressure in the die cavity and the flow behavior inside the shot sleeve.

Two different multi-steps (two-step and three-step) and a constant slow shot were analyzed in order to determine the influence on the parameters mentioned above. Despite that the dwell time ( $t$ ) of the molten metal was higher on the three-step slow speed, it had a greater influence on the vacuum pressure of all three experiments. The vacuum pressure in this case was the lowest of the three, resulting in lower levels of gas porosity of the specimens produced [94].

ESCs (externally solidified crystals) occurs only on the cold chamber process and are defined as crystal's as large as  $200\text{ }\mu\text{m}$  with a dendrite form. They are produced during the ladling of the molten metal into the shot sleeve, duo to the fast heat transfer between the liquid melt and the shot sleeve [95]. These crystals when injected into the die cavity can either be remelted or continue to grow because of the local undercooling [96]. Controlling the formation of these crystal is particularly important, since they can induce the formation of porosities and can also act as a crack initiator, therefore compromising the mechanical properties of the cast component.

#### 4.1.1 Effect of different slow shot speeds on the vacuum pressure and tensile properties

A recent study [97] analyzed the effect of different plunger speeds in the first injection phase (from 0.1 to 0.4 m/s), on the internal die cavity pressure, the components mechanical properties and distribution of air porosities. For this study, a AZ91D magnesium alloy was casted in a 200 ton cold chamber machine. The following situations were observed:

- Figure 75 presents the vacuum pressure function to the plunger's velocity during the first injection speed. It can be observed that higher plunger velocity, during the first injection phase, increases the die cavity pressure before the second phase starts. This evolution follows a cubic polynomial expression;

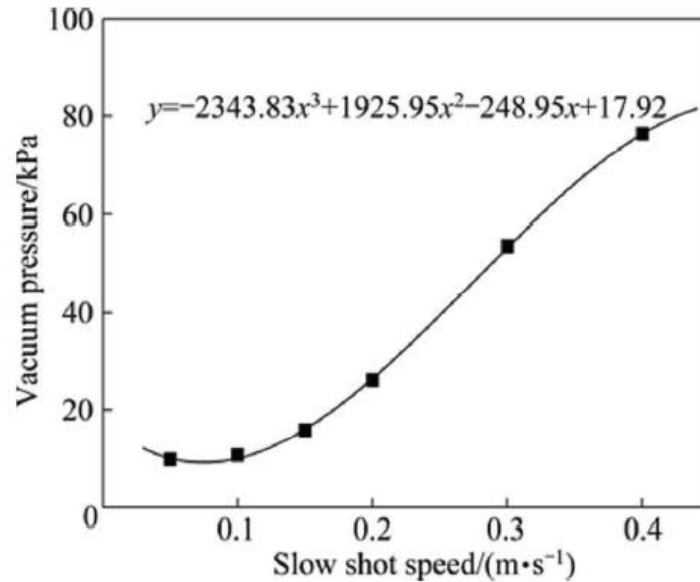


Figure 75- Die cavity pressure with respect to different slow shot speed [97].

- Figure 76 presents the average air fraction evolution, for a conventional and vacuum die casting process, function to the plunger speed in the first injection phase. As shown, a higher slow shot speed increases the porosity levels in a vacuum and conventional die casting process. A probable cause is a decreasing vacuum level in the die cavity at the beginning of the filling. From the literature [97], it is known that a higher vacuum level or a lower internal pressure, less air entrapments are generated in the filling process. It is also visible the benefits of vacuum die casting over the conventional die casting. By using vacuum in die casting, the percentage of gas porosity decreases considerably;

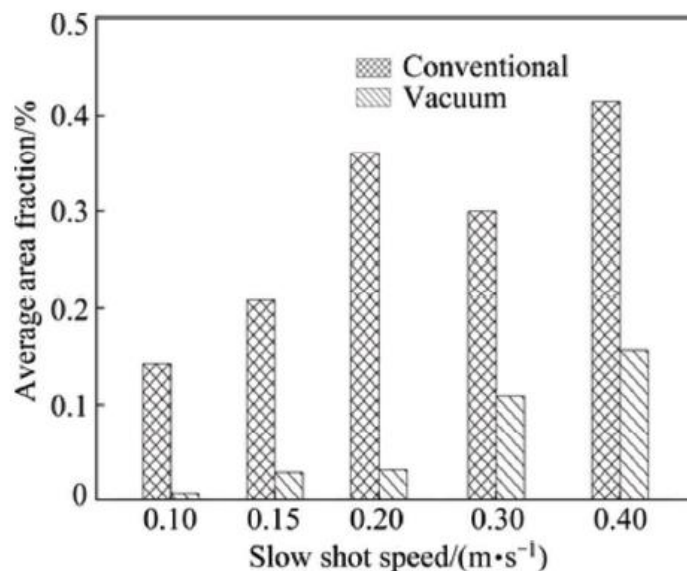


Figure 76- Average area of gas porosity with respect to different slow shot speeds [97].

- Figure 77 presents the components tensile properties evolution function to different plunger velocities during the first injection phase. From plunger's velocities of 0.10 to 0.15 m/s and from 0.20 to 0.40 m/s, the tensile properties increase while from 0.15 to 0.20 m/s decreases. These variations are similar for the conventional and vacuum high pressure die casting pressure. These results are in accordance with the results observed in Figure 75 and 76. Overall, a high plunger velocity in the first injection speed increases the average fraction of air porosity and internal die cavity pressure, which in turn deteriorates the components tensile properties. An optimal slow shot speed shot for the vacuum die casting process, that produces parts with better tensile properties, is 0.15m/s. This is primary related to a good balance between low values for gas porosities and die cavity pressure when the second injection phase starts. It is also visible that die casting with vacuum when comparing to a conventional, produces components with higher tensile properties and ductility.

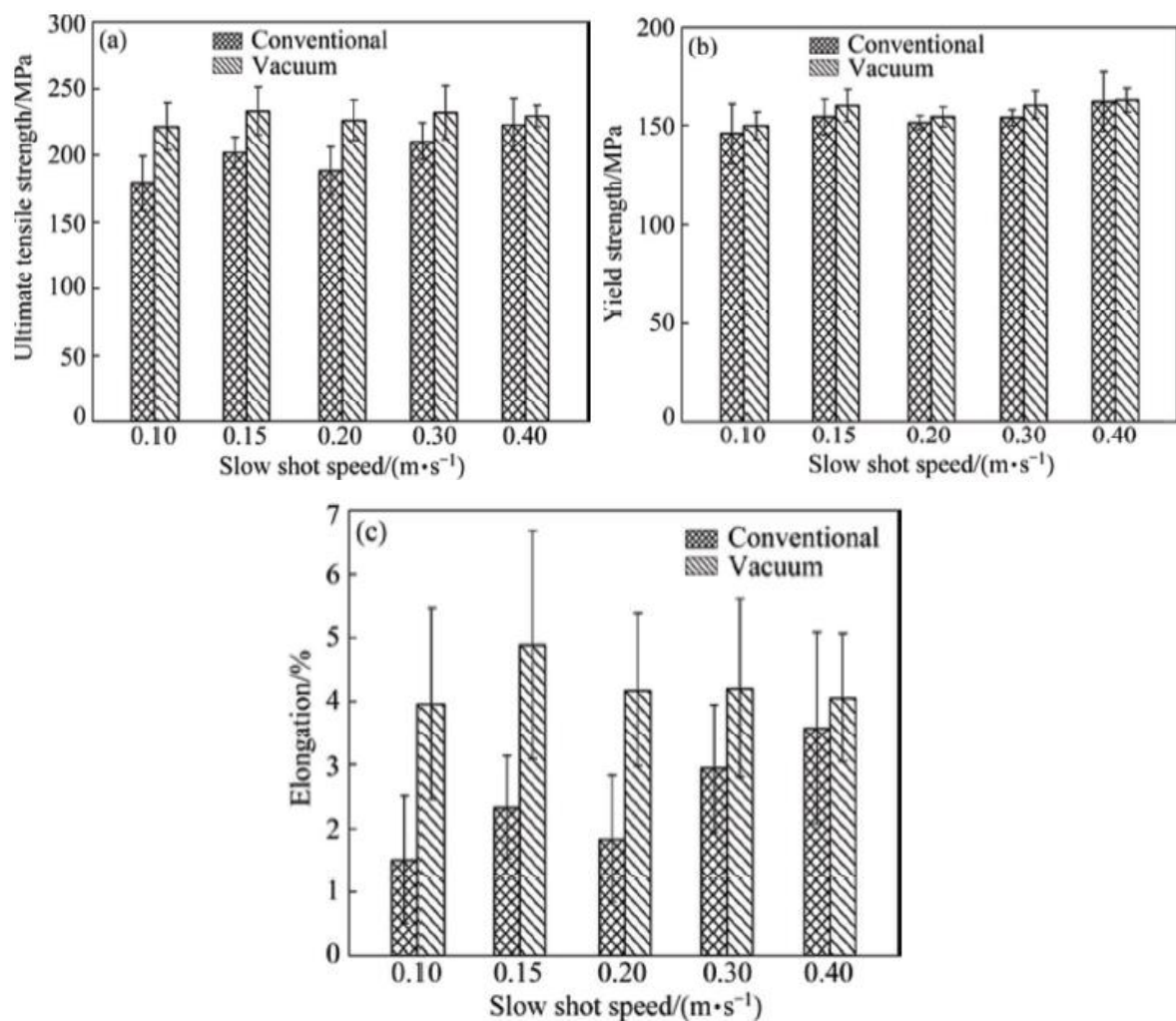


Figure 77- Influence of different slow shot speed on mechanical properties: UTS, YS, elongation [97].

#### 4.1.2 Influence of the second injection phase on the mechanical properties

Figure 78 presents the influence of the velocity at which the molten metal passes through the gate, on the components mechanical properties such as tensile strength, hardness and

elongation. It can be observed that increasing the gate velocity from 16 - 26 m/s has a better effect on improving mechanical properties, compared to values above that range, such as tensile strength and hardness. Elongation was other analyzed property, and it has a linear dependency on the gate velocity. With these results, a critical gate speed of 26 m/s can be identified which enables optimum mechanical properties. With lower injection velocities, the probability of occurring a liquid metal premature freezing is higher compared to higher velocities. In this case, the gate is partially or completely blocked and therefore the remaining metal has difficulties to enter the die cavity. This leads to low mechanical properties mainly due to the existence of shrinkage and gas pores that weren't fed by applying intensification pressure. With a higher injection velocity, this scenario is avoided due to higher metal momentum that enables a better die cavity filling [84].

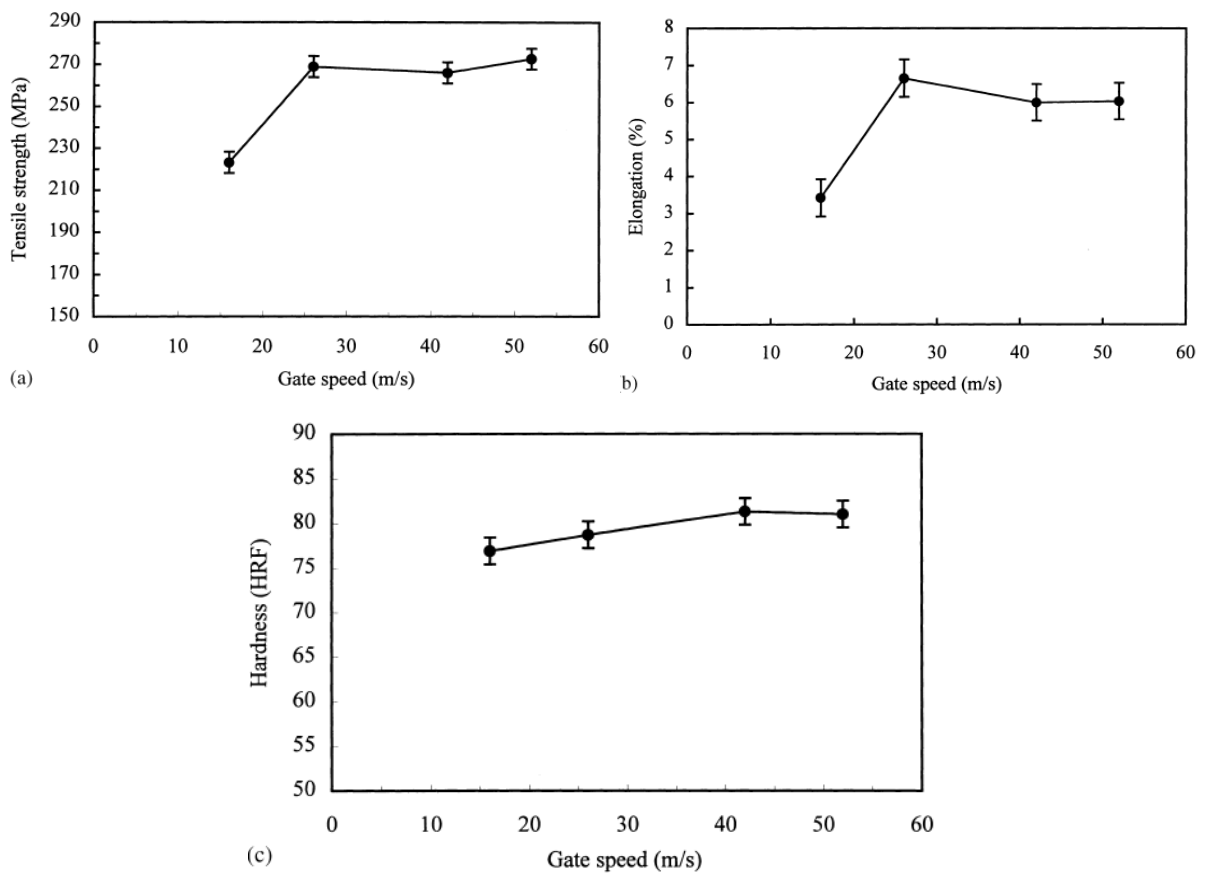


Figure 78- Mechanical properties variation with respect to different gate velocity [84].

## 4.2 Case study of an incorrect vacuum gate system design

The main constraint during the evolution of vacuum high pressure die casting has been the development of a reliable shut-off valve and guaranteeing a close to 100 % seal of the die cavity through the parting line, slides and ejector pins and other components that can develop air leakage.

Also, an inefficient vacuum gate system design, due to trial and error methods, presents a problem guaranteeing quality [92]. An example of this problem is presented in Figure 79. With this vacuum gating design, the vacuum outgates A and B are blocked when the die cavity is 70 % filled, greatly reducing the air venting capacity. An optimization of the vacuum gating

system, represented in Figure 80, led to a different solution which improved the air venting efficiency.

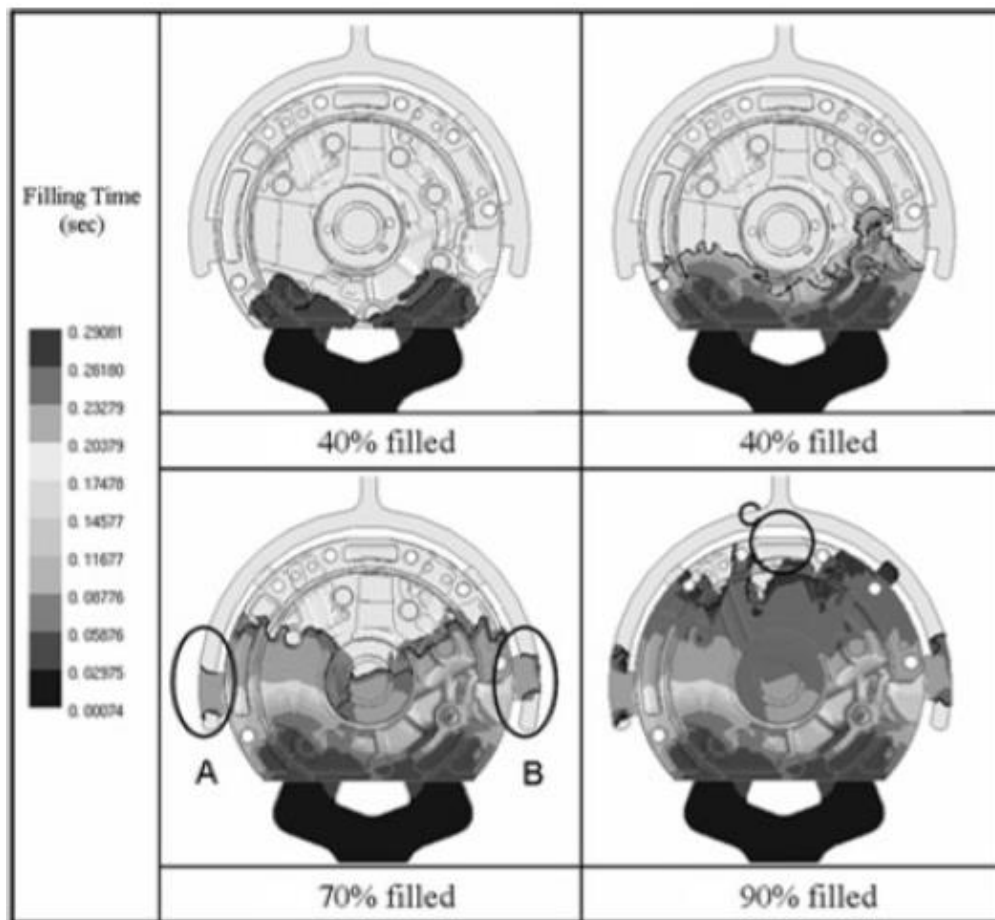


Figure 79- Incorrect vacuum gating system design, with blocked zones A and B [92].

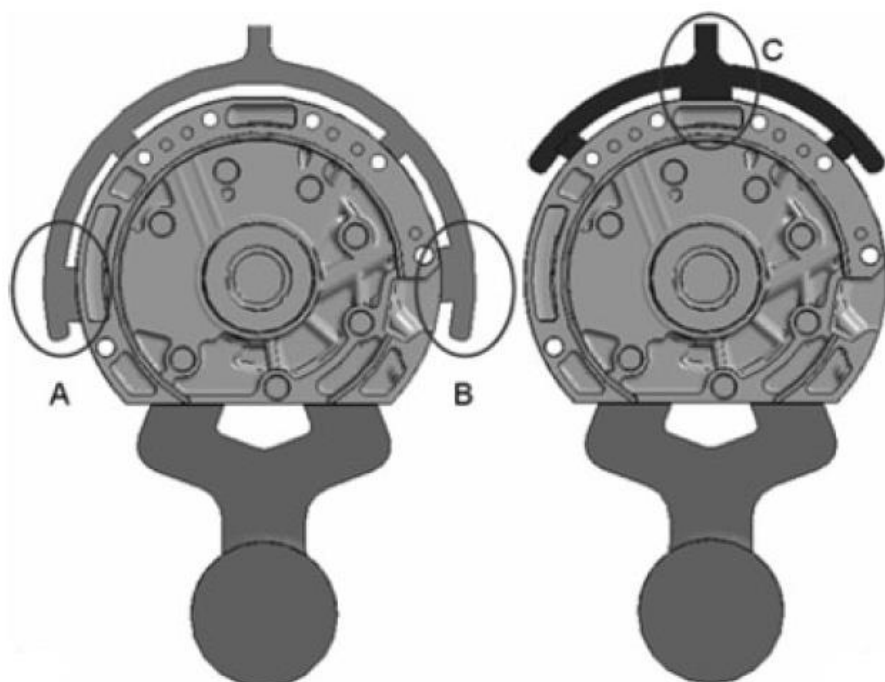


Figure 80- A- Incorrect vacuum gating design; B-Optimized design [92].

### 4.3 Vacuum die casting system

Figure 81 describes a typical vacuum die casting system. It uses a conventional die casting machine with the addition of a system with the following components: vacuum pump, being the most common a rotary vane vacuum pump; vacuum shut-off valve, that prevents the metal entering the pump; vacuum control system; vacuum tank and an unvented die [4].

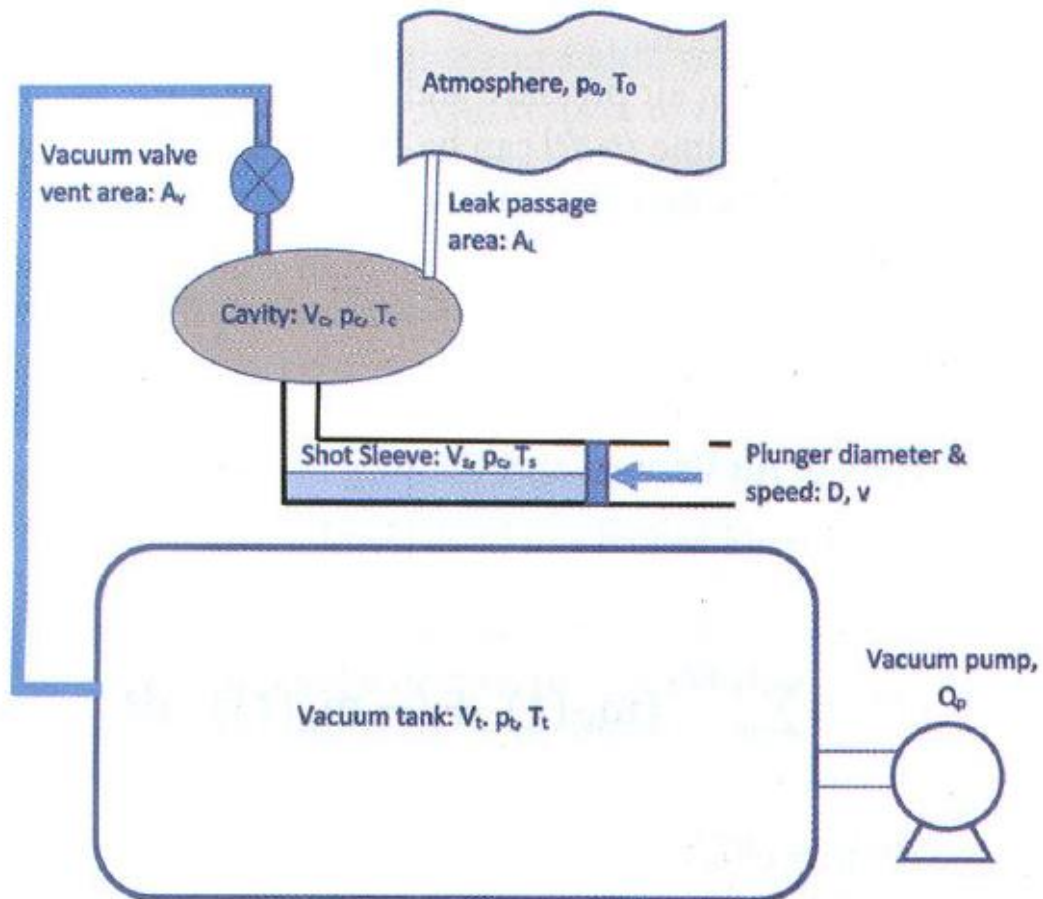


Figure 81- Vacuum die casting system [98].

The volume of the vacuum tank is larger when compared to the die cavities volume and must maintain a pressure of about 1 mBar. This ensures the required evacuation capacity, a high level of vacuum in the die cavity and an effective removal of impurities and dirt after the shot [99].

The size of a vacuum pump must be in accordance with the amount of air that has to be extracted from the die. The sizing procedure uses a vacuum pumps characteristic operation curve, which matches the required volume of air needed to be extracted with the vacuum level [99].

Vacuum should be applied to the die as long as possible, which maximizes the air extraction. As a result, the location and type of vacuum shut-off valve is an important process control parameter. The vacuum shut-off valve is connected to the die cavity by a runner. A gate, connecting the runner, should be located in the last filling location in the die cavity.

There are two types of vacuum shut-off valves [4]:

### 4.3.1 Static vacuum shut-off valve

Characterized by having no movable parts, high thermal conductivity material and internal cooling channels, it allows air to vent from the die cavity during metal filling and can be used as a simple vent or connected to a vacuum pump. Even though it lets air through the outgate, it protects the vacuum system using a thermal gradient, since the liquid metal that passes through solidifies due to multiple direction changes. They're characteristically a robust, low cost and maintenance valve, but hard to maintain during production, since the chill block must be kept clean to maintain a correct gas flow. Another downside is the existing lag between the vacuum pump and die cavity, that can reach up to 50 ms. Also, its venting efficiency is limited by its reduced venting area. This parameter can be improved by using multiple chill blocks or by increasing the chill blocks dimensions, which increases the die projected area. Consequently, the components size is reduced for the same die casting machines capacity. A common dynamic vacuum shut-off valve is the corrugated chill block, presented in Figure 82. It is basically a two half-block, with a clearance between blocks of 0.5 - 1 mm, made of steel or copper. When both halves are engaged, air is vented through a zigzagged gap machined in each face [99; 100].

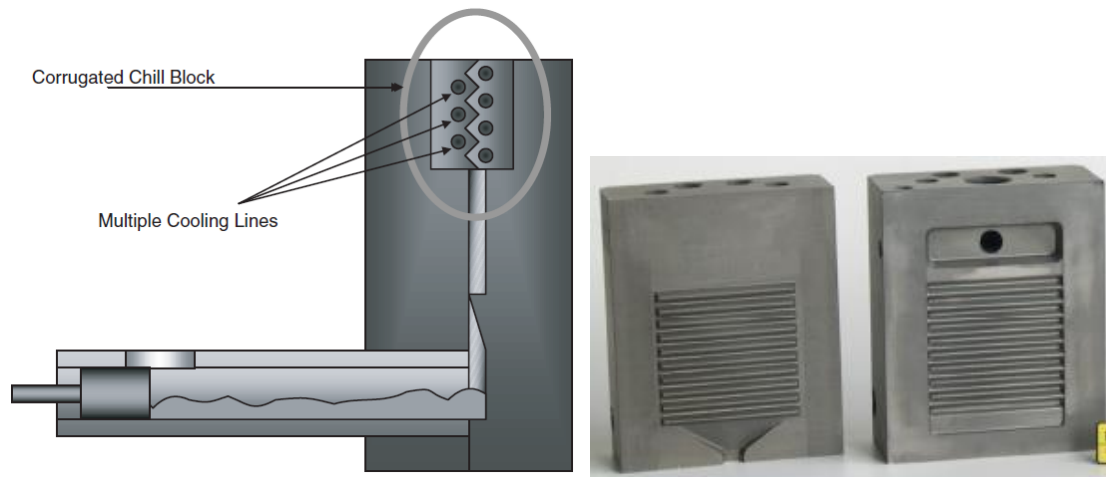


Figure 82- Left- Schematic of a corrugated chill block [4]; Right- ProVac chill vent [99].

Chill blocks differ from each other by its cross-sectional shape. As shown in Figure 83, a chill block may present a trapezoidal or triangular cross-sectional shape. From recent studies, it was proven that this parameter has a major influence on the evacuation efficiency, with the triangular cross-sectional shape presenting the highest efficiency. This happens because the trapezoidal cross-sectional shape has higher flow redirections, which increases the flow resistance when compared to a triangular cross-sectional shape. In terms of the distance that the flow travels in the zigzag gap, it is predicted to be the same for both profiles [101].

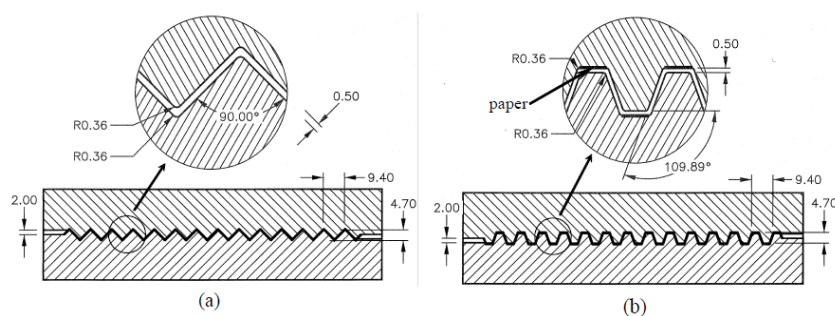


Figure 83- Left: Chill block with a triangular cross-sectional shape; Right: Chill block with a trapezoidal cross-sectional shape [101].



### 4.3.2 Dynamic vacuum shut-off valve

With movable parts, these type of valves offers less resistance to air when compared to static valves, due to higher cross sections. They're divided into mechanical and actuated valves [4]:

The mechanical valve, which is the simplest of all dynamic valves, opens when the die halves closes, and then vacuum can be applied to the die. During the die filling with molten metal, the internal pressure increases until a preset pressure closes the valve, with a response time up to 10 ms. This allows an air extraction from the die cavity up until the last moment of the injection process, making it an efficient vacuum system. Die casting is characteristically a very efficient but harsh manufacturing process. The efficiency is related to the capacity of mass producing components that requires a low post-casting machining. Die casting is a process that deals with many extreme conditions such as high temperatures of the molten metal; high injection and intensification pressures and turbulent flows due to high metal flow velocities. To maintain a process consistency, a robust mechanical valve is required. However, due to a high number of moving parts, the existing mechanical valves are susceptible to malfunction and are quite expensive. [4; 100].



Figure 84- Mechanical shut-off vacuum valve with the Typhon vacuum runners [99].

A special runner, that connects the overflow to the mechanical valve, is required to control the metal flow, avoiding a direct impact to the valves triggering system. This is critical to avoid a malfunction of the valve. Runner design problems emerge from this requirement, since no widespread specific design rules exist. An example of a vacuum runner is presented in Figure 85 [100].



Figure 85- Vacuum runner for a mechanical vacuum valve [100].



Dynamic actuated valves can be either electrical or hydraulic, piloted by the die casting machine, with reaction times of 8 - 10 ms and 120 - 150 ms respectively. Two examples of dynamic actuated valves are presented in Figure 86. Vacuum system which incorporate these valves are often called as simple vacuum systems [93]. These valves offer low resistance to air evacuation due to high cross-sectional areas. This is the most controllable vacuum die casting process and are activated by a signal, triggered by the plunger position or the metal front position. By using electronic controllers, the plunger position can be monitored, and therefore vacuum can be applied to the die by opening the valve, right after the plunger starts displacing. The valve should be kept open as much time as possible, to remove as much air as possible and more importantly to avoid that air is drawn back into the die cavity through leakage areas after the valve closes. This leak will decrease the vacuum level and the end of the injection process at a rate of 230 mBar/s. For this reason, the system is programmed so that the valve closes right before the liquid metal reaches it [4; 93; 100].



Figure 86- Left: Electro-pneumatic valve [102]; Right: Hydraulic vacuum shut-off valve [4].

#### 4.3.3 Choosing the evacuation device

A common dilemma in the vacuum die casting industry is choosing the most suitable type of vacuum evacuation device to obtain high-quality products and to be able to monitor the consistency and performance of the process, for repeatability, safety, statistical process control. There are 3 aspects to be considered when choosing an evacuation device: technical criterion for the choice; monitoring this criterion and practical considerations such as reliability and ease of maintenance [99].

The criterion is the level of vacuum or pressure of the die cavity when the molten metal enters the die cavity at end of the pistons first phase of injection. To choose the most suitable evacuation device for a desired level of vacuum, the critical evacuation section must be equal for a comparing parameter. This represents the smallest section that the exhausting gas passes through and is affected by the size of the evacuation device. The most suitable evacuation device is directly dependant on the quality of the casting. A comparison of the performance of a vacuum valve and a chill vent, with the same critical evacuation area, is illustrated in Figure 87 [99].

By analyzing Figure 87, the vacuum valve has a higher performance in terms of achieving a die cavity pressure in less time, when compared to a chill vent. In other words, a vacuum valve is 2 to 3 time faster in terms of air evacuation comparing to a chill vent. This aspect is very important in relation to casting quality since a higher level of vacuum translates into a higher part quality. These die cavity pressure measurements were carried out in a highly scientific laboratory, with a continues measurement at the die cavity and at the evacuation device and can't be implemented in an industrial process. Other important aspect is that even though performances between the evacuation devices are different, the pressure measured at the vacuum valve or chill is the same. This is particularly important, since normally pressure is only measured at the vacuum extraction devices [99].

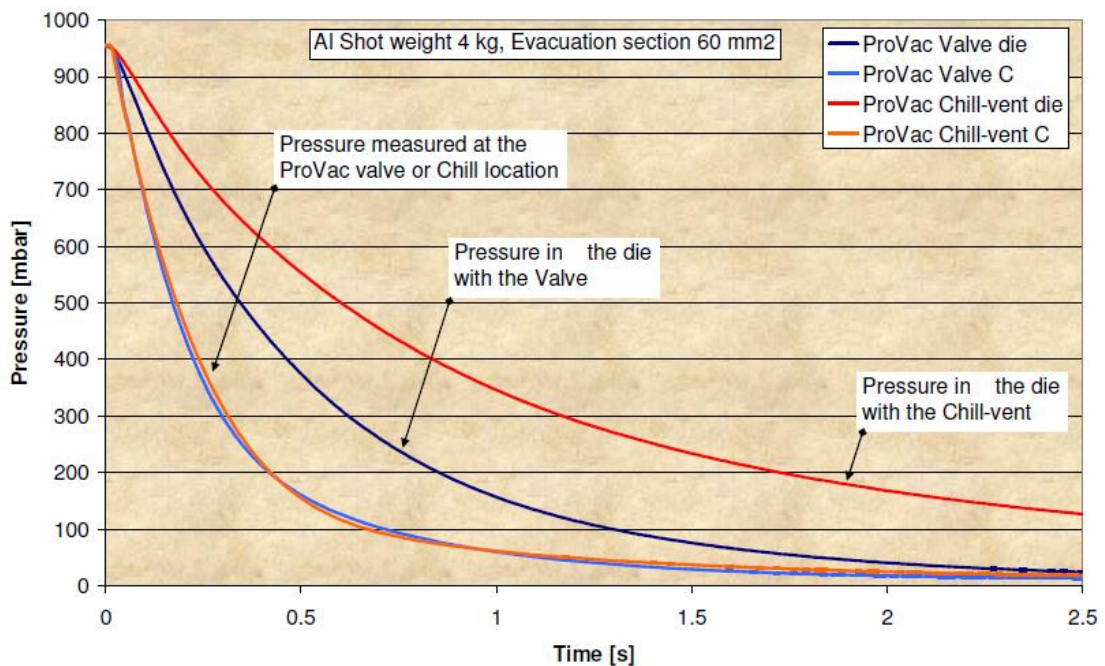


Figure 87- Performance comparing of a vacuum valve and chill vent [99].

A valid measurement of a mechanical vacuum valve that can relate to a vacuum level measurement is presented in Figure 88. As the authors refer, when the aspiration piston closes the aspiration hole, the hole for the measurement of vacuum is closed at the same time. The last pressure before the closure is the measured levels of the vacuum, and this value is recorded and stored. A method is presented in the same report for the case of a chill block, but it ends up being an invalid measurement and therefore not mentioned in this report [99].

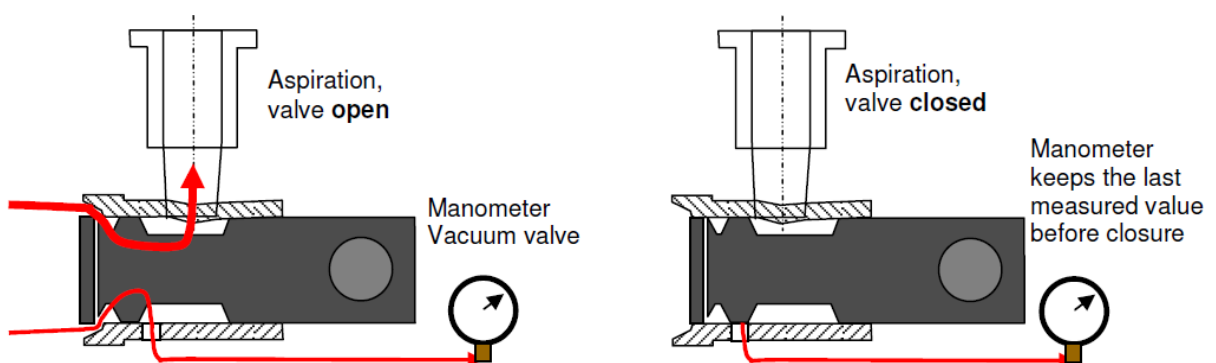


Figure 88- Pressure measurement of a vacuum shut-off valve. Left: Aspiration is opened; Right: Aspiration is closed [99].

Other important aspect to ensure a correct evacuation process for an evacuation device, are the vacuum runner dimensions. Runners must be machined into the ejector die from the overflows or die cavity and must converge, in terms of side runner section and the total gate section area, to the extraction device. This means that the main runner section should be similar or slightly bigger than the critical evacuation section area [99].

Figure 89 compares a chill vent to a vacuum valve from various points of view. A mechanical vacuum valve is a must when a higher quality part is desired even though it represents a higher investment and maintenance cost. A chill vent can still be a better choice over a mechanical vacuum valve when the quality requirements are not high.

High-speed vacuum valve	advant -age	Chill vent	advant -age
High evacuation capacity	yes	Reduced evacuation capacity	
Feedback by vacuum measurement	yes	Wrong feedback	
Security excellent if a high security valve is used	yes	Security excellent if process well under control	
“Low” maintenance		“No” maintenance	yes
Low projected surface	yes	High projected surface	
Aspiration check and readiness for the next shot	yes	No readiness check	
Not sensitive to casting parameter increase	yes	Sensitive to high speed increase or other casting parameter increase	
Affordable cost		Low cost	yes
Satisfies all advanced requirements	yes	Does not satisfy all advanced requirements	
Good process repeatability	yes	Limited process repeatability	
High technology		Old technology	

Figure 89- Differences between a mechanical valve and a chill vent [99].

#### 4.4 CASTvac

Much of the research put into the vacuum systems, is to improve the existing evacuation devices or to create new ones. A new evacuation device was presented 2003, known as CASTvac or a three-dimensional chill vent, which is similar to a conventional chill block. Trials have been conducted on production machines for extended periods, producing thousands of high quality components.

The principal difference is that the zigzagged gap is perpendicular to the die parting line, unlike with the conventional chill vent that is parallel. With this solution, it's possible to have more chill faces, when compared to a chill block with the same dimensions, without increasing the die projected area. It also consists of two die halves (Figure 90. left), and when engaged a vertically corrugated and horizontally wedge-shaped venting gap is created. Like the conventional chill vent, when the metal enters the inlet at the bottom, it loses heat while it flows in the gap section, where it solidifies. Also, this can be incorporated in a vacuum system through the vacuum ports, one on each side, Figure 90. right [100]. Like a conventional chill block, it has no moving parts which never fails to close off the vacuum path.

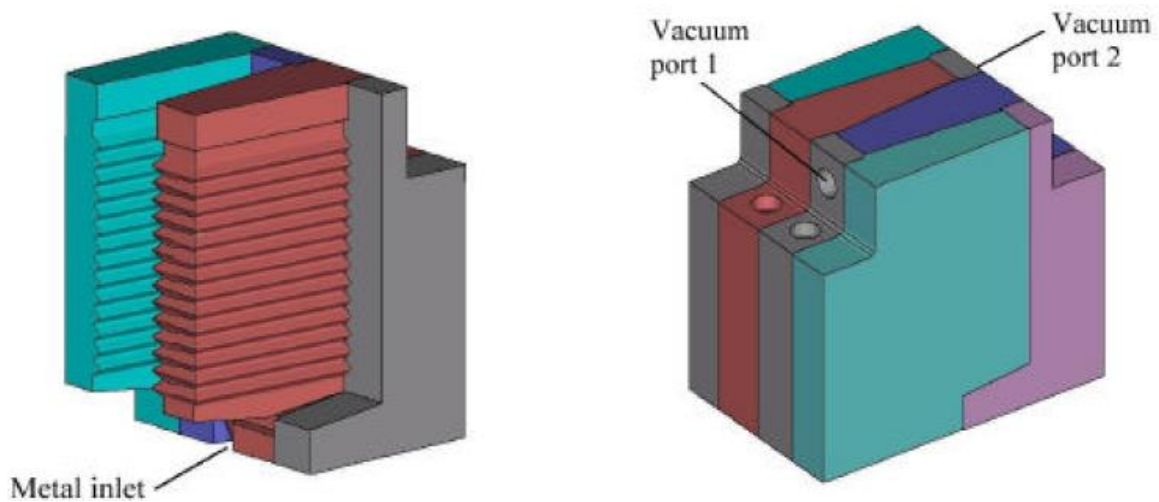


Figure 90- Left: Representation of one half, consisting of wedge-shaped inserts; Right: Engagement of two halves [100].

CASTvac presents the following advantages [100]:

- **Robust.** This is a common characteristic for every static shut-off valves, that has no movable parts. It's also a very reliable evacuation device, since it will never fail to close off the vacuum path;
- **Low cost.** It's a cheaper valve when compared to a mechanical valve and besides, using this valve, rarely introduces machine stoppages and maintenances, thus saving money during the production process;
- **Efficient.** Air extraction happens up until the die cavity is completely filled, which helps to maintain a high vacuum level. Figure 91 compares the efficiency between a CASTvac with a mechanical vacuum valve. With four times the cross-sectional area of the venting path when compared to a conventional chill vent, a higher vacuum efficiency is achieved. Also, it has the same efficiency when compared to a mechanical valve;

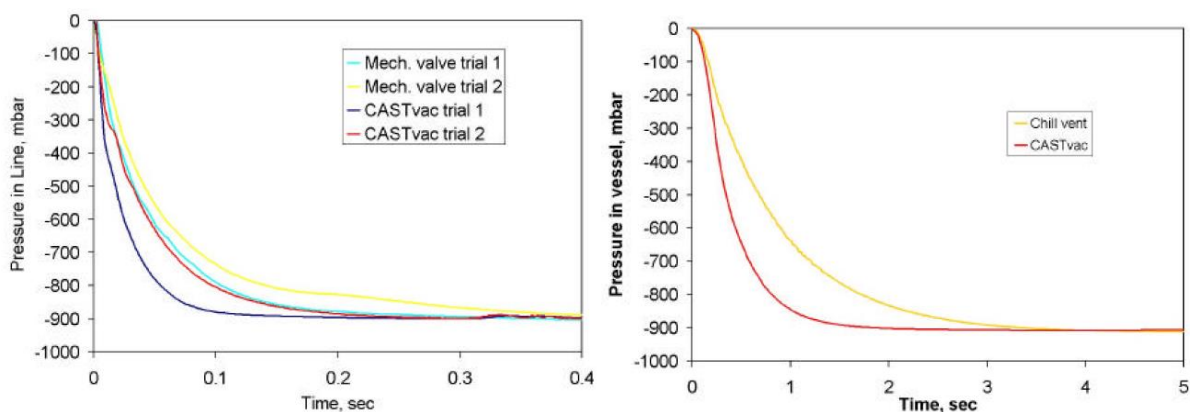


Figure 91- Left: Pressure changes in the vacuum line for a mechanical and a CASTvac valve; Right: Pressure changes in a 3L vacuum vessel for a chill vent and a CASTvac [100].

- **Simple.** Is easier to use when compared to a mechanical valve, since no vacuum runners are required;
- **Easy to adapt.** Occupies the same space of a mechanical valve in the die;

- **Flexible.** When an insert is damaged, only that piece has to be replaced. As shown in Figure 92, a CASTvac fits in the die just like a chill block.

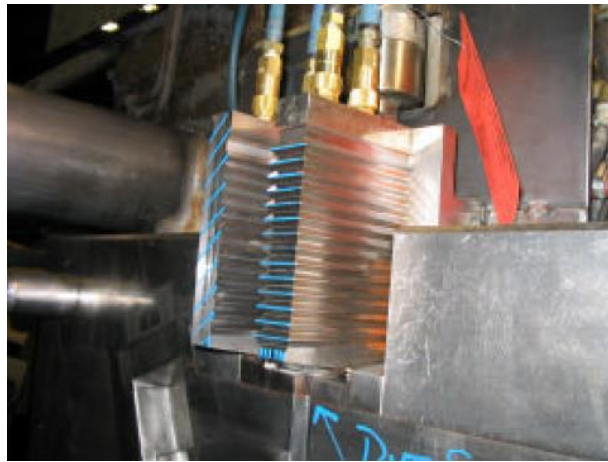


Figure 92- CASTvac installed in a die [100].

A study presented the differences between the venting efficiencies of different venting methods with different evacuation devices, including the CASTvac. These results are presented in the Figure 93 and 94 [93].

The first injection phase plays an important role for the vacuum HPDC process since the highest air extraction occurs during this phase, as there's more time available when compared to the second injection phase. Using both evacuation devices with natural venting, air masses are linearly reduced during the first injection phase. In this study, at the end of the first phase, 62 % of the existing air was extracted using a CASTvac and 61 % for a chill block, both as a vent. The differences in efficiency are accentuated during the second injection phase. Using a CASTvac, 5.8 % of air remained in the cavity, while with a mechanical valve 20.6 %. These results suggest that the CASTvac as a vent becomes more efficient during the second phase. When these evacuation devices are connected to a vacuum system, the greater venting efficiency of a CASTvac becomes more evident when compared to a chill vent. The venting efficiency of a CASTvac when connected to a vacuum system increases 31 % compared to a natural venting, and 10 % for a chill block [93].

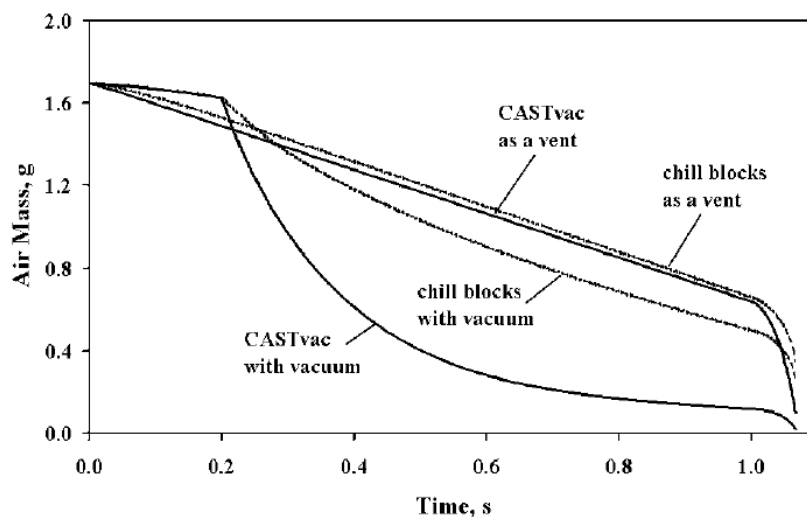


Figure 93- Different venting efficiencies for a CASTvac and a chill block with natural and vacuum venting [93].



From the same case study, the final air mass content was evaluated for different evacuation devices and venting methods. Besides the results discussed above, a CASTvac as a vent has nearly the same venting efficiency as a simple vacuum system, with an actuated valve [93].

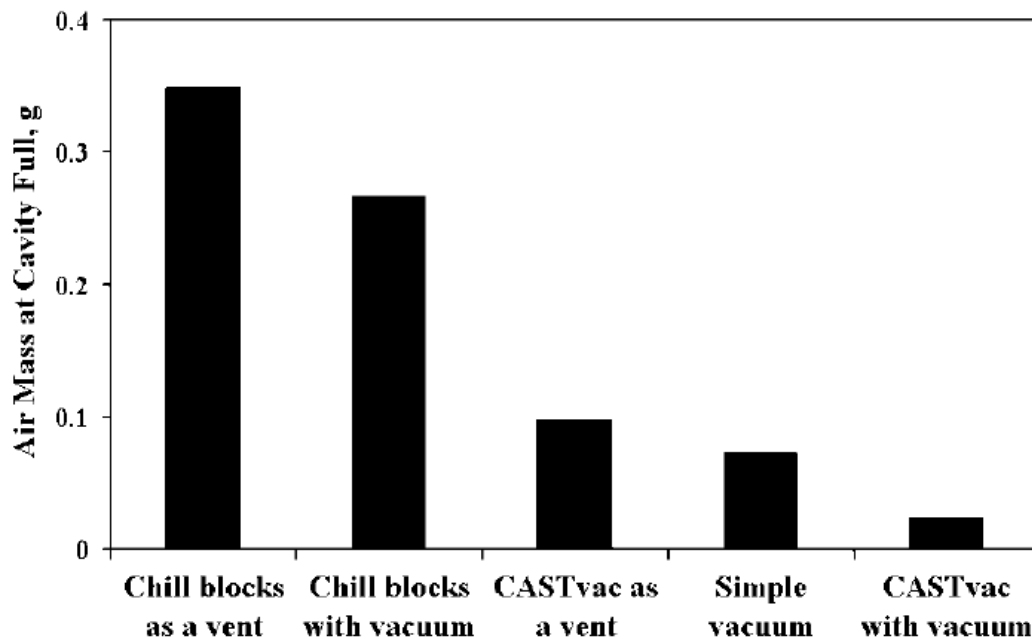


Figure 94- Different venting efficiencies with for different venting methods and evacuation devices [93].

In terms of its capabilities, CASTvac is an optimal choice to reduce air masses using natural venting. Further studies are necessary to determine its effectiveness on a continuous production machine.

#### 4.5 Gibbs die casting machine

Even though there's no reports regarding the application of a vacuum system on a hot chamber machine, there's references to a vertical vacuum die casting machine, developed by Gibbs Die casting used to inject magnesium, presented in Figure 95. This machine is somewhat like a hot chamber machine since some components are immersed in liquid metal and kept in a holding pot. In this process, vacuum system extracts air from the die cavity and feed channels, which also draws the liquid metal through the transfer tube into the injection cylinder. The filling of the cylinder takes about 2 s or less until the plunger starts displacing metal, shutting off the metal flow, into a pore and resistance free die cavity. After the die cavity is completely filled, an intensification pressure is applied to the solidifying part. The vacuum remains active during the entire injection process, even during the solidification process [14].

This process offers the following process benefits [103]:

- Improves casting microstructure, with smaller grains;
- Reduces gas porosity due to the vacuum process;
- With ultra-high pressure, ranging from 827 - 1379 Bar, shrinkage porosity is greatly minimized;
- Allows and easy use of inserts.

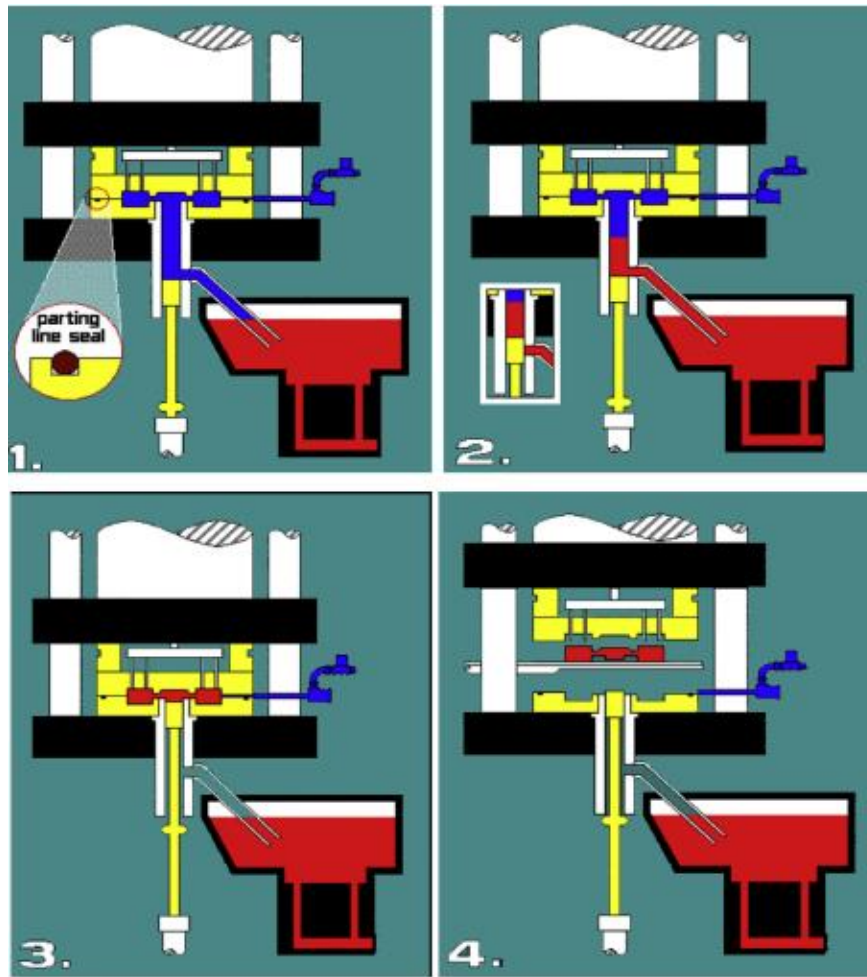


Figure 95- Gibbs vertical vacuum die casting process [14].

## 4.6 Vacuum system design

The vacuum venting design method used in this chapter was proposed by Exco Engineering [65; 98; 104], which offers an easy approach to ensure a correct design of a vacuum system. These articles also resulted in an application that calculates various vacuum venting parameters.

During a venting design process, there's several aspects to be considered such as venting efficiency, vacuum tank size, vacuum pull time, discharge coefficient and air mass flow, that heavily depends upon the desired cast quality [98].

### 4.6.1 Venting efficiency

The first parameter to be considered during a vacuum venting design, is the desired venting efficiency that needs to be achieved at the end of the die casting process. Venting efficiency can be also analyzed for natural venting.

Venting Efficiency is defined as the percentage ratio of air mass being vented out of the die divided by the initial mass being vented, being function of the part quality and casting flow pattern design. Key factors such as vacuum pull time, vent valve effective size, die cavity

temperature and the leakage area of the die assembly directly affects venting efficiency. This parameter can be calculated using Equation 4.1:

$$\eta = 100\% * \frac{M}{(V_c + V_s) * \rho_0} \quad (4.1)$$

Where:

$\eta$ - Venting efficiency (%);

M- Total air mass vented (kg);

$V_c$ - Cavity volume (mm<sup>3</sup>);

$V_s$ - Air volume in the shot sleeve plus the runner volume (mm<sup>3</sup>);

$\rho_0$ - Air density at room temperature (kg/m<sup>3</sup>).

Even though this parameter is difficult to quantify, a higher quality part requires a higher venting efficiency. When assuming the system is at room temperature, a 90 % venting efficiency translates into a 10 % residual air that remains in the die cavity, which is equivalent to 100 mBar. This assumption is made for venting efficiency to be comparable to other processes.

There's some crucial aspects that must be done before analyzing which venting efficiency is necessary, like casting geometry, casting filling pattern and overflow configurations. The filling pattern must be optimized, reducing the air entrapment during the filling process and ensures that air is pushed into the overflows and vacuum runner. This results in a lower efficiency requirement which lowers the process control cost [65].

Post heat-treatments are highly dependent on the venting efficiency, with values that can range from 80 to 97.5 %. Heat treatments like T4 and T6 that require solution treatment a venting efficiency of around 97.5 % must be achieved, otherwise the entrapped air inside the components will explode. For T5 an efficiency ranging from 93 to 95 % is sufficient for a successful treatment [65].

For a vacuum assisted or natural venting process with vent valves, a 90 % venting efficiency is required while 80 % is reserved for non-structural components [65].

#### 4.6.2 Vacuum tank size

According to the author, vacuum tank size depends on various factors such as the volume of air to be remove from the die cavity; overflows and runner; venting efficiency; and the initial tank pressure. A simple process to determine the tank volume with an initial pressure of 5 mBar is to multiple by 150 the cavity volume for a venting efficiency of 97.5 % and 75 for an efficiency of 95 % [65].

The tank pressure is other important aspect to consider in the vacuum tank sizing process, which determines the volume venting flow of an evacuation device. In order to maximize the air flow, the internal tank pressure should be kept 50 % lower than the cavity pressure all time. [65]. The vacuum tank size can be estimated using the Equation 4.2. For this expression some assumptions are made such as air temperature is constant, cavity leakage and pump effect are ignored which results in the need to use a safety constant, K.



$$V_t \geq K \frac{2\eta V_c}{1 - \eta \frac{p_{t0}}{p_0}} \quad (4.2)$$

Where:

$V_t$ - Vacuum tank volume (L);

$K$ - Safety margin factor ( $K=1.5$ );

$\eta$ - Venting efficiency (%);

$V_c$ - Cavity volume to be vented, including overflows and vacuum runners ( $\text{mm}^3$ );

$V_s$ - Volume in the shot sleeve to be vented, including runners and shot sleeve ( $\text{mm}^3$ );

$p_0$ - Initial air pressure, normally atmosphere pressure ( $p_0 = 1 \text{ Bar}$ );

$p_{t0}$ - Initial pressure in the vacuum tank (Bar).

#### 4.6.3 Vacuum pull time

Vacuum pull time is the total time that air is being evacuated through the evacuation device from the die, throughout the first and the second injection phase. Maximizing this parameter is a key parameter for vacuum die casting process optimization. While the cavity filling time is controlled by the second injection phase, the vacuum pull time is controlled by the first. To calculate this parameter, the response time of the evacuation device must be subtracted from the ideal vacuum pull time. The ideal vacuum pull time is the maximum available time to apply vacuum, only considering the duration of the first and the second injection phase until the flow hits the overflows [65].

If the effective vent area (defined as the product of the vent aspiration area and discharge coefficient) is known, increasing the vacuum pull time results in a venting efficiency increase [65].

#### 4.6.4 Discharge coefficient of the evacuation device

Discharge coefficient of the evacuation device, normally provided by the manufactures, is determined by the valve's performance, which is a function of valve geometry design, material selection and manufacturing quality. Values for a mechanical vacuum valve are typically in the range of (0.4 - 0.9); chill block (0.2 - 0.5); for natural vent (0.05 - 0.2) and for leak passages resulting from fitting clearances such as ejection pins (0.044) [104] and slide seal-off surfaces (0.041) [104]. Even though a chill block has the same sectional evacuation area, by having a lower discharge coefficient it has a lower evacuation performance, represented in Figure 96. The discharge coefficient is directly proportional to the evacuation devices venting efficiency.

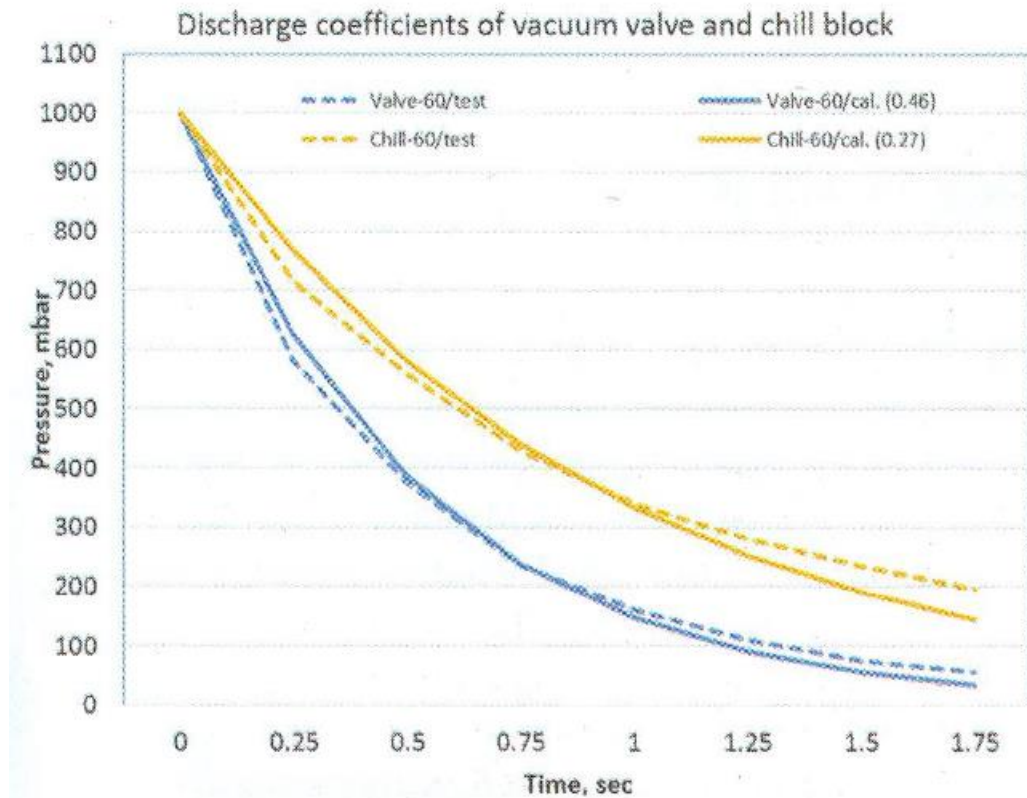


Figure 96- Discharge coefficient of vacuum valve and chill block [98].

A die with a temperature below the optimal range, can play an important role on reducing leakage area. It cannot be generalized, because it could cause flashing which increases the leakage area. Lowering the effective leakage venting area is a method to increase the evacuation performance [104].

#### 4.6.5 Venting mass flow rate

Both natural and vacuum venting produce lower mass flow rates during the first injection phase (slow phase) when compared to the second phase (fast phase). This is because, the die cavity pressure is strongly affected by the plunger velocity. Figure 97 demonstrates the influence of the die cavity pressure on the mass flow rates. For natural venting, by having a higher die cavity pressure in the second phase, a higher mass flow rate will be produced comparing to a vacuum venting process [98].

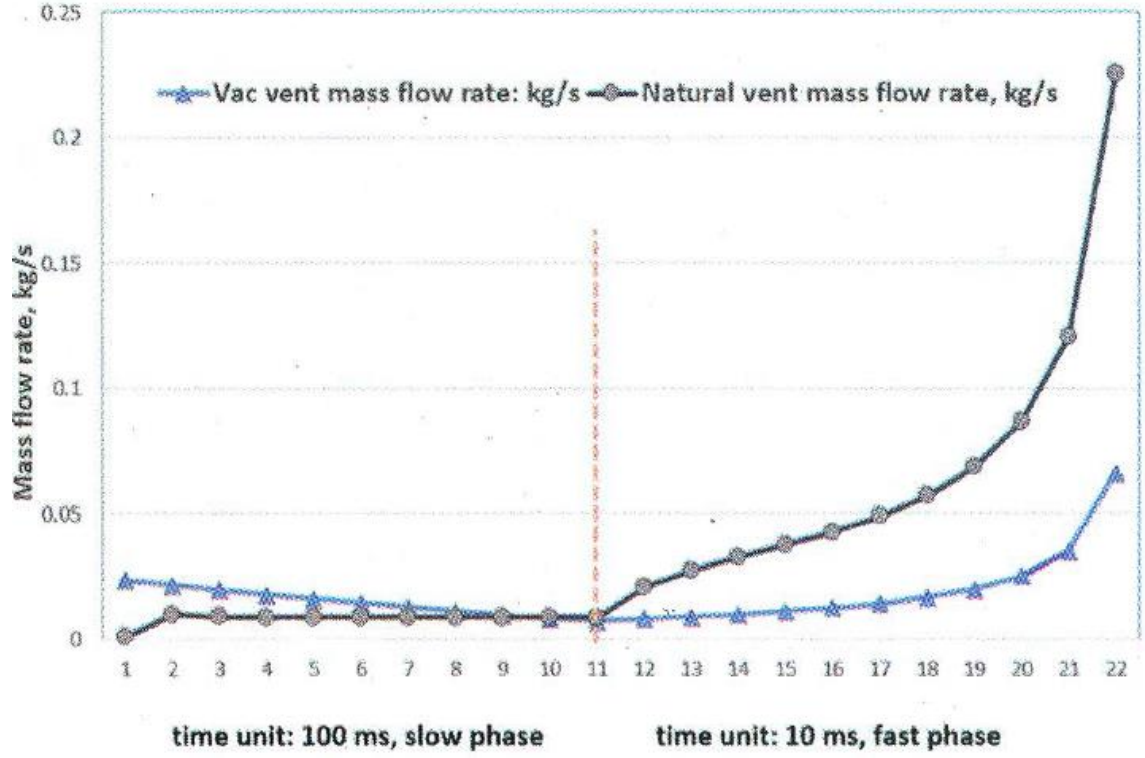


Figure 97- Venting mass flow rates [98].

The maximum flow rate can be calculated using Equation 4.3. Using a sufficient vacuum tank size, this parameter can be achieved throughout the entire evacuation pull time.

$$\dot{Q}_v = A_e * \sqrt{\gamma * R * T_c * \left(\frac{2}{\gamma + 1}\right)^{\frac{\gamma+1}{\gamma-1}}} \quad (4.3)$$

Where:

A<sub>e</sub>- Effective vent area, product of the vent aspiration area and discharge coefficient;

γ- Adiabatic exponent of air;

R- Specific gas constant of air;

T<sub>c</sub>- Air temperature in the die cavity, initially it can be considered as room temperature.

Equation 4.4. establishes a relationship between vacuum pull time and maximum venting flow rate. Considering that the maximum venting flow rate is independent of plunger velocity and cavity pressure, it could be a standard product specification of an evacuation device.

$$t = \frac{V_s + V_c}{\dot{Q}_v} \ln\left(\frac{1}{2(1-\eta)}\right) \quad (4.4)$$

## 4.7 Case study

In this case study, a vacuum system will be designed for the CAD model presented in section 3. The Exco Engineering App will be used, which is based on theoretical and empirical data underlying the following three technical publications [65; 98; 104]. This app is an easy to use tool for a venting and design analysis. This analysis is divided into 2 sub-analysis: first a vacuum tank sizing step; next a vent valve sizing or vacuum pull time estimation.

### 4.7.1 Vacuum tank sizing

For this analysis, the following input values are required to calculate the vacuum tank sizing:

- Efficiency Target = 90 %. This value is considered by the author to ensure a low percentage of air mass during the injection process. Also, this is the lowest value used for a vacuum die casting process;
- Volume to vent- Includes runners, die cavity, sprue and overflows:  
 $V_c = 55915.5 \text{ mm}^3 = 0.056 \text{ L}$ ;
- Safety factor = 1.5;
- Initial cavity pressure = 1000 mBar;
- Initial tank pressure- the application recommends a value of 50 mBar;

Figure 98 presents the App's interface which calculates the vacuum tank size. With these values, the App calculates the required vacuum tank volume of 3.007 L.

Vacuum Tank Sizing

Efficiency Target (%)	<input type="text" value="90"/>		
Volume to Vent (l)	<input type="text" value="0.0556915"/>		
Safety Factor	<input type="text" value="1.5"/>	>	Tank Size (l) <input type="text" value="3.0073e+000"/>
Initial Cavity Pressure (mbar)	<input type="text" value="1000"/>		
Initial Tank Pressure (mbar)	<input type="text" value="50"/>		
Recommended Initial Tank Pressure (mbar) <= 50			

Figure 98- Vacuum tank sizing using the Exco Engineering application.

### 4.7.2 Vent Valve sizing

For this analysis, an evacuation pull time must be known to calculate the necessary evacuation device cross sectional-area to achieve the desired venting efficiency.

For this analysis, the following input values are required to calculate the valves aspiration are:

- Efficiency target = 90 %;
- Volume to vent-  $V_c = 55915.5 \text{ mm}^3 = 0.056 \text{ L}$ ;

- Available pull time- This parameter is calculated based upon the total duration of the first and the second injection phase minus the evacuation devices response time. For this case a 0.45 s will be used for the vent valve sizing, which represents only the available time from injection phase 1 and 2 until the flow hits the overflows. This value is set based on simulations from iteration 2 and is considered an ideal available pull time since the valve response time isn't considered.
- Cavity surface time = 140 °C.

Figure 99 represents the App's interface that calculates the cross-sectional area for a vacuum valve. Using these input values, the application calculates two evacuation device areas: for a mechanical vacuum valve, which is 1.88 mm<sup>2</sup>, and for a chill block which is 3.38 mm<sup>2</sup>. As mentioned before, the vacuum runner must converge in terms of cross sectional area from the outgate, which was 2.65 mm<sup>2</sup>, towards the evacuation device, which happens only for the mechanical vacuum valve. For this reason, only the mechanical vacuum valve can be used as an evacuation device, which ensures a correct evacuation for the efficient target.

Vent Valve Sizing	
Efficiency Target (%)	90
Volume to Vent (l)	0.0556915
Available Pull Time (s)	0.45
Cavity Surface Temp (°C)	140
Effective Vent Area (mm²)	8.4468e-001
Area for Mechanical Valve (mm²)	1.8771e+000
Area for Chill Block (mm²)	3.3787e+000

Figure 99- Vent valve sizing using Exco engineering application.

#### 4.7.3 Vacuum pull time

Figure 100 and 101 represents the App's interface to calculate the required vacuum pull time and effective vent area. This analysis is performed in the case that the designer already has an evacuation device, and the application calculates the required evacuation pull time to achieve the venting efficiency target.

Input parameters:

- Efficiency target = 90 %;
- Volume to vent-  $V_c = 55915.5 \text{ mm}^3 = 0.056 \text{ L}$ ;
- Cavity surface = 140 °C;
- Area for a mechanical valve: If a mechanical valve is used for the design then the input value for a chill block is zero. For both cases the cross-sectional area for the evacuation device must be lower than 2.65, which is the calculated outgate area. It is already known from the previous vacuum pull time calculation, that a 0.45 s pull time requires an area of 1.88 mm<sup>2</sup>. If the designer has a mechanical valve with an area of 2.5 mm<sup>2</sup>, 337 ms would be required to achieve a venting efficiency target of 90 %.

Vacuum Pull Time Estimation

Efficiency Target (%)	90		
Volume to Vent (l)	0,0556915		
Cavity Surface Temp (°C)	140	>	Total Effective Vent Area (mm2) 1,1250e+000
Area for Mechanical Valve (mm2)	2,5		Required Vacuum Pull Time (S) 3,3787e-001
Area for Chill Block (mm2)	0		

Figure 100- Vacuum pull time estimation using a mechanical vacuum valve.

Or

- Area for a chill block: If a chill block is used instead of a mechanical valve, then the input value for the mechanical valve is 0. Using the same evacuation area, a chill block would require 608 ms to achieve a 90 % efficiency, which is nearly double when compared to a mechanical valve. This means that a chill block is less effective evacuating air when compared to a mechanical valve, which was discussed previously. This also proves that a vacuum chill block can't achieve the required venting efficiency venting the ideal vacuum pull time. Increasing the vacuum pull time is also possible by: increasing the furnace temperature and increasing the first injection phase if necessary.

Vacuum Pull Time Estimation

Efficiency Target (%)	90		
Volume to Vent (l)	0,0556915		
Cavity Surface Temp (°C)	140	>	Total Effective Vent Area (mm2) 6,2500e-001
Area for Mechanical Valve (mm2)	0		Required Vacuum Pull Time (S) 6,0817e-001
Area for Chill Block (mm2)	2,5		

Figure 101- Vacuum pull time estimation using a chill block.

#### 4.7.4 Validation of the calculated vacuum system parameters

The application also offers the possibility to validate values calculated previously. By inputting several parameters, some of them calculated during the vacuum venting design, the designer can plot various charts that relates two process parameters. One of these charts can validate the calculations previously calculated by plotting the internal die cavity pressure at the end of the evacuation pull time. This is important to evaluate if the vacuum die casting system is well dimensioned, that ensures that the desired venting efficiency is achieved.

Unfortunately, as the application is bugged, the analysis of the internal pressure variation function to the plunger position, using parameters calculated in the previous section cannot be done.

Even so, a practical case study will be discussed, which was carried out by the author of the application. In this analysis, two processes with different evacuation times, 1.5 s and 2.1 s, are

analyzed. As shown in Figure 102, the cavity air pressure as metal hits the gate is 270.5 mBar for process 1 and 91.8 mBar for process 2. This means that if the designer's target is 100 mBar, only process 2 achieves this target [105]. With a totally functional app, the same analysis could be made on the authors case study to in some way validate the designed vacuum system.

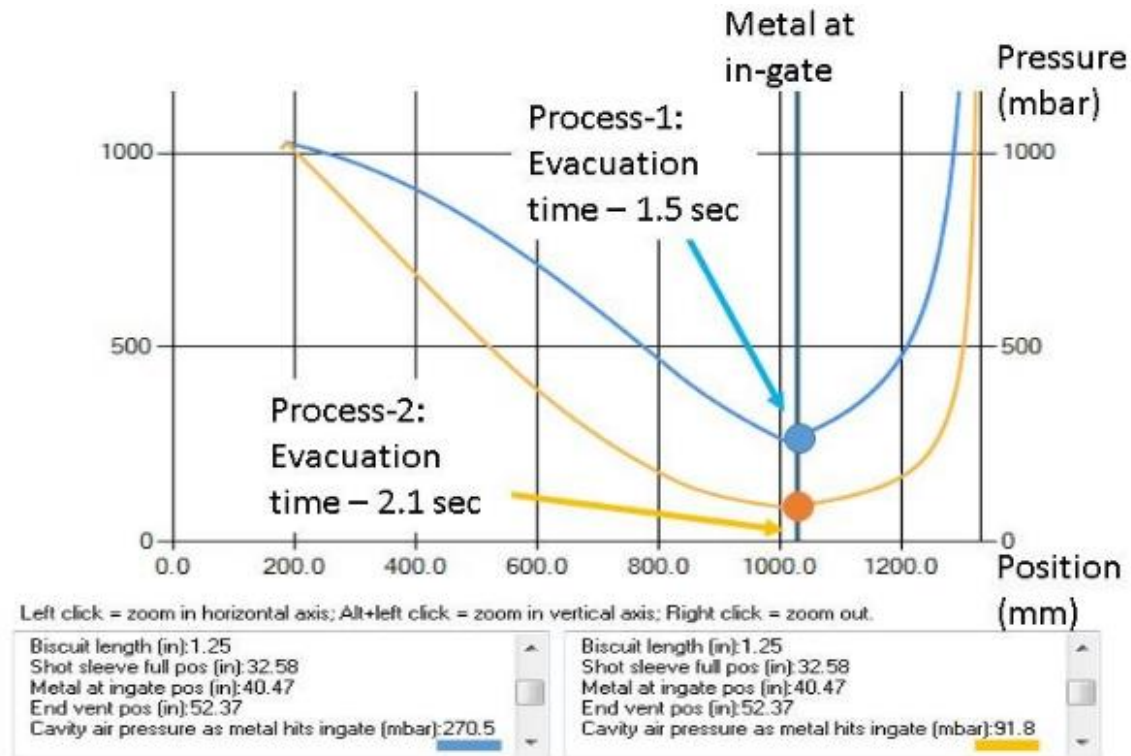


Figure 102- Evolution of the die cavity pressure with respect to the plunger position [105].

#### 4.8 Design of vacuum runners

As discussed previously, no widespread rules for the design of vacuum runners exist, as it happens for the design of gating system. A starting point to design vacuum runners is by applying a converging rule from the outgate to the evacuation device. This means that the runner system cross-sectional area decreases until the evacuations device. Apart from this rule, no widespread calculations are used for the design of vacuum runners. An example of a vacuum runner system layout is presented in Figure 103.

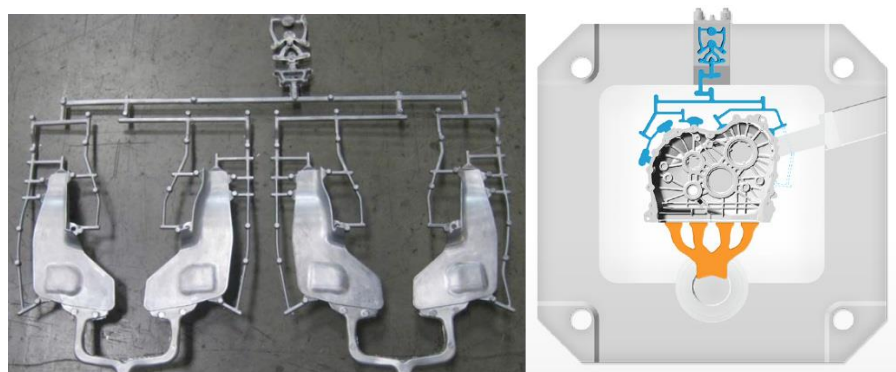


Figure 103- Examples of a vacuum runner system layout with a mechanical vacuum valve [106].



Fondarex [79] presents some guide lines for designing a vacuum runner system, presented in Figure 104. The runner system can be also machined into the die, adjacent to the parting line, with trapezoidal cross section as observed in Figure 104. The total vacuum cross-sectional area is recommended to be 100 to 250 % the area of the main vacuum channel [106].

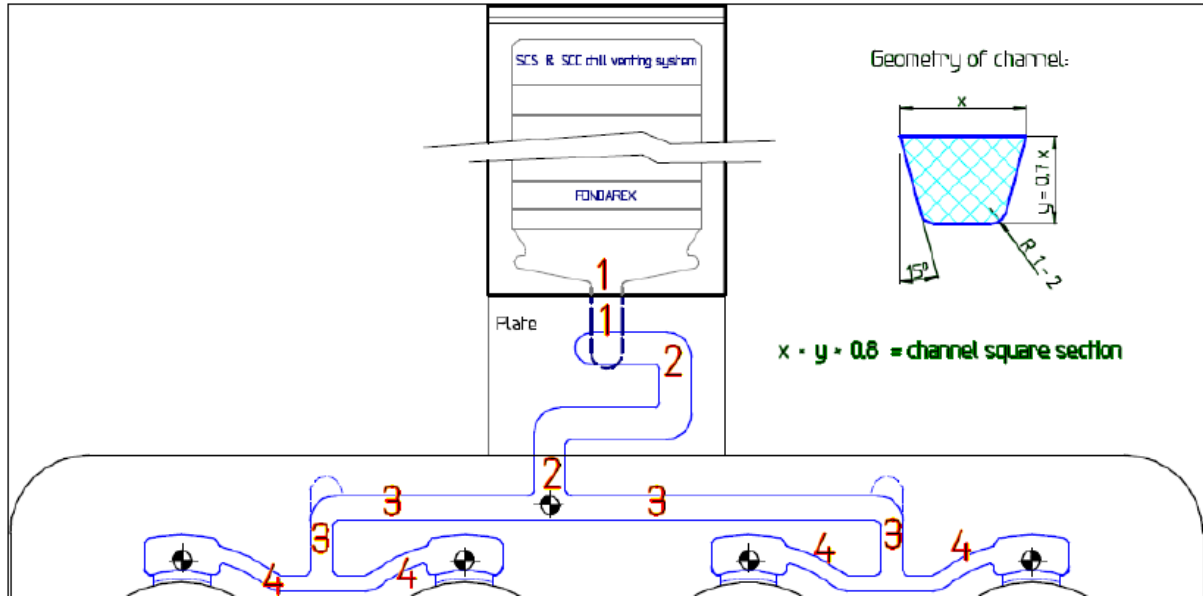


Figure 104- Cross-sectional area variation of the vacuum runner system [106].

Figures description:

- 1 Evacuation device;
- 2 Main vacuum channel – channel capacity – 100 %;
- 3 Distributor vacuum channel – channel capacity – 110 %;
- 4 Distributor vacuum channel – channel capacity – 120 %;

In the vacuum channel design presented in Figure 104, the total cross-sectional area of the gate is 20 % higher, compared to the main vacuum channel. This ensures the convergence rule of the cross-sectional area of the vacuum runner system.

Also, a spreadsheet could be developed using the information presented above that automatically calculates every necessary dimension, used in the designing of vacuum runner systems.

## 4.9 Conclusions

In this section, various topics regarding the application of the vacuum technology in the high pressure die casting were discussed.

It was discussed that an effective approach to remove air porosity related defects of a casted component is by applying vacuum to the die cavity. During this process, air is removed from the die cavity, during the first and second injection phase. Components manufactured using this technology presents higher mechanical properties, when compared to those conventionally produced.

Before analysing the possibility to apply vacuum, the optimization of process parameters and gating system must be ensured. Generally, this process is applied to a high added value market for aluminium and magnesium alloys. These components must maintain high mechanical



properties while being a “light weight”. For zinc alloys, this process isn’t as relevant, because these alloys are primarily used for applications where the mechanical properties aren’t critical. Other reason are the necessary costs to implement this process, which for zinc alloys may not be viable. Components manufactured with zinc alloys, are reserved for a lower added value market, when compared to the aluminium alloys. Even though, for a majority of these application, an excellent surface quality is required which in some cases isn’t obtained only via the optimization of process parameters and the gating system. In these cases, the vacuum technology might be useful.

Both injection phases play an important role during the air evacuation process. It was proved that, during the first injection phase a minimum of 60 % of the air is removed, which depends on the evacuation device used. This is because, in the first injection phase there is more time available for the air to be evacuated. From the literature, it is known that a higher molten metal velocity produces more air entrapments, due to the turbulence generation. Therefore, a value of 0.15 m/s for the plunger’s velocity in the first injection phase, that gives an optimal balance of air porosities and tensile properties. This value is valid for both the conventional process and with vacuum. For the second injection phase of HPDC process using vacuum, a 26 m/s metal flow is indicated. This value allows an optimal balance between air porosity and mechanical properties.

During the design of a vacuum system, the vacuum activation valve is considered a critical component. This will allow that the air is correctly evacuated from the die, without allowing molten metal to enter the system. Among every available evacuation device, the electro-pneumatic valve represents the most optimal choice in terms of low air resistance, low response times and can be easily controlled to evacuate as much air as possible.

Finally, a venting design procedure was presented, which is based on empirical and theoretical data. In this design various parameters are considered such as: venting efficiency, vacuum tank size, vacuum pull time, discharge coefficient of the evacuation device and the venting air mass flow rate. Also, the Exco Engineering App was explored. It is an easy to use tool for the designing process of a venting system. This procedure was applied to the component presented in section 3, to analyse the influence of vacuum on the air porosity generation. An unexpected problem using the App didn’t allow the validation of the parameters calculated during the design. Although, this App is very useful for the designing process of a vacuum system.



## 5 Conclusions and future studies

---

This study presents numerous topics related to the high pressure die casting process of Zamak alloys.

It was discussed that the main problems concerning the Zamak alloys are high density and creep resistance at low temperatures, inherent properties of zinc. Problems related to the high alloy density, can be minimized using a new high fluidity alloy (HF), which allows wall thicknesses as low as 0.25 mm. A new alloy, EZAC™, is a promising solution to overcome the characteristic creep resistance problem. Even though zinc alloys don't have the ability to compete with aluminium and magnesium alloys, their highly appreciated in small dimension applications, where an excellent surface quality finishing is required.

The application of water soluble cores in the HPDC process enhances the capacity of the HPDC process to produce highly complexed shape components. Currently, the water-soluble cores with the highest bending strength (45 MPa), that can be used for a zinc alloy are: KCl salt cores with reinforcing particles such as 15 wt.% of bauxite powders with 15 wt.% glass fibers or 15 wt.% bauxite powders with 15 wt.% sericite powders. Other alternative that could also produce functional cavities, is by using the gas injection technology, originally used for the thermoplastics industry. This technology isn't being used in a continuous production, but it has great potential of creating components with hollow cavities, which are impossible to produce using the conventional process.

A manual of good practices for the design of gating system was developed. This manual surged from the need to create a standard design procedure, which allows the design of optimized gating systems. A real case study was presented, which developed blistering during the painting process. A common associated problem is a non-optimized gating system, which produces a high quantity of air entrapments during the filling process. Using the simulation die casting tool, it was observed that these defects were generated due to problems related to the filling process: a non-convergent sprue, this couldn't be corrected using this manual, since it is provided by the company; a non-convergent gating system; generation of air pockets and metal front collisions. Using this manual, the gating system non-convergent problem was effectively corrected. The other two problems, still occurred, but in a location where the generated air could be effectively pushed into the overflows. This proved that an optimized gating system is a must to obtain an optimal filling pattern. From the CAD model of iteration 3, the first batches were produced with a rejection rate of 5 %. This represents a reduction of 30% when compared to the solution presented in iteration 1. These results are important, since the analyses made based on the simulation were validated experimentally, which proves that the simulation software is somewhat accurate in the defect prediction. Even though a gating system can be effectively designed using only the designers experience, this often leads to incorrect designs which results in higher manufacturing costs.

It was also discussed that even with an optimized gating system, air can be generated during the filling process. This leads to the need to use other alternatives. In this thesis, the application of the vacuum technology was discussed in detail, to minimize the air entrapments during the filling process. The application of the vacuum technology for the zinc die casting industry, isn't used as much as for aluminium and magnesium alloys. This is because, a vacuum system represents a high investment cost, and only in a high added value market it is compensated. But, in some cases applying the vacuum technology might be the solution to achieve the desired components quality. Also, a vacuum system design was presented, based on empirical and theoretical calculations. During this design, it was discussed that the evacuation device is a critical component, which limits the evacuation efficiency of the vacuum system. Also, the Exco Engineering App was explored, which is a useful tool to calculate a number of parameters of the vacuum system. With this App, a validation of the designed vacuum system is possible,

but unfortunately due to a bug, the designed vacuum system for the CAD model couldn't be performed.

## 5.1 Future studies

Throughout this thesis, many subjects were applied to the zinc die casting industry, with theory used in the aluminium die casting industry. There are some subjects that would be interesting to discuss in future works:

- Influence of heat treatments, T4, T5 and T6 on the mechanical properties for Zamak alloys, for the high pressure die casting;
- Implementation of the gating system CAD model from iteration 2 in practice, in order to analyse the influence of an optimized gating system on the blistering problem and also to experimentally validate the simulation;
- Implementation of the vacuum system design method in a real case study using a Zamak alloy, to discuss its influence on the occurrence of filling related defects and on the components mechanical properties.

## References

1. Butler, W. A., Timelli, G., Battaglia, E., & Bonollo, F. (2016). *Die Casting (Permanent Mold)*.
2. Bonollo, F., Gramegna, N., & Timelli, G. (2015). High-Pressure Die-Casting: Contradictions and Challenges. *JOM*, 67(5), 901-908. doi:10.1007/s11837-015-1333-8.
3. Andresen, B. (2005). *Die casting engineering a hydraulic, thermal, and mechanical process*. New York: Marcel Dekker.
4. Vinarcik, E. J. (2002). *High Integrity Die Casting Processes*: Wiley.
5. Murray, M., & Murray, M. (2011). High pressure die casting of aluminium and its alloys *Fundamentals of Aluminium Metallurgy* (pp. 217-261): Elsevier.
6. Kwon, H.-J., & Kwon, H.-K. (2018). Computer aided engineering (CAE) simulation for the design optimization of gate system on high pressure die casting (HPDC) process. *Robotics and Computer-Integrated Manufacturing*. doi:<https://doi.org/10.1016/j.rcim.2018.01.003>.
7. Larsen, D., & Colvin, G. (1999). Vacuum-Die casting titanium for aerospace and commercial components. *JOM*, 51(6), 26-27. doi:10.1007/s11837-999-0089-4.
8. Singh, R. (2014). Modeling of surface hardness in hot chamber die casting using Buckingham's  $\pi$  approach. *Journal of Mechanical Science and Technology*, 28(2), 699-704. doi:10.1007/s12206-013-1133-4.
9. Peti, F., & Grama, L. (2011). Analyze of the possible causes of porosity type defects in aluminium high pressure diecast parts. *Scientific Bulletin of the "Petru Maior" University of Targu Mures*, 8(1), 41.
10. Becker, M., Kallien, L., & Weidler, T. (2015). *Production of magnesium die castings with hollow structures using gas injection technology in the hot chamber die casting process*.
11. Wang, L., Turnley, P., & Savage, G. (2011). Gas content in high pressure die castings. *Journal of Materials Processing Technology*, 211(9), 1510-1515. doi:<https://doi.org/10.1016/j.jmatprotec.2011.03.024>.
12. Rzychoń, T., Adamczk-Cieślak, B., Kielbus, A., & Mizera, J. (2012). The influence of hot-chamber die casting parameters on the microstructure and mechanical properties of magnesium-aluminum alloys containing alkaline elements  
Einfluss der Ofenparameter beim Druckgießen auf die Mikrostruktur und mechanischen Eigenschaften von Magnesium-Aluminium Legierungen mit alkalischen Elementen. *Materialwissenschaft und Werkstofftechnik*, 43(5), 421-426. doi:10.1002/mawe.201200976.
13. Sharma, S. (2014). Modeling and Optimization of Die Casting Process for ZAMAK Alloy. *Journal of Engineering and Technology*, 4(2), 87-94. doi:10.4103/0976-8580.141176.
14. Luo, A. A. (2013). Magnesium casting technology for structural applications. *Journal of Magnesium and Alloys*, 1(1), 2-22.
15. North American Die Casting Association, A. H., Illinois. (2007). *NADCA- Introduction to Die Casting*.

16. Gariboldi, E., Bonollo, F., & Parona, P. (2010). Handbook of Defects in HPDC. AIM, Milano.
17. Walkington, W. G. (2003). *Gas Porosity: A Guide to Correcting the Problems*: North American Die Casting Association.
18. Walkington, W. G. (1997). *Die casting defects. \*. Troubleshooting guide*: NADCA.
19. Derek Cocks, M. C. E. S. DIECASTING DEFECTS: IDENTIFICATION - - CAUSES & CURES: EASTERN ALLOYS, INC.
20. Midson, D. S. (2017 ). NADCA EC-515 Die Casting Defects Course Review: Hill and Griffith Company.
21. Fiorese, E., Bonollo, F., Timelli, G., Arnberg, L., & Gariboldi, E. (2015). New classification of defects and imperfections for aluminum alloy castings. *International Journal of Metalcasting*, 9(1), 55-66.
22. Höök, T. Tampere University of Technology, HPDC runner and gating system design, CAE Mould Design.
23. Data, A. (2003). NADCA product specification standards for die castings. *Arlington Heights, NADCA*.
24. Ward, M. (2006). *Gating manual*: NADCA.
25. Comparison of processes. Casting versatility leads to further savings. Retrieved from <https://www.eazall.com/comparison-of-processes>
26. Rosindale, I., & Davey, K. (1998). Steady state thermal model for the hot chamber injection system in the pressure die casting process. *Journal of Materials Processing Technology*, 82(1-3), 27-45.
27. Winter, R. (2011). EZACTM–High Strength, Creep Resistant, Zinc Die Casting Alloy.
28. Kumar Das, S., & Kumar Bhattacharya, D. (2003). Corrosion failure of Zn–Al detonator housing. *Engineering Failure Analysis*, 10(6), 639-643. doi:[https://doi.org/10.1016/S1350-6307\(03\)00045-1](https://doi.org/10.1016/S1350-6307(03)00045-1).
29. Pola, A., Roberti, R., & Montesano, L. (2010). New Zinc alloys for semisolid applications. *International Journal of Material Forming*, 3(1), 743-746.
30. Dynacast. Retrieved from <https://www.dynacast.co.uk/>
31. da Costa, E. M., da Costa, C. E., Dalla Vecchia, F., Rick, C., Scherer, M., dos Santos, C. A., & Dedavid, B. A. (2009). Study of the influence of copper and magnesium additions on the microstructure formation of Zn–Al hypoeutectic alloys. *Journal of Alloys and Compounds*, 488(1), 89-99.
32. Reveko, V., & Møller, P. (2018). *Special Aspects of Electrodeposition on Zinc Die Castings* (Vol. 82).
33. Stefanescu, D., Davis, J., & Destefani, J. (1988). Metals Handbook, Vol. 15--Casting. *ASM International*, 1988, 937.
34. Wanhill, R., & Hattenberg, T. (2005). Corrosion-induced cracking of model train zinc-aluminium die castings.
35. Zaid, A. I., & Mostafa, A. O. (2017). Effect of hafnium addition on wear resistance of zinc-aluminum 5 alloy: A three-dimensional presentation. *Advanced Materials Letters*, 8(9), 910-915. doi:10.5185/amlett.2017.1662.

36. Goodwin, F. E., Zhang, K., Filc, A. B., Holland, R. L., Dalter, W. R., & Jennings, T. M. (2007). *Development of zinc die casting alloys with improved fluidity: progress in thin section zinc die casting technology*. Paper presented at the Proc. NADCA Metalcasting Congress, Houston Google Scholar.
37. Goodwin, F., Kallien, L., & Leis, W. The High Fluidity (HF) Zinc Alloy: Process-Property and Ageing Characteristics.
38. Goodwin, F., Leis, W., & Kallien, L. (2011). *Ageing Properties of Zinc Alloys*. Paper presented at the NADCA 2011 Congress, Columbus, OH.
39. Kim, C.-H., & Kwon, T. H. (2001). A runner–gate design system for die casting.
40. Hansson, P. (2009). Modern Prehardened Tool Steels in Die-Casting Applications. *Materials and Manufacturing Processes*, 24(7-8), 824-827. doi:10.1080/10426910902841753.
41. RAVEENDRAN, N. A. K., & PATIL, A. N. (2017). OPTIMIZATION OF RUNNER DESIGN IN HIGH PRESSURE DIE CASTING (HPDC) DIE. *International Journal of Engineering Research & Technology (IJERT)*, 3(4).
42. Pinto, H., & Silva, F. (2017). Optimisation of die casting process in Zamak alloys. *Procedia Manufacturing*, 11, 517-525.
43. Yangqing, D., Kun, B., Yangliu, D., & Yiwei, D. (2010). Reversing design methodology of investment casting die profile based on ProCAST. *Research & Development*.
44. Dadić, Z., Živković, D., Čatipović, N., & Bilić, J. (2017). *High pressure die casting mould repair technologies*. Paper presented at the 7th International Conference" Mechanical Technologies and Structural Materials 2017".
45. Huang, R., & Zhang, B. (2017). Study on the composition and properties of salt cores for zinc alloy die casting. *International Journal of Metalcasting*, 11(3), 440-447. doi:<https://doi.org/10.1007/s40962-016-0086-7>.
46. Adámková, E., Jelínek, P., Beňo, J., & Mikšovský, F. (2015). Water-soluble cores—verifying development trends. *Materiali In Tehnologije*, 49(1), 61-67. Retrieved from <http://mit.imt.si/Revija/izvodi/mit151/adamkova.pdf>
47. Kallien, L., Böhnlein, C., Dworak, A., & Müller, B. (2013). Ergebnisse aus dem Forschungsprojekt 3-D-Freiform–medienführende Kanäle im Druckguss. *Giesserei Praxis*, 100(12), 36-43.
48. Jelínek, P., Adámková, E., Mikšovský, F., & Beňo, J. (2015). Advances in technology of soluble cores for die castings. *Archives of foundry engineering*, 15(2), 29-34.
49. Jelínek, P., & Adámková, E. (2014). Lost cores for high-pressure die casting. *Archives of foundry engineering*, 14(2), 101-104.
50. Tu, S., Liu, F., Li, G., Jiang, W., Liu, X., & Fan, Z. (2018). Fabrication and characterization of high-strength water-soluble composite salt core for zinc alloy die castings. *The international journal of advanced manufacturing technology*, 95(1-4), 505-512.
51. Gramegna, N. (2006). Analysis of the factors contributing to the heat balance of an high pressure die-casting mould. *EnginSoft SpA, Padova*.
52. Fiorese, E., Bonollo, F., Battaglia, E., & Cavaliere, G. (2017). Improving die casting processes through optimization of lubrication. *International Journal of Cast Metals Research*, 30(1), 6-12. doi:10.1080/13640461.2016.1162387.

53. Asthana, S. (2013). Innovative die lubricant trends for evolving productivity and process requirements. *NADCA Die casting Cong.*
54. Andreoni, L., Casè, M., & Pomesano, G. Lubrificazione della cavità dello stampo, quaderni della colata a pressione delle leghe di alluminio, quaderno Nr. 7, 1<sup>a</sup> edizione, 1996. *Brescia, Edimet.*
55. BERTHOLD, J., VAN DER STEEN, S., KRUGMANN, J., & RÜHMANN, H. R. (2004). Profitabler Spritzgiessen mit Stickstoff oder Wasser? *Kunststoffe*, 94(9), 203-207.
56. KALLIEN, L. H., WEIDLER, T., HERMANN, C., & STIELER, S. U. (2006). Druckgussteile mit funktionalen Hohlräumen durch Gasinjektion. *Giesserei*, 93(11).
57. Kallien, L. H. (2009). *Using gas injection in high pressure die casting technology*. Paper presented at the 113th Metalcasting Congress, Las Vegas, Nevada.
58. Kallien, L. H., Weidler, T., Hermann, C., Stieler, U., Kallien, L., Weidler, T., . . . Kunststoff, S. (2006). Pressure die castings with functional cavities produced by gas injection. *Giessereiforschung*, 58(4), 2-9.
59. Kim, E., Lee, K., & Moon, Y. (2000). A feasibility study of the partial squeeze and vacuum die casting process. *Journal of Materials Processing Technology*, 105(1-2), 42-48.
60. Thirugnanam, M. (2013). *Modern high pressure die-casting processes for aluminium castings*. Paper presented at the Transaction of Indian Foundry Congress.
61. De Cicco, M. P., Li, X., & Turng, L.-S. (2009). Semi-solid casting (SSC) of zinc alloy nanocomposites. *Journal of Materials Processing Technology*, 209(18-19), 5881-5885.
62. Lee, J. K., Kim, S. K., & Lee, Y. C. (2008). Development of Novel Hot Chamber Rheo-Diecasting Process. *Solid State Phenomena*, 141-143, 191-194. doi:10.4028/[www.scientific.net/SSP.141-143.191](http://www.scientific.net/SSP.141-143.191).
63. Lumley, R., O'Donnell, R., Gunasegaram, D., & Givord, M. (2007). Heat treatment of high-pressure die castings. *Metallurgical and Materials Transactions A*, 38(10), 2564-2574.
64. Kasprzak, W., Sokolowski, J., Yamagata, H., Aniolek, M., & Kurita, H. (2011). Energy efficient heat treatment for linerless hypereutectic Al-Si engine blocks made using vacuum HPDC process. *Journal of Materials Engineering and Performance*, 20(1), 120-132.
65. Changhua (Joshua) Huang, W. B. (2014). *Venting Design and Process Optimization of Die Casting Process for Structural components - Part II Venting Design and Process Optimizationn*. Paper presented at the Die casting Congress & Tabletop.
66. Lumley, R. (2011). Progress on the heat treatment of high pressure die castings *Fundamentals of aluminium metallurgy* (pp. 262-303): Elsevier.
67. ZHANG, S., WEI, X., YU, W., LIAN, Z., & ZHAO, H. (2015). Microstructural Characterization of Zinc Alloy ZA27 with Modification and Heat Treatments.
68. Kallien, L. H., & Leis, W. (2011). Ageing of Zink Alloys. *Giessereiforschung including CD ROM*, 63(1), 2.
69. Babić, M., Ninković, R., Mitrović, S., & Bobić, I. (2007). *Influence of heat treatment on tribological behavior of Zn-Al Alloys*. Paper presented at the Proceedings of 10th International Conference on Tribology, SERBIATRIB.



70. Bobic, B., Bajat, J., Acimovic-Pavlovic, Z., Rakin, M., & Bobic, I. (2011). The effect of T4 heat treatment on the microstructure and corrosion behaviour of Zn27Al1. 5Cu0. 02Mg alloy. *Corrosion Science*, 53(1), 409-417.
71. Liu, Y., Li, H.-y., Jiang, H.-f., & Lu, X.-c. (2013). Effects of heat treatment on microstructure and mechanical properties of ZA27 alloy. *Transactions of Nonferrous Metals Society of China*, 23(3), 642-649. doi:[https://doi.org/10.1016/S1003-6326\(13\)62511-X](https://doi.org/10.1016/S1003-6326(13)62511-X).
72. Choudhury, P., Das, K., & Das, S. (2005). Evolution of as-cast and heat-treated microstructure of a commercial bearing alloy. *Materials Science and Engineering: A*, 398(1), 332-343. doi:<https://doi.org/10.1016/j.msea.2005.03.098>.
73. Michalik, R., & Tomaszewska, A. (2014). Influence of Heat Treatment on the Hardness of ZnAl22Cu3 Alloy. *Solid State Phenomena*, 212, 35-38. doi:10.4028/[www.scientific.net/SSP.212.35](http://www.scientific.net/SSP.212.35).
74. Prasad, B. K., Patwardhan, A. K., & Yegneswaran, A. H. (1996). Influence of heat treatment parameters on the microstructure and properties of some zinc-based alloys. *Journal of Materials Science*, 31(23), 6317-6324. doi:10.1007/bf00354455.
75. Kumar, V., & Madan, J. (2017). A system for computer-aided gating design for multi-cavity die-casting dies. *Proceedings of the Institution of Mechanical Engineers, Part B: Journal of Engineering Manufacture*, 231(11), 1983-1999.
76. Renukananda, K. H., & Ravi, B. (2016). Multi-Gate Systems in Casting Process: Comparative Study of Liquid Metal and Water Flow. *Materials and Manufacturing Processes*, 31(8), 1091-1101. doi:10.1080/10426914.2015.1037911.
77. Wu, S., Lee, K., & Fuh, J. (2002). Feature-based parametric design of a gating system for a die-casting die. *The international journal of advanced manufacturing technology*, 19(11), 821-829.
78. Uchida, M. (2009). Development of vacuum die-casting process. *China Foundry*, 6(2), 137-144.
79. . Retrieved from <https://www.fondarex.com/>
80. Zyska, A., Konopka, Z., Łągiewka, M., & Nadolski, M. (2015). Porosity of Castings Produced by the Vacuum Assisted Pressure Die Casting Method. *Archives of foundry engineering*, 15(1), 125-130.
81. NOURI, B. A. (2004). Analysis of vacuum venting in Die Casting.
82. HU, B., XIONG, S., Murakami, M., Matsumoto, Y., & Ikeda, S. Study on vacuum die casting process of aluminum alloys.
83. Wang, X., Zhu, S., Easton, M. A., Gibson, M. A., & Savage, G. (2014). Heat treatment of vacuum high pressure die cast magnesium alloy AZ91. *International Journal of Cast Metals Research*, 27(3), 161-166.
84. Niu, X., Hu, B., Pinwill, I., & Li, H. (2000). Vacuum assisted high pressure die casting of aluminium alloys. *Journal of Materials Processing Technology*, 105(1-2), 119-127.
85. Cao, H., Hao, M., Shen, C., & Liang, P. (2017). The influence of different vacuum degree on the porosity and mechanical properties of aluminum die casting. *Vacuum*, 146, 278-281.
86. Li, S.-y., Li, D.-j., Zeng, X.-q., & Ding, W.-j. (2014). Microstructure and mechanical properties of Mg-6Gd-3Y-0.5 Zr alloy processed by high-vacuum die-casting. *Transactions of Nonferrous Metals Society of China*, 24(12), 3769-3776.

87. Li, X.-b., Xiong, S., & Guo, Z.-p. (2016). Improved mechanical properties in vacuum-assist high-pressure die casting of AZ91D alloy. *Journal of Materials Processing Technology*, 231, 1-7.
88. Siedersleben, M. (2003). Vacuum Die-Casting of Magnesium Parts with High Pressure. *Magnesium-Alloys and Technology*, 45-55.
89. Hu, B., Xiong, S., Masayuki, M., Yoshihide, M., & Shingo, I. (2006). Experimental study of vacuum die casting process of AZ91D magnesium alloy. *Magnesium Technology 2006*, 51-55.
90. Bar-Meir, G., Eckert, E., & Goldstein, R. (1996). Pressure die casting: A model of vacuum pumping. *Journal of Manufacturing Science and Engineering*, 118(2), 259-265.
91. Jin, C. K., Jang, C. H., & Kang, C. G. (2015). Vacuum die casting process and simulation for manufacturing 0.8 mm-thick aluminum plate with four maze shapes. *Metals*, 5(1), 192-205.
92. Yoon, J., Kim, S., Yim, Y., & Park, J. (2008). Numerical simulation of molten metal flow under vacuum condition in high pressure and low pressure die casting process. *International Journal of Cast Metals Research*, 21(1-4), 299-303.
93. Wang, L. (2007). Mathematical modelling of air evacuation in die casting process via CASTvac and other venting devices. *International Journal of Cast Metals Research*, 20(4), 191-197.
94. Wang, Q.-l., & Xiong, S.-m. (2015). Effect of multi-step slow shot speed on microstructure of vacuum die cast AZ91D magnesium alloy. *Transactions of Nonferrous Metals Society of China*, 25(2), 375-380. doi:[https://doi.org/10.1016/S1003-6326\(15\)63613-5](https://doi.org/10.1016/S1003-6326(15)63613-5).
95. Otarawanna, S., Gurlay, C. M., Laukli, H. I., & Dahle, A. K. (2009). Microstructure formation in high pressure die casting. *Transactions of the Indian Institute of Metals*, 62(4), 499-503. doi:10.1007/s12666-009-0081-2.
96. Li, X.-B., Xiong, S.-M., & Guo, Z.-P. (2016). Characterization of the Grain Structures in Vacuum-Assist High-Pressure Die Casting AM60B Alloy. *Acta Metallurgica Sinica (English Letters)*, 29(7), 619-628. doi:10.1007/s40195-016-0430-1.
97. Wang, Q.-l., & Xiong, S.-m. (2014). Vacuum assisted high-pressure die casting of AZ91D magnesium alloy at different slow shot speeds. *Transactions of Nonferrous Metals Society of China*, 24(10), 3051-3059.
98. Bishenden, C. J. H. W. (2014). venting design and process optimization of die casting process for structural components - Part I Venting efficiency analysis of die casting process. *Die casting Engineer*.
99. Dr.Christophe Bagnoud, R. B. Die evacuation: Valve or chill vent. VDS/SA Vacuum Die-casting service, Montreux, Switzerland. Retrieved from [http://www.soundcastproject.eu/files/2013/10/Evacuation\\_performance\\_of\\_a\\_ProVac\\_vacuum\\_valve\\_and\\_a\\_chill-vent.pdf](http://www.soundcastproject.eu/files/2013/10/Evacuation_performance_of_a_ProVac_vacuum_valve_and_a_chill-vent.pdf)
100. Wang, L., Gershenzon, M., Nguyen, V., & Savage, G. (2005). An Innovative Device for Vacuum and Air Venting. *CastExpo*, 5, 16-19.
101. Wang, L., Gershenzon, M., Nguyen, V., & Savage, G. (2007). *Air evacuation and metal solidification with varied profiles of chill surfaces*. Paper presented at the 111th Metalcasting Congress.
102. SA, V. (2018). PROVAC® ULTRA EASY VALVES. Retrieved from <http://www.vdssa.ch/provac-ultra-easy/>

103. corp., G. D. c. Process Controls. Retrieved from [http://www.gibbsdc.com/us/quality/process\\_control.htm](http://www.gibbsdc.com/us/quality/process_control.htm)
104. Changhua (Joshua) Huang, W. B. (2015). *Experimental investigation into leakage of die casting die for vacuum venting process*. Paper presented at the Die casting Congress & Exposition.
105. Huang, J. (2016). Vacuum Die Casting Process Design. Retrieved from <https://www.linkedin.com/pulse/vacuum-die-casting-process-design-joshua-huang/>
106. Emmenegger, J. (2016). Innovations in Vacuum Die Casting: Vacuum Technology for High Quality Die Casting Parts. *Fondarex*.



## Appendix A

### Gating system design manual using Excel

Table A 1- Cavity filling time.

t- max filling time, s	0,0361	[s]
K - thermal constant of a die steel	0,0346	[s/mm]
T - characteristic thickness (average or minimum)	1,8	[mm]
T <sub>f</sub> - liquidus temperature	382	[°C]
T <sub>i</sub> - metal temperature in the gate	420	[°C]
T <sub>d</sub> - die temperature before the shot	230	[°C]
S- percent solids before at the end	20	[%]
Z- solids units conversion	2,5	[°C/%]

Table A 2- Flow rates.

Segment		#1	Total
t- cavity fill time	[s]	0,036	
V <sub>g</sub> - volume of a segment	[mm <sup>3</sup> ]	10206,70	
V <sub>o</sub> - volume of overflow segment	[mm <sup>3</sup> ]	5103,35	50 % of V <sub>g</sub>
V <sub>i</sub> -total segment volume	[mm <sup>3</sup> ]	15310,05	
Gate velocity	[m/s]	40	range [30-60] m/s
Q <sub>i</sub> - Volumetric flow rate of each segment	[m <sup>3</sup> /s]	0,00043	
Q- $\sum Q_i$ - Volumetric flow rate for the entire casting	[m <sup>3</sup> /s]		0,00043
A <sub>i</sub> -Ingate area of segment	[mm <sup>2</sup> ]	10,62	
A - Total Ingate area	[mm <sup>2</sup> ]		10,62

Table A 3- Ingate data.

Gate number	#1	#2	#3	#4	Total
Total gate area	10,62				10,62
Gate thickness	0,55				0,55
Gate length	19,30				19,30

Table A 4- Nozzle data in second phase.

Diameter	[mm]	8,7
Nozzle Area	[mm <sup>2</sup> ]	59,41665
Nozzle velocity	[m/s]	7,15
Volumetric flow rate	[m <sup>3</sup> /s]	0,00042

Table A 5- Plunger data in the second phase.

<b>Diameter</b>	[mm]	60
<b>Plunger Area</b>	[mm <sup>2</sup> ]	2826
<b>Plunger velocity</b>	[m/s]	0,15
<b>Mass flow</b>	[m <sup>3</sup> /s]	0,000425
<b>PQ<sup>2</sup>- Pm - Metal Pressure during 2 phase</b>	MPa	1,54

Table A 6- Curved sided fan gate-runner and runner segment data.

<b>Gate Land Length [mm]</b>	Flow angle = 40 degrees								
<b>Section</b>	A	B	C	D	E	F	G	H	I
<b>Area [mm<sup>2</sup>]</b>	11,68	13,14	14,60	16,06	17,52	18,97	20,43	21,89	23,35
<b>Distance [mm]</b>	0,00	2,50	5,00	7,50	10,00	12,50	15,00	17,50	20
<b>Depth (h) [mm]</b>	0,61	0,78	0,95	1,13	1,30	1,48	1,65	1,83	2,00
<b>Average Width [mm]</b>	19,30	16,85	15,30	14,23	13,45	12,85	12,38	11,99	11,68
<b>Base (b) [mm]</b>	19,41	16,99	15,47	14,43	13,68	13,11	12,67	12,31	12,03
<b>Top (t) [mm]</b>	19,19	16,72	15,14	14,03	13,22	12,59	12,08	11,67	11,32
<b>Side (c) [mm]</b>	0,11	0,14	0,17	0,20	0,23	0,26	0,29	0,32	0,35
<b>Side (d) [mm]</b>	0,11	0,14	0,17	0,20	0,23	0,26	0,29	0,32	0,35

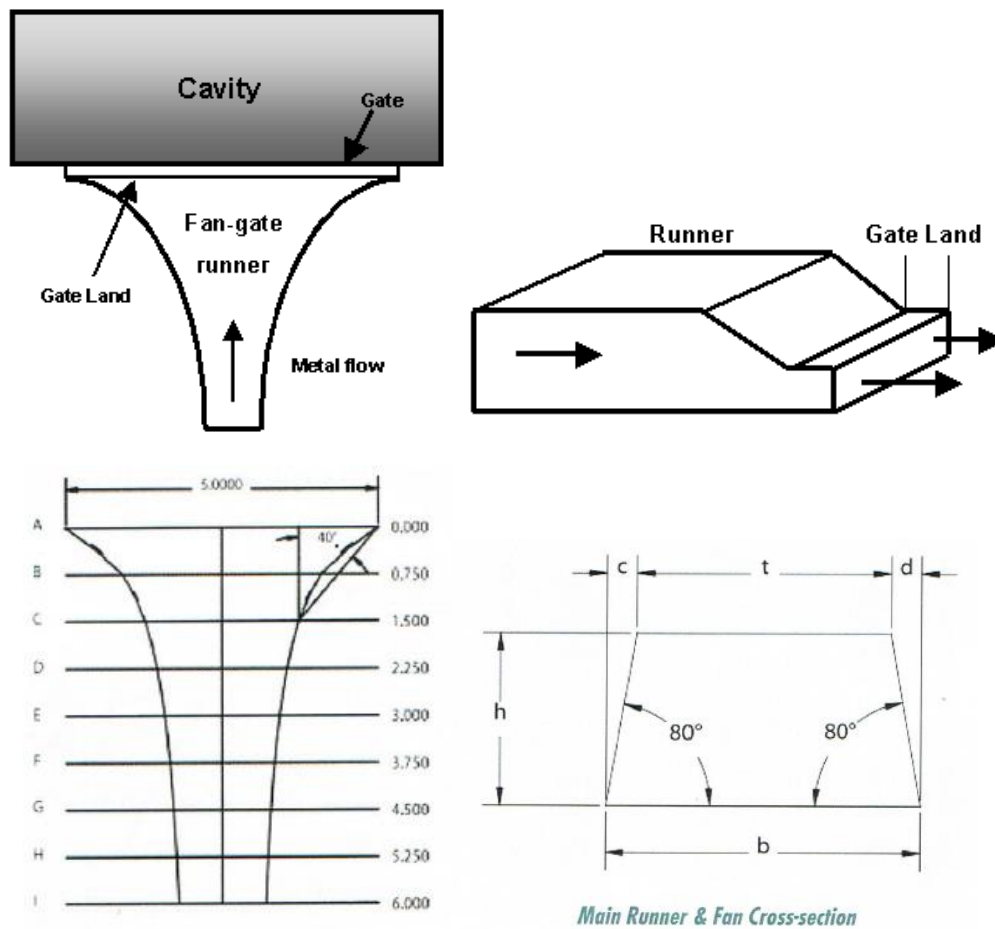


Figure A 1- Figure presenting different dimensions of the fan gate-runner calculated in Table A 6.

Table A 7- Outgates, overflows and vents.

<b>Outgates data</b>	<b>#1</b>	<b>#2</b>	<b>#3</b>	<b>#4</b>	<b>#5</b>
Total Outgate Area [mm <sup>2</sup> ]	5,308				
Number of Outgates	2				
Outgate Area [mm <sup>2</sup> ]	2,65	2,65			
Outgate thickness, C [mm]	0,275	0,275			
Outgate width [mm]	9,65	9,65			
<b>Overflow data</b>	<b>#1</b>	<b>#2</b>	<b>#3</b>	<b>#4</b>	<b>#5</b>
Number of overflows	2				
Total Overflow volume [mm <sup>3</sup> ]	5103,35				
Outgate overflow length, B [mm]	6,5	<b>Range [6-8] mm</b>			
Land length, A [mm]	2,5	<b>Range [2-5] mm</b>			
Volume [mm <sup>3</sup> ]	2551,675	2551,675			
Overflow length, L [mm]	32,567909	32,56791			
Overflow height, H [mm]	5	5			
Overflow upper side length, W [mm]	20	20			
Overflow lower side length, w [mm]	11,339746	11,33975			
<b>Vent data</b>	<b>#1</b>	<b>#2</b>	<b>#3</b>	<b>#4</b>	<b>#4</b>
Total Vent area [mm <sup>2</sup> ]	2,65				
Number of vents	2				
Vent thickness [mm]	0,254	0,254			
Vent area [mm <sup>2</sup> ]	1,33	1,33			
Vent width [mm]	5,22	5,22			
Vent length [mm]	<b>Function of the gate thickness</b>				50,8

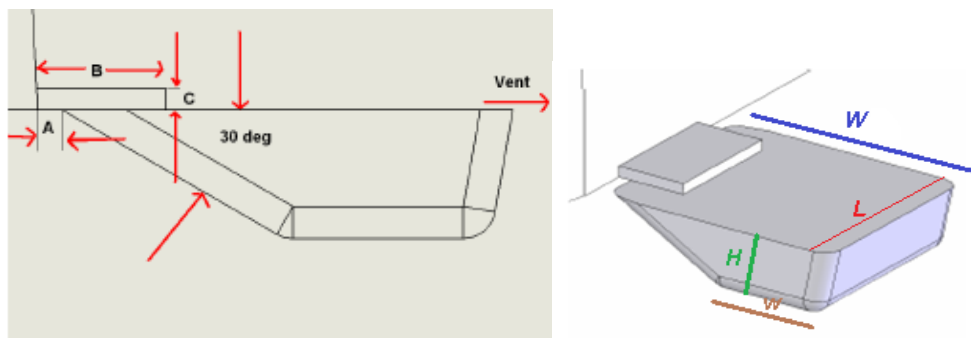
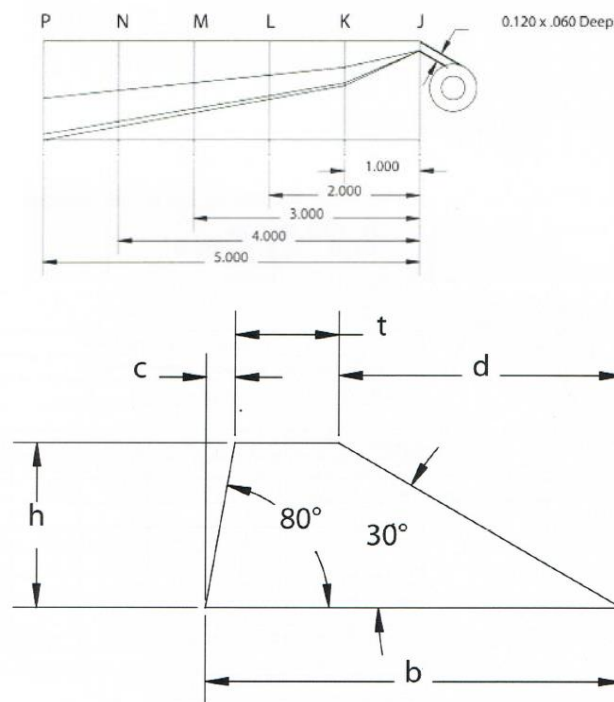
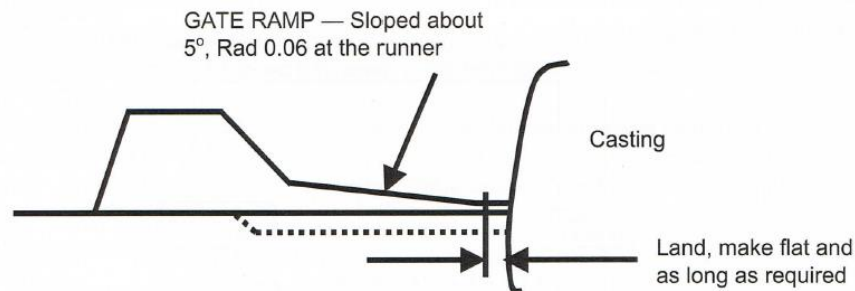


Figure A 2- Various dimensions of an overflow.

Table A 8 represents the dimensions of a tangential gate-runner in case it would be used.

Table A 8- Tangential gate-runner

2:1 Aspect Ratio; 30° approach angle; 10° Draft; Flow angle = 40°						
Gate Thickness [mm]	0,55					
Section	J	K	L	M	N	P
Distance [mm]	0	3,86	7,72	11,58	15,44	19,3
Flow angle (°)	0	40	40	40	40	40
Area [mm <sup>2</sup> ]	1,676	2,771	5,543	8,314	11,086	13,857
h [mm]	0,55	1,177	1,665	2,039	2,354	2,632
b [mm]	3,048	3,475	4,914	6,019	6,950	7,770
d [mm]	0	0,207	0,293	0,359	0,414	0,463
t [mm]	0	1,231	1,741	2,133	2,463	2,753
c [mm]	0	2,036	2,880	3,527	4,073	4,554



Tangential Runner Cross-section 30° Approach

Figure A 3- Dimensions of a tangential gate-runner.